Cell Reports

Article

The RNA Binding Protein Mex-3B Is Required for IL-33 Induction in the Development of Allergic Airway Inflammation

Graphical Abstract

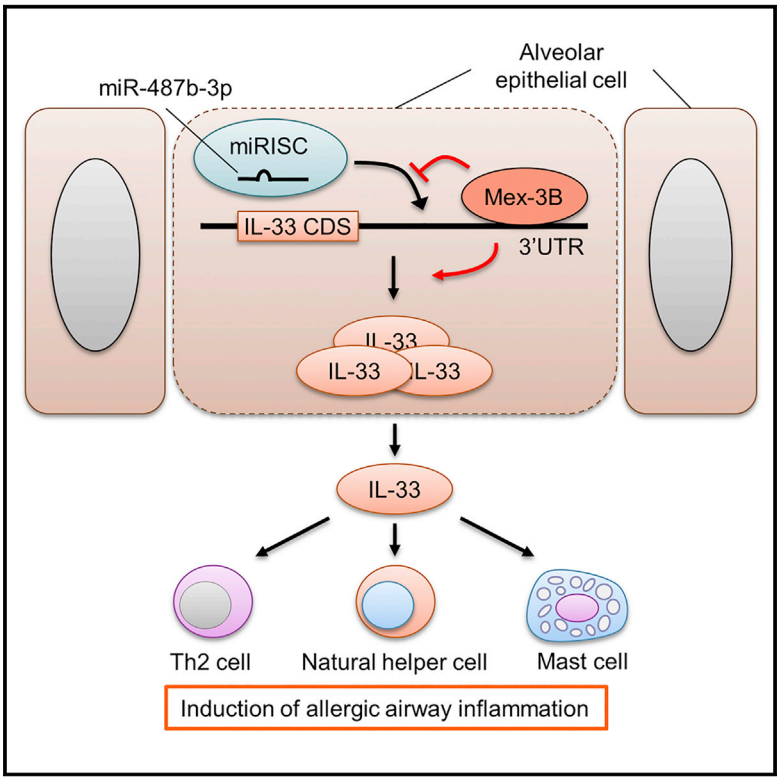

Highlights

- Mex-3B induces IL-33 in the development of allergic airway inflammation
- *Mex3b*$^{-/-}$ mice develop less airway inflammation due to reduced induction of IL-33
- Mex-3B upregulates IL-33 expression by inhibiting miR-487b-3p-mediated repression
- Inhalation of an antisense oligo targeting Mex-3B suppresses airway inflammation

Authors

Yusuke Yamazumi, Oh Sasaki, Mitsuru Imamura, ..., Makoto Dohi, Shigeo Koyasu, Tetsu Akiyama

Correspondence

akiyama@iam.u-tokyo.ac.jp

In Brief

Yamazumi et al. show that Mex-3B-mediated post-transcriptional upregulation of IL-33 is required for the development of allergic airway inflammation. Inhalation of an antisense oligonucleotide targeting Mex-3B suppresses allergic airway inflammation, suggesting that Mex-3B could be a promising molecular target for the treatment of allergic asthma.

Yamazumi et al., 2016, Cell Reports *16*, 2456–2471
August 30, 2016 © 2016 The Author(s).
http://dx.doi.org/10.1016/j.celrep.2016.07.062

OPEN ACCESS
CellPress

Cell Reports
Article

The RNA Binding Protein Mex-3B Is Required for IL-33 Induction in the Development of Allergic Airway Inflammation

Yusuke Yamazumi,[1] Oh Sasaki,[2] Mitsuru Imamura,[2] Takeaki Oda,[1] Yoko Ohno,[1] Yumi Shiozaki-Sato,[1] Shigenori Nagai,[3] Saki Suyama,[1] Yuki Kamoshida,[1] Kosuke Funato,[1] Teruhito Yasui,[4] Hitoshi Kikutani,[4] Kazuhiko Yamamoto,[2] Makoto Dohi,[2,5] Shigeo Koyasu,[6] and Tetsu Akiyama[1,7,*]

[1]Laboratory of Molecular and Genetic Information, Institute for Molecular and Cellular Biosciences, The University of Tokyo, 1-1-1 Yayoi, Bunkyo-ku, Tokyo 113-0032, Japan
[2]Department of Allergy and Rheumatology, Graduate School of Medicine, University of Tokyo, 7-3-1 Hongo, Bunkyo-ku, Tokyo 113-8655, Japan
[3]Department of Molecular Immunology, Graduate School of Medical and Dental Sciences, Tokyo Medical and Dental University, 1-5-45 Yushima, Bunkyo-ku, Tokyo 113-8549, Japan
[4]Department of Molecular Immunology, Research Institute for Microbial Diseases, Osaka University, 3-1 Yamada-oka, Suita, Osaka 565-0871, Japan
[5]Institute of Respiratory Immunology, Shibuya Clinic for Respiratory Diseases and Allergology, Tokyo 150-0002, Japan
[6]Laboratory for Immune Cell Systems, RIKEN Research Center for Integrative Medical Sciences (IMS), 1-7-22 Suehiro-cho, Tsurumi-ku, Yokohama 230-0045, Japan
[7]Lead Contact
*Correspondence: akiyama@iam.u-tokyo.ac.jp
http://dx.doi.org/10.1016/j.celrep.2016.07.062

SUMMARY

Allergic airway inflammation is one of the primary features of allergic asthma. Interleukin-33 (IL-33) is recognized as a key pro-inflammatory cytokine that mediates allergic airway inflammation, and its expression is elevated in this condition, but little is known about the regulatory mechanisms underlying IL-33 induction. Here, we show that the RNA binding protein Mex-3B plays a critical role in the induction of IL-33 in the development of allergic airway inflammation. We generated *Mex3b*$^{-/-}$ mice and found that they develop significantly less airway inflammation than wild-type mice due to reduced induction of IL-33. Furthermore, we show that Mex-3B directly upregulates IL-33 expression by inhibiting miR-487b-3p-mediated repression of IL-33. Moreover, we show that inhalation of an antisense oligonucleotide targeting Mex-3B suppresses allergic airway inflammation. Our data identify a signaling pathway that post-transcriptionally regulates IL-33 expression and suggest that Mex-3B could be a promising molecular target for the treatment of allergic asthma.

INTRODUCTION

Allergic asthma is a chronic inflammatory disease of the lungs that affects nearly 300 million people worldwide. Allergic airway inflammation is one of the primary features of allergic asthma and is generally considered to be mediated by a T helper type 2 (Th2) response (Kim et al., 2010). Leucocytes have long been focused as the key players in the development of allergic airway inflammation. However, there is increasing evidence that epithelial cells act as active immune regulators that produce inflammatory factors, such as TSLP and interleukin-33 (IL-33) (Liew et al., 2010; Ziegler and Artis, 2010). IL-33 is a member of the IL-1 family, which plays important roles in type 2 innate immunity and human asthma (Cayrol and Girard, 2014). It has been shown that mice deficient for IL-33 are resistant to allergen-induced airway inflammation (Oboki et al., 2010). Furthermore, *IL-33* has been identified as a susceptibility gene for human asthma (Gudbjartsson et al., 2009; Moffatt et al., 2010). In addition, its expression in epithelial cells is higher in patients with allergic asthma than in healthy individuals (Préfontaine et al., 2010), and upregulation of IL-33 expression is observed in an experimental asthma model (Louten et al., 2011). Although several studies have shown that IL-33 expression is induced upon pro-inflammatory cytokine stimulation in several cell types (Masamune et al., 2010; Sponheim et al., 2010), the importance of IL-33 induction in the development of allergic airway inflammation, and the mechanisms underlying this induction are not well understood.

MicroRNAs (miRNAs) are small non-coding RNAs that can regulate gene expression and have been shown to play a role in various pathologies, including inflammation and cancer. miRNAs interact with Argonaute (Ago) and other proteins to form RNA-induced silencing complexes (RISCs), and guide these RISCs to 3′ UTRs of target RNAs via sequence-specific binding (Bartel, 2009; Fabian et al., 2010). This results in the destabilization of the target RNA and inhibition of translation. RNA binding proteins can also interact with 3′ UTRs and regulate gene expression (Filipowicz et al., 2008; Kedde and Agami, 2008). Recently, several groups have obtained evidence that miRNAs and RNA binding proteins can co-operate at common

 © 2016 The Author(s).
This is an open access article under the CC BY-NC-ND license (http://creativecommons.org/licenses/by-nc-nd/4.0/).

target 3′ UTRs under certain conditions (Bhattacharyya et al., 2006; Ray et al., 2009).

Mex-3B, a member of the Mex-3 family, contains two K homology (KH)-type RNA-recognition domains and a RING finger domain (Buchet-Poyau et al., 2007). It has been shown that these family members associate with specific mRNAs and regulate expression of their proteins (Cano et al., 2012; Donnini et al., 2004; Pereira et al., 2013). Mex-3D (also known as TINO or RKHD1) has been shown to destabilize *BCL2* mRNA by binding to an AU-rich element in its 3′ UTR (Donnini et al., 2004). Mex-3C regulates HLA-A2 levels through its mRNA 3′ UTR (Cano et al., 2012). Mex-3A has been shown to repress CDX2 expression post-transcriptionally through binding to the CDX2 3′ UTR (Pereira et al., 2013). *Mex3b*-deficient mice exhibit defects in Sertoli cells and have low fertility (Le Borgne et al., 2014). However, the physiological role of post-transcriptional regulation of target genes by Mex-3B has not been elucidated.

In this study, we generated *Mex3b*$^{-/-}$ mice and used them in an experimental model of allergic airway inflammation. We show that *Mex3b*$^{-/-}$ mice develop significantly less airway inflammation, due to reduced induction of IL-33. We also demonstrate that Mex-3B binds to the IL-33 3′ UTR and upregulates IL-33 expression by inhibiting miR-487b-3p-mediated repression of IL-33. Furthermore, we show that inhalation of a locked nucleic acid (LNA)-modified antisense oligonucleotide targeting Mex-3B (LNA-anti-Mex-3B) suppresses the development of allergic airway inflammation.

RESULTS

Mice Deficient in *Mex3b* Have Normal Phenotype

To gain insight into Mex-3B function in vivo, we generated *Mex3b*$^{-/-}$ mice through homologous recombination in mouse embryonic stem cells (Figures S1A–S1E). Homozygous *Mex3b* mutant animals were born in a Mendelian ratio (~25% of progeny), showing no evidence of embryonic lethality. *Mex3b*$^{-/-}$ newborns were indistinguishable from wild-type littermates except that they were smaller and had reduced body weight (Figure S1F). Consistent with a previous report (Le Borgne et al., 2014), *Mex3b*$^{-/-}$ mice were fertile, but fertility is low. Macroscopic and histological examination did not reveal any morphological abnormalities in the major organs of young adult mice. In addition, *Mex3b*$^{-/-}$ mice showed no detectable abnormalities in the development of B cells in the spleen or T cells in the thymus (Figure S1G).

Mex-3B Is Required for the Ovalbumin-Induced Allergic Airway Inflammation

It has previously been reported that Mex-3B is relatively highly expressed in human lung and thymus (Buchet-Poyau et al., 2007). Consistent with these results, we found that Mex-3B is also highly expressed in mouse lung and thymus (Y.Y., unpublished data). We therefore speculated that Mex-3B could play a role in the immune system in the lung. We examined this possibility using an experimental model of allergic airway inflammation (Figure 1A). Mice were sensitized with ovalbumin (OVA)/alum and then challenged with nebulized OVA or PBS. Compared to wild-type mice, *Mex3b*$^{-/-}$ mice exhibited decreased lung leukocytic infiltration and mucus secretion (Figure 1B) and decreased numbers of bronchoalveolar lavage (BAL) eosinophils (Figure 1C) in response to OVA challenge. The Th2-type cytokines, IL-4, IL-5, and IL-13, were less efficiently induced in the lungs of *Mex3b*$^{-/-}$ mice (Figure 1D). By contrast, the Th1-type cytokine interferon-γ (IFN)-γ was induced normally. We also examined the number of Th2 cells in bronchial lymph nodes by measuring intracellular cytokine levels of lung bronchial lymph node cells stimulated ex vivo with leukocyte activation cocktail. We observed decreased percentages of IL-4-positive CD4^{+} cells in primary cultured bronchial lymph node cells from *Mex3b*$^{-/-}$ mice (Figure S2A). These results suggest that Mex-3B is required for the development of allergic airway inflammation.

Th2 cells are known to play critical roles in the pathogenesis of allergic airway inflammation by producing a variety of cytokines such as IL-4, IL-5, IL-9, and IL-13 (Herrick and Bottomly, 2003). In addition to Th2 cells, it has recently been shown that Th1, regulatory T (Treg), and Th17 cells play important roles in allergic airway inflammation (Lloyd and Hessel, 2010). To understand how Mex-3B regulates the induction of allergic airway inflammation, we first examined T cell differentiation in *Mex3b*$^{-/-}$ mice. Effector and regulatory T cells were generated from wild-type and *Mex3b*$^{-/-}$ CD4^{+}CD62L^{+} naive T cells by standard methods. We found that the percentage of each T cell subset generated was very similar regardless of their *Mex3b* status (Figure S2B). Furthermore, we stimulated CD4^{+} T cells with anti-CD3/CD28 antibody in vitro and examined the expression of Mex-3B and the other family members. IFN-γ was used as a marker of T cell activation. We found that stimulation with anti-CD3/CD28 antibody resulted in reduced expression of only Mex-3B (Figure S2C). We next examined antigen-induced immune responses in the spleens. When splenocytes from OVA-sensitized mice were cultured with OVA, similar levels of IL-5 were secreted into the culture media by wild-type and *Mex3b*$^{-/-}$ splenocytes (Figure S2D). These results suggest that immune cell function in the spleen is comparable between wild-type and *Mex3b*$^{-/-}$ mice.

To further clarify the role of Mex-3B in hematopoietic cells, we performed bone marrow transplantation experiments. BAL fluid analysis revealed that *Mex3b*$^{-/-}$ mice transplanted with bone marrow cells from wild-type mice had less inflammation than wild-type mice transplanted with bone marrow cells from *Mex3b*$^{-/-}$ mice (Figures S2E and S2F). These results exclude the possibility that Mex-3B in hematopoietic cells plays a critical role in the development of allergic airway inflammation.

IL-33 Induction Is Suppressed in *Mex3b*-Deficient Mice

Recent studies have shown that airway epithelial cells play critical roles in the regulation of airway inflammation: airway epithelial cells influence the function of immune-competent cells, such as dendritic cells (Hammad and Lambrecht, 2008), mast cells (Allakhverdi et al., 2007), and Th2 cells (Wang et al., 2007) by producing many inflammatory factors in response to allergen exposure. We therefore examined the expression of Mex-3B in lung tissues from control and OVA-challenged mice. We separated airway epithelial and non-epithelial cells using anti-CD45 antibody and performed qRT-PCR analysis. IL-13 and SP-C were used as markers of inflammation and airway epithelial cells,

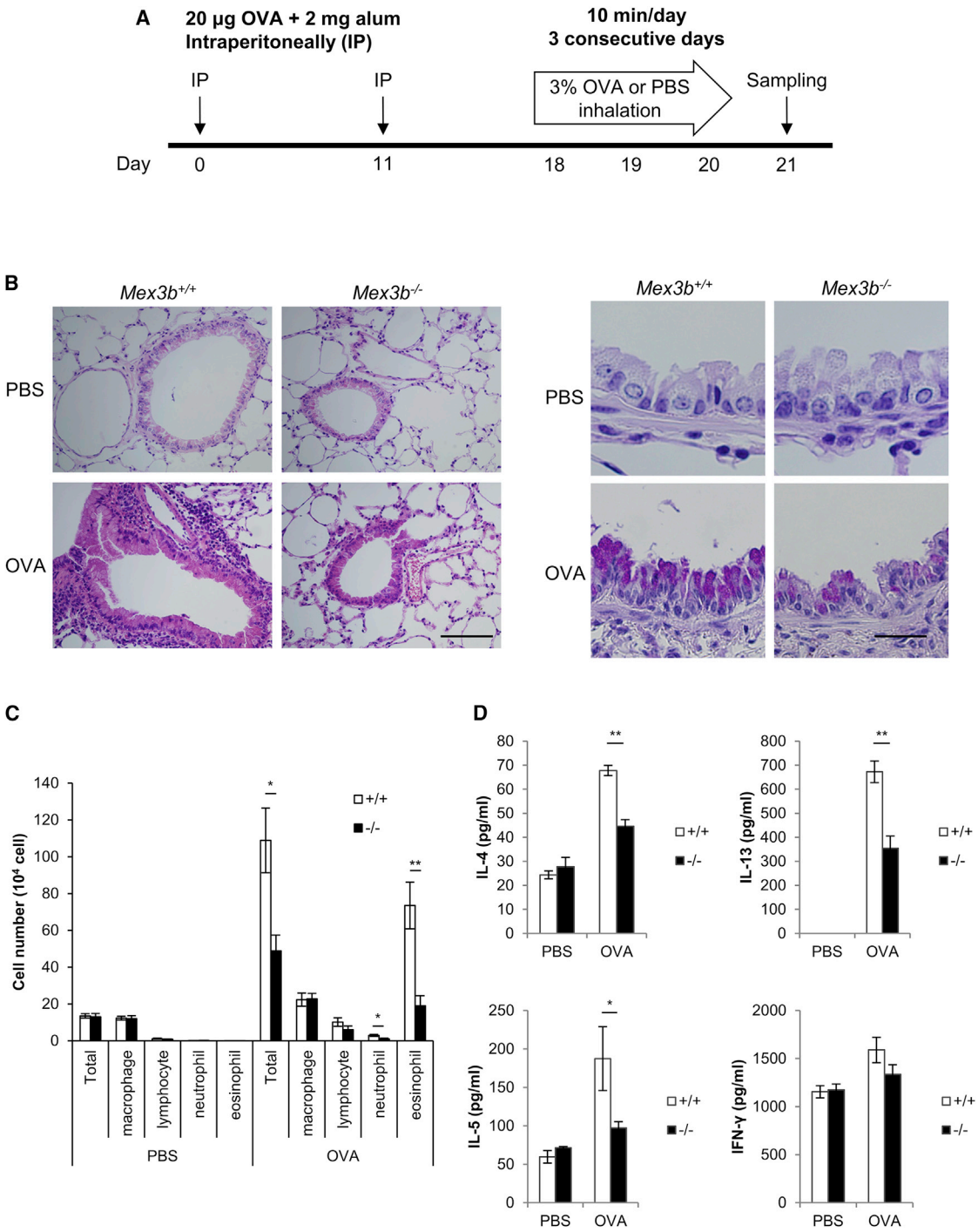

Figure 1. Mex-3B Is Critical for the Development of Airway Inflammation

(A) Scheme of the experimental asthma model. *Mex3b*$^{+/+}$ and *Mex3b*$^{-/-}$ mice were sensitized with OVA/alum on days 0 and 11. The mice were nebulized with OVA or PBS from day 18 to 20 and analyzed on day 21.

(B) OVA-induced infiltration of eosinophils into the peribronchial area and mucus hypersecretion by bronchial epithelial cells. (left) H&E staining. Scale bar, 100 μm. (right) Periodic acid-Schiff staining. Scale bar, 15 μm.

(C) Bronchoalveolar lavage (BAL) fluid analyses were performed. Leukocytes were identified by morphological criteria.

(D) Cytokine concentrations in the lungs of OVA-challenged or control mice. Lung homogenates were assayed for cytokine concentrations by ELISA. Data are represented as mean ± SEM (n = 3–7). *$p < 0.05$, **$p < 0.01$.

See also Figures S1–S3.

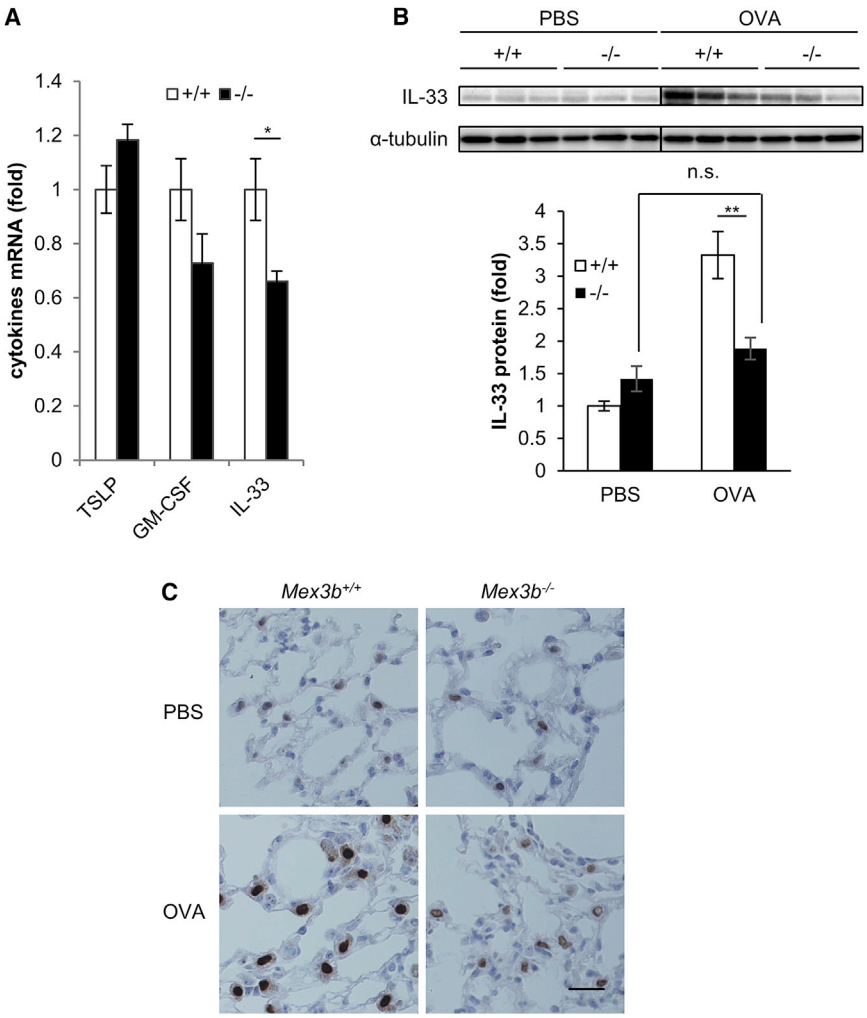

Figure 2. Mex-3B Is Required for the Induction of IL-33 Expression in the Development of Allergic Airway Inflammation

(A) The levels of inflammatory factor mRNAs in OVA-inflamed lungs of *Mex3b*$^{+/+}$ and *Mex3b*$^{-/-}$ mice.

(B) Immunoblot analysis of IL-33 protein in control or OVA-inflamed lungs.

(C) Lung sections were stained with anti-IL-33 antibody and counterstained with hematoxylin. Scale bar, 20 μm. Data are represented as mean ± SEM (n = 3–7). *p < 0.05, **p < 0.01.

See also Figure S4.

respectively. We found that Mex-3B was expressed in both airway epithelial and non-epithelial cells at similar levels and was upregulated by OVA challenge (Figure S3). We also found that the other Mex family genes, Mex-3A, -3C, and -3D, were highly expressed in airway epithelial cells compared with non-epithelial cells, and that only Mex-3A was upregulated by OVA challenge in airway epithelial cells. These results suggest that Mex-3B plays a role in airway epithelial cells in the development of allergic airway inflammation.

To investigate the role of Mex-3B in inflammatory factor production from airway epithelial cells, we examined the mRNA levels of epithelial cell-derived inflammatory factors in the lung tissues of OVA-challenged wild-type and *Mex3b*$^{-/-}$ mice. Among the inflammatory factors examined, IL-33 and GM-CSF mRNAs were found to be less efficiently induced in *Mex3b*$^{-/-}$ compared to wild-type lung (Figure 2A). Similarly, IL-33 protein was not significantly induced in the inflamed lungs of *Mex3b*$^{-/-}$ mice compared with wild-type mice (Figure 2B). In agreement with a previous report (Louten et al., 2011), immunostaining with anti-IL-33 antibody revealed that IL-33 was localized to the nuclei of alveolar epithelial cells of both wild-type and *Mex3b*$^{-/-}$ mice (Figure 2C). Following OVA challenge, we detected strong expression of IL-33 in the nuclei of alveolar epithelial cells from wild-type, but not *Mex3b*$^{-/-}$ mice (Figure 2C). By contrast, IL-33 was induced to similar levels in the cytoplasm of alveolar macrophages from either wild-type or *Mex3b*$^{-/-}$ mice (Figure S4A). Furthermore, the levels of IL-33 mRNA induced by LPS in OVA-sensitized or unsensitized alveolar macrophages were similar in wild-type and *Mex3b*$^{-/-}$ mice (Figure S4B). These results suggest that Mex-3B is required for the inflammation-induced upregulation of IL-33 in alveolar epithelial cells.

Mex-3B Deficiency Does Not Significantly Affect IL-33-Induced Airway Inflammation

IL-33 is a central player in the development of allergic inflammation. IL-33 stimulates Th2 cells (Schmitz et al., 2005), mast cells (Iikura et al., 2007), and natural helper cells (Moro et al., 2010). To clarify whether decreased IL-33 production in *Mex3b*$^{-/-}$ mice is responsible for the impaired development of airway inflammation, we examined the effects of intranasal administration of IL-33 on lung inflammation in wild-type and *Mex3b*$^{-/-}$ mice (Figure S4C). Administration of IL-33 for 4 consecutive days resulted in airway inflammation in both wild-type and *Mex3b*$^{-/-}$ mice, similar to that reported by Kondo et al. (2008), and was manifested by an increase in the numbers of eosinophils (Figure S4D), induction of Th2 cytokines (Figure S4E), and epithelial thickening and leukocytic infiltration (Figure S4F). Thus, in contrast to OVA-induced airway inflammation, IL-33-induced inflammation is not affected by *Mex3b* status. These results suggest that *Mex3b*$^{-/-}$ mice develop less airway inflammation than wild-type littermates due to reduced induction of IL-33.

Mex-3B Promotes IL-33 Expression Post-transcriptionally

We next investigated the mechanisms by which Mex-3B induces IL-33 expression using the transformed murine respiratory

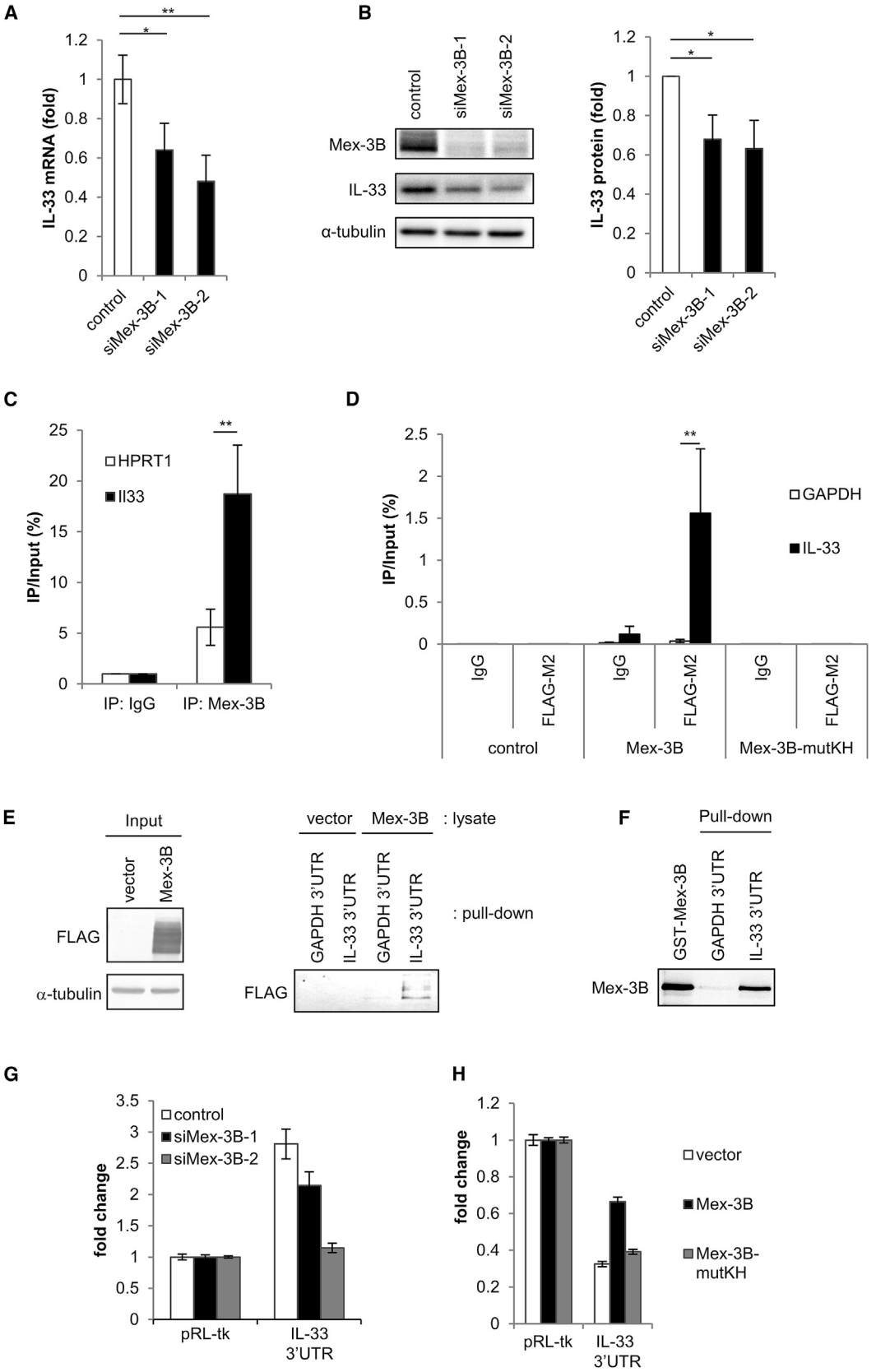

(legend on next page)

epithelial cell-derived cell line MLE-15 (Wikenheiser et al., 1993). We first examined whether IL-33 expression in MLE-15 cells is also regulated by Mex-3B. We found that knockdown of Mex-3B by small interfering RNA (siRNA) caused a decrease in both IL-33 mRNA and protein expression (Figures 3A and 3B). We therefore set out to examine whether Mex-3B directly regulates IL-33 expression using MLE-15 cells.

Since Mex-3B is a KH-type RNA binding protein, we investigated whether Mex-3B is associated with the IL-33 mRNA. We performed RNA immunoprecipitation assays: lysates prepared from MLE-15 cells were subjected to immunoprecipitation with anti-Mex-3B antibody and the IL-33 mRNA associated with the immunoprecipitates was detected by qRT-PCR analysis. We found that Mex-3B is associated with IL-33 mRNA, but not significantly with HPRT1 mRNA (Figure 3C). To examine the role of the KH domain in Mex-3B binding to IL-33 mRNA, we transfected FLAG-tagged wild-type or KH domain mutant Mex-3B into the alveolar epithelial cell-derived adenocarcinoma cell line A549 (Lieber et al., 1976) and performed RNA immunoprecipitation assays. We found that Mex-3B is associated with IL-33 mRNA, but not with GAPDH mRNA (Figure 3D). By contrast, we found that Mex-3B-mutKH did not co-precipitate with the IL-33 mRNA. Mex-3B-mutKH is mutated in key residues involved in RNA binding, i.e., Gly-83 and Gly-177 in the KH domains, which are replaced with Asp. Thus, Mex-3B may associate with the IL-33 mRNA through its KH domains.

An array of RNA binding proteins recognizes the 3′ UTR of target genes and exerts post-transcriptional control (Khabar, 2010). To examine whether Mex-3B binds to the IL-33 3′ UTR, we performed RNA binding protein pull-down assays. Lysates prepared from A549 cells transfected with FLAG-tagged Mex-3B were incubated with biotin-labeled IL-33 3′ UTR and subjected to precipitation with streptavidin-Dynabeads. Immunoblotting with anti-FLAG antibody revealed that Mex-3B co-precipitated with the IL-33 3′ UTR, but not with the GAPDH 3′ UTR (Figure 3E). Furthermore, we produced recombinant Mex-3B fused to glutathione *S*-transferase (GST-Mex-3B) (Figure S5) and examined its ability to interact directly with the IL-33 3′ UTR by RNA binding protein pull-down assays. Immunoblotting of the precipitates with anti-Mex-3B antibody revealed that GST-Mex-3B directly binds to the IL-33 3′ UTR (Figure 3F).

To clarify the significance of the association of Mex-3B with the IL-33 3′ UTR, we constructed a reporter vector containing the IL-33 3′ UTR region fused downstream of the luciferase gene. We found that knockdown of Mex-3B by siRNA caused a decrease in luciferase activity in MLE-15 cells (Figure 3G). Furthermore, we found that overexpression of Mex-3B, but not of Mex-3B-mutKH resulted in the enhancement of reporter activity in A549 cells (Figure 3H). These results suggest that Mex-3B post-transcriptionally activates IL-33 expression through binding to the IL-33 3′ UTR.

Identification of a Mex-3B-Responsive Region in the IL-33 3′ UTR

We next investigated which region of the IL-33 3′ UTR (region 1–12 in Figures S6A–S6D) is involved in Mex-3B-mediated upregulation of IL-33. We found that luciferase reporters containing region 9 [3′ UTR-9 (nucleotides 1414–1674)] were significantly upregulated by Mex-3B (Figure S6C). Furthermore, RNA binding protein pull-down assays revealed that Mex-3B binds 3′ UTR-9 (Figure S6D). These results suggest that Mex-3B regulates IL-33 expression through binding to 3′ UTR-9.

Mex-3B Promotes IL-33 Expression by Inhibiting miR-487b-3p-Mediated Repression

It has been shown that miRNAs suppress the expression of target genes by binding to their 3′ UTRs (Bartel, 2009). We therefore speculated that the Mex-3B-mediated regulation of IL-33 expression via the 3′ UTR might involve an miRNA species. We therefore searched for potential miRNA binding sites in 3′ UTR-9 using the microRNA.org database (John et al., 2004) and identified seven candidate sites (Figure 4A). Among these miRNAs, overexpression of miR-487b-3p most significantly suppressed IL-33 mRNA and protein expression in MLE-15 cells (Figures 4B and 4C). Overexpression of miR-487b-3p also resulted in a decrease in the activity of the luciferase reporters containing either the entire 3′ UTR or 3′ UTR-9 (Figure 4D). By contrast, overexpression of miR-487b-3p did not inhibit the activity of a luciferase reporter containing a mutated miR-487b-3p binding site (3′ UTR-9-mt487b in Figures 4E and 4F). In addition, this mutant reporter showed enhanced activity in the absence of Mex-3B. These results suggest that miR-487b-3p directly regulates IL-33 expression.

We next examined the significance of miR-487b-3p in Mex-3B-mediated upregulation of IL-33. We found that knockdown of miR-487b-3p by a locked nucleic-acid-modified antisense oligonucleotide (LNA-anti-miR487b-3p) (Ørom et al., 2006)

Figure 3. Mex-3B Post-transcriptionally Upregulates IL-33 Expression in the Alveolar Epithelial Cells

(A and B) Effects of Mex-3B knockdown on IL-33 mRNA (A) and protein (B) expression in MLE-15 cells.

(C) qRT-PCR analysis of IL-33 mRNA co-immunoprecipitated with rabbit immunoglobulin G (IgG) or anti-Mex-3B antibody in MLE-15 cells. HPRT1 mRNA was used as a negative control.

(D) qRT-PCR analysis of IL-33 mRNA co-immunoprecipitated with mouse IgG or anti-FLAG-M2 antibody in A549 cells, transfected with control vector, FLAG-tagged Mex-3B or FLAG-tagged Mex-3B-mutKH. GAPDH mRNA was used as a negative control.

(E) Immunoblot analysis of exogenously expressed FLAG-tagged Mex-3B protein co-precipitated with the indicated in vitro transcribed biotin-labeled RNAs. (left) Input. (right) Mex-3B pulled-down with biotin-labeled RNAs. GAPDH 3′ UTR was used as a negative control.

(F) Immunoblot analysis of GST-Mex-3B co-precipitated with the indicated in vitro transcribed biotin-labeled RNAs. GAPDH 3′ UTR was used as a negative control.

(G) Luciferase activity of Mex-3B-knockdowned MLE-15 cells transfected with a luciferase reporter fused to the IL-33 3′ UTR.

(H) Luciferase activity of A549 cells transfected with a luciferase reporter fused to the IL-33 3′ UTR along with control vector, FLAG-tagged Mex-3B or FLAG-tagged Mex-3B-mutKH. Data are represented as mean ± SD (n = 3). *$p < 0.05$, **$p < 0.01$.

See also Figure S5.

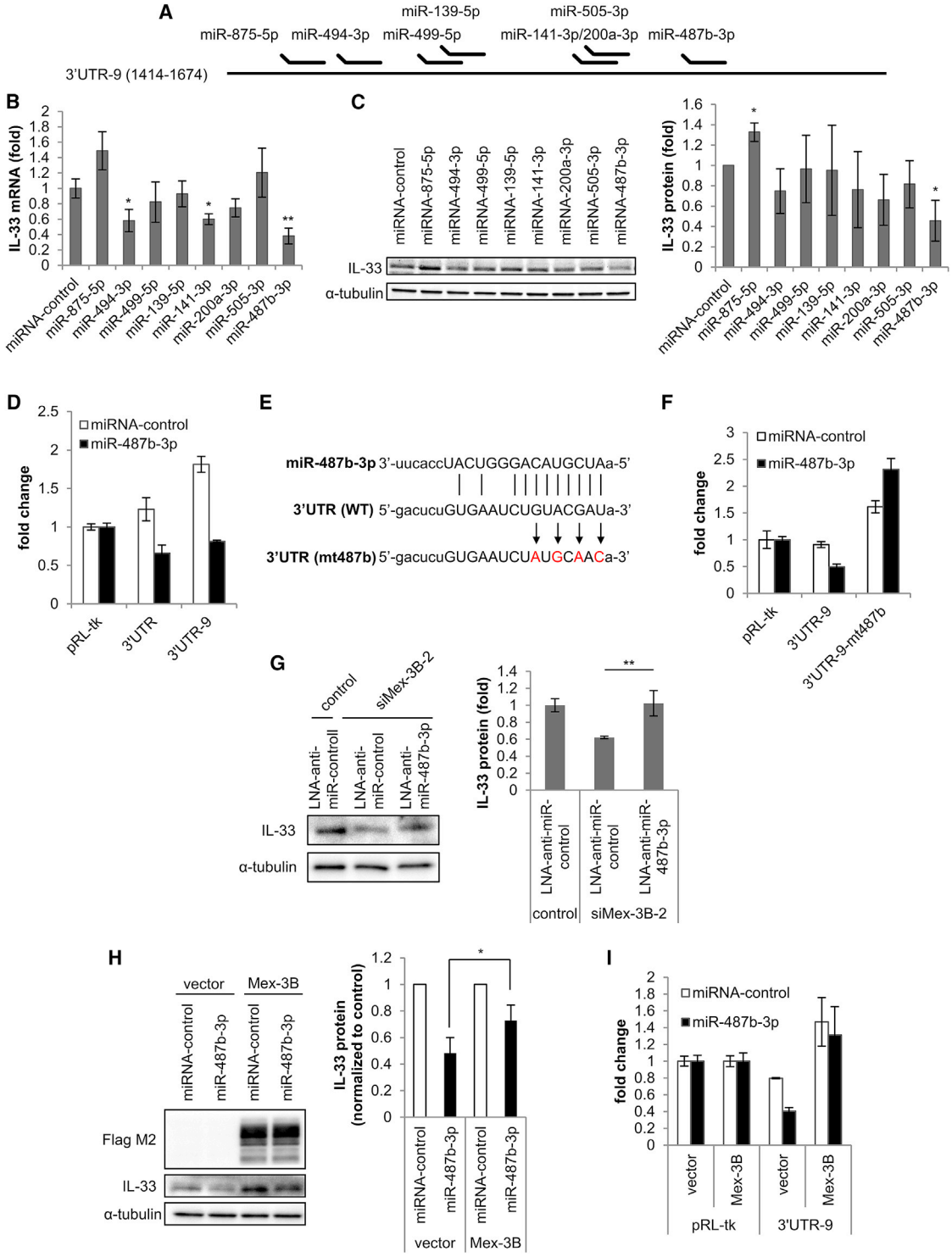

Figure 4. Mex-3B Inhibits the Effect of miR-487b-3p on the IL-33 3′ UTR

(A) Target sites of conserved miRNAs in IL-33 3′ UTR-9 predicted by mirSVR score (http://www.microRNA.org).

(B and C) Effect of miRNA overexpression on IL-33 mRNA (B) and protein (C) expression in MLE-15 cells.

(D) Luciferase activity of MLE-15 cells transfected with each reporter plasmid along with control miRNA or miR-487b-3p.

(E) Schematic representation of wild-type and mutated 3′ UTR-9 reporters.

(F) Luciferase activity of MLE-15 cells co-transfected with each reporter plasmid along with control miRNA or miR-487b-3p.

(G) Immunoblot analysis of IL-33 in MLE-15 cells transfected with the indicated anti-miRNAs along with the indicated siRNAs.

(legend continued on next page)

resulted in a restoration of IL-33 protein expression in MLE-15 cells in which Mex-3B was knocked down (Figure 4G). In addition, overexpression of Mex-3B restored IL-33 protein expression, as well as the activity of a luciferase reporter containing 3′ UTR-9 in cells in which miR-487b-3p was overexpressed (Figures 4H and 4I). We also found that knockdown of Mex-3B resulted in a decrease in miR-487b-3p expression (Figure S6E). These results suggest that Mex-3B promotes IL-33 expression by inhibiting miR-487b-3p-mediated suppression of IL-33.

Mex-3B Inhibits the Interaction of the miR-487b-3p-Ago2 Complex with the miR-487b-3p Target Site in the IL-33 3′ UTR

RNA binding proteins such as Dnd1 have been shown to inhibit miRNA access to their target mRNAs (Kedde et al., 2007). Thus, it is possible that Mex-3B competes with the miR-487b-3p-RISC complex for binding to the 3′ UTR of IL-33. To examine this possibility, we performed RNA binding protein pull-down assays. When miR-487b-3p was transfected into A549 cells, Ago2 was found to co-precipitate with 3′ UTR-9 (Figure 5A). However, co-transfection of Mex-3B with miR-487b-3p interfered with the co-precipitation of Ago2 and 3′ UTR-9 (Figure 5A). These results suggest that Mex-3B inhibits the interaction of the miR-487b-3p-Ago2 complex with the miR-487b-3p target site in the IL-33 3′ UTR.

We therefore examined whether the Mex-3B binding site overlaps with the miR-487b-3p binding site. However, we found that Mex-3B coprecipitated with a mutated 3′ UTR, 3′ UTR-9-Δseed, in which the miR-487b-3p seed match sequence in 3′ UTR-9 has deleted (Figures 5B and 5C). Thus, Mex-3B may not directly compete with the miR-487b-3p-RISC complex for binding to the 3′ UTR of IL-33 but indirectly inhibits their interaction presumably by changing the RNA secondary structure.

As shown in Figure S6C, we found that Mex-3B activated a luciferase reporter containing 3′ UTR-9, but not 3′ UTR-11 or 3′ UTR-12, which are the 5′ and 3′ halves of 3′ UTR-9, respectively. This may indicate that a region straddling 3′ UTR-11 and 3′ UTR-12 is important for Mex-3B binding. In addition, RNA secondary structure prediction indicated the presence of a stem-loop structure, within which this region is contained. We therefore constructed a mutated 3′ UTR-9, 3′ UTR-9-ΔSL, in which this predicted stem-loop structure (nucleotides 1514–1547) is deleted. Luciferase assays revealed that Mex-3B did not enhance the activity of a reporter containing 3′ UTR-9-ΔSL (Figure 5E). Moreover, RNA binding protein pull-down assays revealed that Mex-3B coprecipitated only weakly with 3′ UTR-9-ΔSL (Figure 5F). We also found that Ago2 coprecipitated only weakly with 3′ UTR-9-ΔSL and that miR-487b-3p did not affect this interaction (Figure 5G). Thus, the region containing nucleotides 1514–1547 is required for the interaction of both Mex-3B and the miR-487b-3p-Ago2 complex with the IL-33 3′ UTR.

miR-487b-3p Is Important for the Development of Allergic Airway Inflammation

To investigate whether miR-487b-3p plays a role in the negative regulation of allergic airway inflammation, LNA-anti-miR-487b-3p was administered into OVA-sensitized wild-type or *Mex3b*$^{-/-}$ mice according to the protocol shown in Figure 6A. Cytological analysis of BAL fluid revealed that nebulization of either LNA-anti-miR-487b-3p or a control LNA antisense oligonucleotide (LNA-anti-miR-control) had no effect on OVA-induced inflammation in wild-type mice (Figure 6B). By contrast, nebulization of LNA-anti-miRNA-487b-3p, but not an LNA-anti-miR-control, caused an increase in eosinophil infiltration in *Mex3b*$^{-/-}$ mice challenged with OVA (Figures 6A and 6B). We also found that nebulization of LNA-anti-miR-487b-3p restored IL-33 protein levels in *Mex3b*$^{-/-}$ mice (Figure 6C). In addition, we confirmed that Alexa-488-labeled LNA-anti-miR-487b-3p administered in a nebulized form accumulated in lung epithelial cells 24 hr after exposure (Figure S7A). These observations are consistent with the notion that miR-487b-3p plays an important role in the downregulation of IL-33 and thereby suppresses airway inflammation.

We performed qRT-PCR analysis to measure the approximate copy numbers of miR-487b-3p and IL-33 RNA per cell in the lung tissues of control and OVA-challenged *Mex3b*$^{+/+}$ and *Mex3b*$^{-/-}$ mice. We used miRNA-505-3p and miRNA-875-5p as controls, which are expressed in MLE-15 cells but do not suppress IL-33 expression. We found that the expression of miR-487b-3p and miR-875-5p was lower than that of IL-33 mRNA, while the expression of miR-505-3p was similar to that of IL-33 mRNA (Figure S7B). In addition, we observed that the expression of miR-487b-3p was similar between control and OVA-challenged mice. These results suggest that the suppression of IL-33 expression observed in OVA-challenged mice is not simply the result of altered expression of miR-487b-3p.

LNA Antisense Oligonucleotide-Mediated Knockdown of Mex-3B Suppresses Allergic Airway Inflammation

We finally investigated whether administration of an LNA antisense oligonucleotide targeting Mex-3B (LNA-anti-Mex-3B) could suppress the development of allergic airway inflammation. We confirmed that overexpression of LNA-anti-Mex-3B resulted in a decrease in the levels of Mex-3B and IL-33 in MLE-15 cells (Figure 7A). When LNA-anti-Mex-3B was administered into OVA-sensitized wild-type mice according to the protocol shown in Figure 7B, eosinophil infiltration was significantly inhibited (Figure 7C). Immunostaining with anti-IL-33 antibody revealed that LNA-anti-Mex-3B nebulization caused a decrease in the number of cells that were strongly positive for IL-33 (Figure 7D). These results suggest that suppression of Mex-3B expression using LNA antisense oligonucleotides suppresses allergic airway inflammation.

(H) Immunoblot analysis of IL-33 in MLE-15 cells transfected with the indicated miRNAs along with control vector or FLAG-tagged Mex-3B.
(I) Luciferase activity of MLE-15 cells co-transfected with each reporter plasmid and vector or FLAG-tagged Mex-3B along with control miRNA or miR-487b-3p. Data are represented as mean ± SD (n = 3). *$p < 0.05$, **$p < 0.01$.
See also Figure S6.

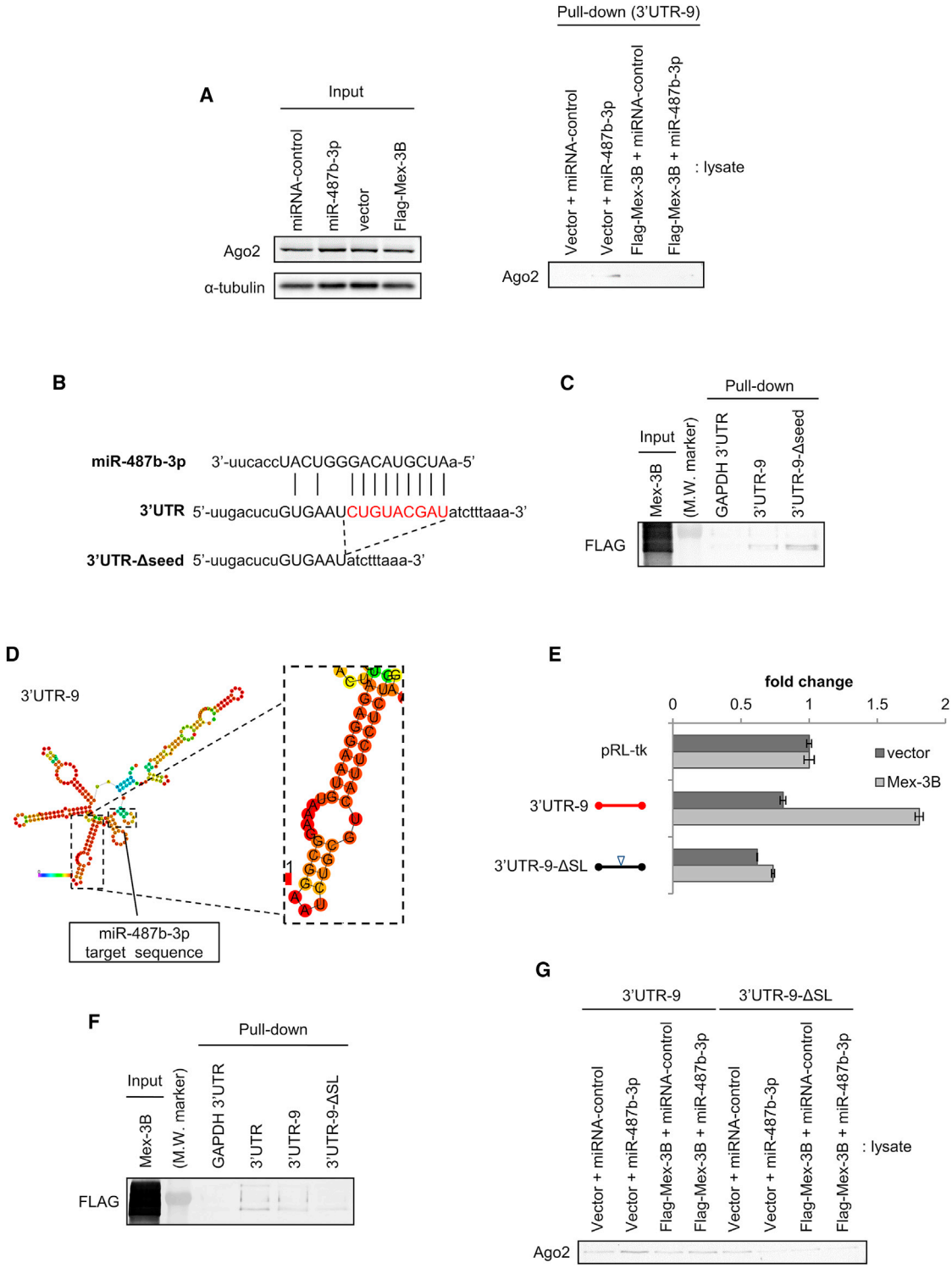

Figure 5. Mex-3B Inhibits the Interaction of the miR-487b-3p-Ago2 Complex with Its miR-487b-3p Target Site in the IL-33 3′ UTR

(A) Immunoblot analysis of Ago2 protein co-precipitated with the in vitro transcribed biotin-labeled 3′ UTR-9. Cell lysates mixed at 1:1 ratio as indicated were used in this assay. (left) Input. (right) Ago2 pulled down with biotin-labeled RNA.

(B) Schematic representation of wild-type and mutated 3′ UTR-9-Δseed reporters.

(C) Immunoblot analysis of exogenously expressed FLAG-tagged Mex-3B protein co-precipitated with the indicated in vitro transcribed biotin-labeled RNAs. GAPDH 3′ UTR was used as a negative control.

(legend continued on next page)

DISCUSSION

Post-transcriptional control of mRNAs encoding pro-inflammatory molecules by RNA binding proteins is considered to be a key determinant of many immunological responses (Kafasla et al., 2014). In the present study, we generated *Mex3b*$^{-/-}$ mice and found that the RNA binding protein Mex-3B plays an essential role in the development of allergic airway inflammation. *Mex3b*$^{-/-}$ mice had fewer inflammatory cell infiltrates and bronchovascular bundles as well as lower mucin production in pulmonary tissues compared to wild-type controls. Furthermore, Th2 cytokines such as IL-4, IL-5, and IL-13 were induced less efficiently in *Mex3b*$^{-/-}$ mice. Although the expression of Mex-3B in CD4^{+} T cells was suppressed by stimulation with anti-CD3/CD28 antibody in vitro, our bone marrow transplantation experiments suggest that the functions of Mex-3B in hematopoietic cells are not crucial for the development of allergic airway inflammation. Additionally, we observed that Mex-3B is upregulated in airway epithelial cells, but not in non-epithelial cells during the development of allergic airway inflammation. We therefore focused on inflammatory factors produced by airway epithelial cells and found that IL-33 induction is suppressed in *Mex3b*$^{-/-}$ mice. Furthermore, we showed that Mex-3B directly binds to the 3′ UTR of IL-33 and post-transcriptionally activates its expression. Thus, our results suggest that Mex-3B plays an important role in the development of airway inflammation by inducing IL-33, a cytokine required for the initiation of allergic airway inflammation.

Consistent with this notion, the degree of airway inflammation in *Mex3b*$^{-/-}$ mice provoked by intranasal administration of recombinant IL-33 was comparable to that in wild-type mice. In particular, we note that although several studies have shown that Th2 cytokines are post-transcriptionally regulated by RNA binding proteins such as HuR (Casolaro et al., 2008; Yarovinsky et al., 2006), the levels of Th2 cytokines induced by the administration of IL-33 in *Mex3b*$^{-/-}$ mice were comparable to those seen in wild-type mice. Thus, the effect of Mex-3B on Th2 cytokine expression appears to be indirect.

It has been shown that miRNAs play important roles in the development of allergic airway inflammation (Simpson et al., 2014). For example, it has been reported that miR-155 is overexpressed in the nasal mucosa of patients with allergic rhinitis and the skin of patients with atopic dermatitis (Suojalehto et al., 2013). It has also been shown that miR-155 deficiency abolishes allergic airway inflammation (Malmhäll et al., 2014). In this study, we found that miR-487b-3p directly suppresses IL-33 expression and that Mex-3B upregulates IL-33 by inhibiting the function of miR-487b-3p. Consistent with our results, it has recently been reported that miR-487b-3p negatively regulates macrophage activation by targeting IL-33 production (Xiang et al., 2016). Furthermore, we showed that inhalation of anti-miR-487b-3p restores IL-33 expression and causes airway inflammation in *Mex3b*$^{-/-}$ mice.

We found that the expression levels of miR-487b-3p are similar between control mice and OVA-challenged wild-type and *Mex3b*$^{-/-}$ mice. Thus, the suppression of IL-33 expression observed in OVA-challenged mice may be not be the simple result of altered expression of miR-487b-3p. Since the expression of Mex-3B is also not altered, activation of Mex-3B, presumably by modification and/or association with other proteins, may play an important role in the upregulation of IL-33 in OVA-challenged mice. Consistent with our results, it has recently been reported that miRNA-mediated mRNA repression in vivo does not necessarily require an alteration in specific miRNA expression (La Rocca et al., 2015) but may also be caused by alterations in the RISC assembly in response to intracellular signaling. Thus, it is possible that upregulation of IL-33 is induced by alterations in RISC assembly in OVA-challenged wild-type mice.

We showed that Mex-3B inhibits the interaction of the miR-487b-3p-Ago2 complex with the miR-487b-3p target site in the IL-33 3′ UTR. However, this inhibition may be indirect, since we found that the Mex-3B- and miR-487b-3p binding sites do not overlap. We therefore speculate that Mex-3B may induce a change in the IL-33 3′ UTR secondary structure that inhibits access of the miR-487b-3p-RISC complex. In line with this notion, it has been reported that the RNA binding protein Pumilio 1 (Pum 1) binds to the 3′ UTR of the p27 mRNA and induces a change in its secondary structure, which exposes miRNA target sites and promotes miRNA-mediated translational repression (Kedde et al., 2010). In addition, we found that Mex-3B binds only weakly to 3′ UTR-9-ΔSL, a mutant lacking a predicted stem-loop structure close to the miR-487b-3p binding site in the IL-33 3′ UTR. However, this result does not tell us whether the stem-loop structure itself is important for Mex-3B binding: it is also possible that this deletion simply removes a conventional binding sequence for Mex-3B. It is further possible that deletion of the stem-loop structure induces a change in mRNA secondary structure that is not favorable for Mex-3B binding. We also observed that the miR-487b-3p-RISC complex binds poorly to 3′ UTR-9-ΔSL, which could be similarly explained by a change in mRNA secondary structure. Further study is needed to determine the detailed regulatory mechanisms underlying Mex-3B-mediated upregulation of IL-33.

It has recently been reported that the expression levels of miRNAs can be regulated by their target mRNAs (Ameres et al., 2010; de la Mata et al., 2015). These reports show that target mRNAs accelerate the decay rate of miRNAs. Consistent with these reports, we found that knockdown of Mex-3B results in a decrease in miR-487b-3p expression. Our results suggest that, in the absence of Mex-3B, miR-487b-3p targets IL-33, and IL-33 may, in turn, accelerate the decay rate of miR-487b-3p.

(D) Predicted secondary structure of 3′ UTR-9. A characteristic stem-loop structure is enlarged in the right panel. The miR-487b-3p target site is also indicated.
(E) Luciferase activity of A549 cells transfected with the indicated reporter plasmid along with control vector or FLAG-tagged Mex-3B.
(F) Immunoblot analysis of exogenously expressed FLAG-tagged Mex-3B protein co-precipitated with the indicated in vitro transcribed biotin-labeled RNAs. GAPDH 3′ UTR was used as a negative control.
(G) Immunoblot analysis of Ago2 co-precipitated with the indicated in vitro transcribed biotin-labeled RNAs. Cell lysates mixed at 1:1 ratio as indicated were used in this assay. Data are represented as mean ± SD (n = 3).

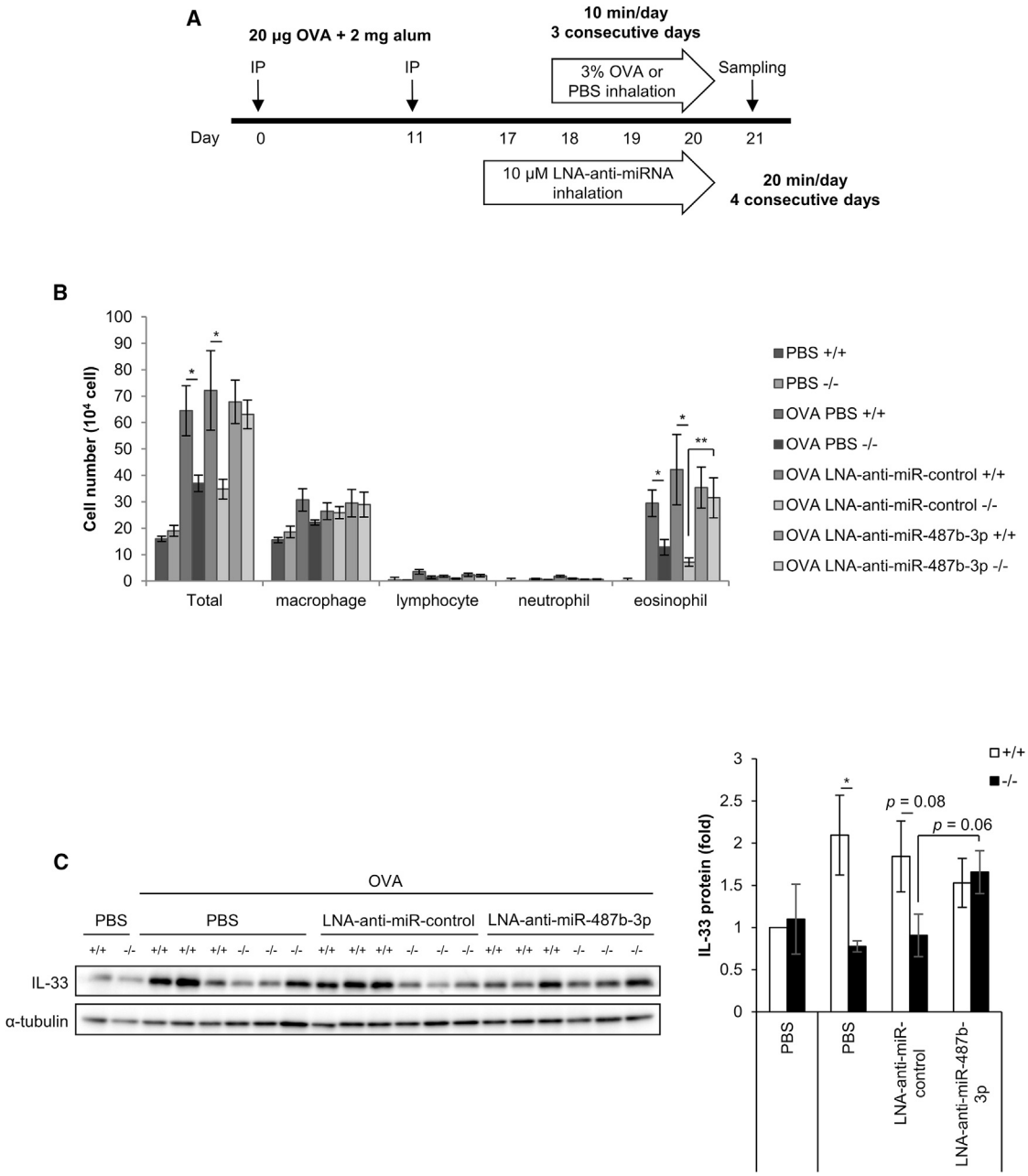

Figure 6. miR-487b-3p Is Important for the Development of Allergic Airway Inflammation

(A) Protocol for the administration of anti-miR-487b-3p into OVA-sensitized *Mex3b*$^{+/+}$ and *Mex3b*$^{-/-}$ mice.

(B) Bronchoalveolar lavage (BAL) fluid analyses. Leukocytes were identified by morphologic criteria.

(C) Immunoblot analysis of IL-33 protein in lungs. Data are represented as mean ± SEM (n = 3–7). *$p < 0.05$, **$p < 0.01$.

See also Figure S7.

Antisense oligonucleotides have been shown to be useful for the treatment of various diseases, including cancer and viral, inflammatory, and neurodegenerative diseases (Evers et al., 2015; Lindow and Kauppinen, 2012). For instance, simultaneous administration of two modified phosphorothioate antisense oligonucleotides targeting CCR3 and CCR4 (ASM8) has been shown to efficiently inhibit allergen-induced eosinophilia and airway dysfunction in sensitized rats and human asthmatics (Allakhverdi et al., 2006). These reagents are currently being evaluated in phase II clinical trials of asthma (Pharmaxis, 2012). We have also found that nebulized administration of an antisense oligonucleotide targeting Mex-3B (LNA-anti-Mex-3B) suppresses the development of allergic airway inflammation. In our experiments, we used LNA antisense

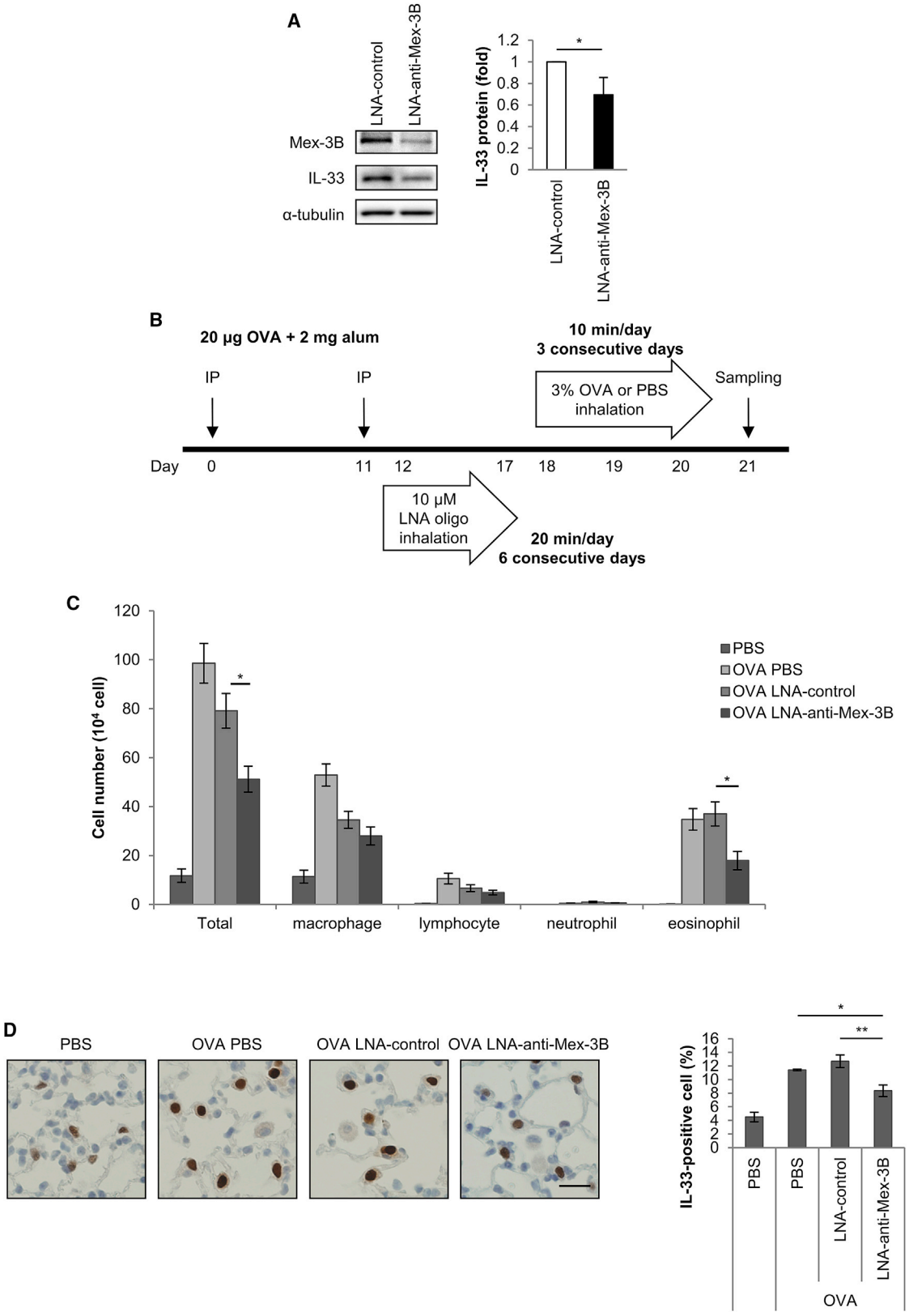

(legend on next page)

oligonucleotides, which contain an engineered O2′ to C4′ linkage within the ribose sugar and have markedly high target mRNA binding affinity and tissue stability (Lundin et al., 2015). We speculate that LNA-anti-Mex-3B could hold promise as a novel anti-asthma reagent. In particular, LNA-anti-Mex-3B could be effective against severe steroid-resistant asthma, a disease in which IL-33 plays an important role by promoting airway remodeling (Saglani et al., 2013).

Accumulating evidence indicates that IL-33 also plays critical roles in the development of various other inflammatory diseases, including chronic obstructive pulmonary disease (COPD) (Byers et al., 2013), inflammatory bowel diseases (Nunes et al., 2014), and atopic dermatitis (Kim and Artis, 2015). It would therefore be interesting to examine whether Mex-3B is involved in these inflammatory diseases and whether LNA-anti-Mex-3B is effective against them.

In conclusion, we showed that Mex-3B-mediated upregulation of IL-33 is critical for the development of allergic airway inflammation. We further showed that Mex-3B upregulates IL-33 by inhibiting miR-487b-3p-mediated repression of IL-33. Our results suggest that LNA-anti-Mex-3B could be useful for the treatment of inflammatory diseases in which the Mex-3B-IL-33 axis plays critical roles.

EXPERIMENTAL PROCEDURES

Mex3b$^{-/-}$ Mice

To construct the Mex-3B targeting vector, exon 1-2 of the *Mex3b* gene was replaced with a neomycin-resistant gene cassette using the bacterial artificial chromosome system (Yang and Seed, 2003). BALB/c embryonic stem cells were electroporated with the linearized Mex-3B targeting vector. G418-resistant clones were screened for homologous recombination by fluorescent in situ hybridization and PCR. *Mex3b*$^{+/-}$ mice were intercrossed to generate *Mex3b*$^{-/-}$ mice. All mice were housed under specific pathogen-free conditions at the Institute of Molecular and Cellular Biosciences, and animal care and experimental procedures were performed in accordance with the guidelines established by the Office for Life Science Research Ethics and Safety of the University of Tokyo.

In Vivo Treatment of Mice

For the OVA-induced model of allergic airway inflammation, mice were immunized as reported previously (Nakagome et al., 2009). For treatment with LNA-anti-miR-487b-3p, mice were exposed to LNA-control or LNA-anti-miR-487b-3p in PBS for 20 min on days 17–20. For treatment with LNA-anti-Mex-3B, mice were exposed to LNA-control or LNA-anti-Mex-3B in PBS for 20 min on days 12–17. Twenty-four hours after the final treatment, samples of BAL fluid and lungs were obtained for examination of the BAL cell profiles and lung histology. After centrifugation, BAL cells were resuspended in PBS and counted with a hemocytometer. A portion of each right lung was lysed in Trisure (Bioline) for qRT-PCR analysis or in RIPA-T buffer (50 mM Tris-HCl [pH 7.5], 150 mM NaCl, 1% Triton X-100, 0.5% NaDOC, 0.1% SDS) for immunoblotting, respectively. The left lungs were homogenized in 1.0 ml of PBS containing 0.5% Triton X-100 and complete protease inhibitor cocktail (Roche) and used for measurements of cytokine concentrations. Bronchial lymph nodes were also examined. Recombinant IL-33 (Invitrogen) treatment was performed as described previously (Kondo et al., 2008). Then, 24 hr after the final treatment, BAL fluid and lung tissues were harvested.

Histology

Tissues were fixed in 10% neutralized buffered formalin (Nacalai Tesque) and embedded in paraffin. Sections were subjected to H&E or periodic acid-Schiff staining. For immunohistochemical staining of lung tissues, rehydrated antigen-retrieved sections were incubated with anti-IL-33 antibody (AF3636: R&D Systems) and visualized by the avidin-biotin complex method using the chromogen diaminobenzidine (Vector Laboratories). For quantification of IL-33-positive cells, a total of 400 alveolar epithelial cells were counted and cells staining more intensely than the threshold value were counted as IL-33 positive. Results were expressed as the percentage of IL-33-positive cells over the total number of lung epithelial cells. Quantification was performed using automated computerized image analysis (CellSens dimension: Olympus). For immunofluorescence staining, nuclei were stained with DAPI (4′6-diamidino-2-phenylindole; Molecular Probes) and observed by fluorescence microscopy (BZ-X700; KEYENCE).

Cell Culture and Transfection

A549 cells were cultured in complete DMEM (Nissui) supplemented with 10% fetal bovine serum (FBS). MLE-15 cells were cultured in RPMI-1640 medium (Sigma-Aldrich) supplemented with 5% FBS, ITS (5 μg/ml insulin, 5 μg/ml transferrin, 5 μg/ml selenium: Sigma-Aldrich), 10 nM hydrocortisone (Sigma-Aldrich), 10 nM β-estradiol (Sigma-Aldrich), and 10 mM HEPES (GIBCO). Spleen cells were cultured in complete DMEM supplemented with 10% FBS. Alveolar macrophage, bronchial lymph node cells and CD4^{+} T cells were cultured in RPMI-1640 medium supplemented with 10% FBS. Plasmids were transfected into A549 or MLE-15 cells with Lipofectamine LTX (Invitrogen) or Lipofectamine 2000 (Invitrogen), respectively. Small oligonucleotides (siRNAs, miRNAs, and LNA oligonucleotides) were transfected into cells with Lipofectamine RNAiMAX (Invitrogen).

Immunoblotting

Cells were lysed in RIPA-T buffer. Samples were separated by SDS-PAGE and probed with specific antibodies. Antibodies were diluted as follows: anti-Mex-3B antibody (Ab) (Atlas), 1:1,000; anti-FLAG M2 Ab (Sigma-Aldrich), 1:2,000; anti-α-tubulin Ab (Calbiochem), 1:2,000; anti-IL-33 Ab (AF3626: R&D Systems), 1:1,000; anti-Ago2 Ab (Wako Pure Chemicals Industries), 1:500. α-tubulin was used as a loading control.

Oligonucleotide

Stealth siRNA targeting Mex-3B and Negative Control siRNA were purchased from Invitrogen. The sequences of siRNA targeting the mouse *Mex3b* cDNA were CACTCAGCTTTGCTCACAATGGGAA for siRNA-1 and TATGGTTTGTAA TCCGTCACAATCG for siRNA-2. Synthetic miRNAs and *mir*Vana mimic negative control were purchased from Ambion. The LNA oligonucleotides were synthesized as unconjugated and fully phosphorothiolated oligonucleotides (Gene Design). The perfectly matching LNA-anti-miR-487b-3p oligonucleotide: 5′-Atga^{m}C^{m}CcTgTa^{m}CGatT-3′ (uppercase, LNA; lowercase, DNA) was complementary to nucleotides 1–16 in the mature miR-487b-3p sequence. The mismatch control LNA oligonucleotide (LNA-anti-miR-control) was synthesized with the following sequence: 5′-aTga^{m}CTcTaTaTGacT-3′. For immunofluorescence analysis, Alexa 488 was conjugated to the 5′ UTR of LNA-anti-miR-487b-3p. LNA-anti-miR-control or LNA-anti-Mex-3B were synthesized by Exiqon.

Figure 7. Inhalation of Antisense Oligonucleotides Targeting Mex-3B Suppresses Allergic Airway Inflammation

(A) Effect of LNA-anti-Mex-3B on Mex-3B and IL-33 protein in MLE-15 cells.

(B) Protocol for the administration of LNA-anti-Mex-3B into OVA-sensitized wild-type mice.

(C) Bronchoalveolar lavage (BAL) fluid analyses. Leukocytes were identified by morphological criteria.

(D) Lung sections were stained with anti-IL-33 antibody and counterstained with hematoxylin. The numbers of IL-33-positive cells were counted. Scale bar, 20 μm. Data are represented as mean ± SEM (n = 3–7). *$p < 0.05$, **$p < 0.01$.

RNA Immunoprecipitation Assay

MLE-15 cells were lysed in NP-40 buffer (20 mM Tris-HCl [pH 7.5], 150 mM NaCl, 1 mM EDTA, 0.5 mM DTT, 0.5% Nonidet P-40, 120 U/ml RNase inhibitor, protease inhibitor cocktail). A549 cells were transfected with the Mex-3B expression constructs. Twenty-four hours after transfection, cytoplasmic cell extracts were prepared in buffer B (10 mM PIPES [pH 6.8], 300 mM sucrose, 100 mM NaCl, 3 mM $MgCl_2$, 1 mM EGTA, 0.5% Triton X-100, 120 U/ml RNase inhibitor, protease inhibitor cocktail). Immunoprecipitation was performed using Dynabeads protein G (Invitrogen). The beads were washed and bound RNA was eluted from the beads by directly adding Trisure (Bioline), followed by RNA extraction and qRT-PCR.

In Vitro Transcription

Murine IL-33 3′ UTRs were cloned into pBluescript II SK (+) at the KpnI and XhoI sites. These constructs were linearized by digestion with EcoRI and in vitro transcription was performed with the T7 MAXIscript Kit (Ambion). Biotin-labeled RNAs were synthesized in the presence of biotin-labeled dCTP during in vitro transcription. GAPDH 3′ UTR was used as a control.

mRNA Binding Protein Pull-down Assay

A549 cells were transfected with the Mex-3B expression construct. Twenty-four hours after transfection, cells were lysed in IP buffer (10 mM Tris-HCl [pH 7.5], 100 mM NaCl, 2.5 mM $MgCl_2$, 0.5% Triton X-100, 120 U/ml RNase inhibitor, protease inhibitor cocktail). Protein extracts were incubated with 350 ng of biotin-labeled UTRs with 15 μg tRNA in IP buffer for 1 hr at 4°C with constant mixing. The biotin-labeled RNA and associated mRNA binding proteins were incubated with 20 μl of paramagnetic streptavidin Dynabeads (Invitrogen) for 1 hr at 4°C with constant mixing. The beads were washed and associated proteins were solubilized in SDS sample buffer and subjected to immunoblotting to detect Mex-3B. For in vitro mRNA binding protein pull-down assays, GST-Mex-3B was incubated with 1 μg of biotin-labeled UTRs.

Luciferase Reporter Assay

A549 cells were transfected with the luciferase reporter construct along with the Mex-3B expression construct. Twenty-four hours after transfection, cells were lysed and luciferase activities were measured. For siRNA or miRNA experiments, MLE-15 cells were transfected with siRNA or miRNA 24 hr before reporter transfection. Twenty-four hours after reporter transfection, cells were lysed and luciferase activities were measured. Luciferase assays were performed with the Dual-Luciferase Reporter Assay System (Promega).

qRT-PCR

RNA extraction and reverse transcription were performed as described previously (Matsuura et al., 2011). Mouse β-actin, mouse GAPDH, and human GAPDH were used as control genes for normalization. Primers used are listed in Table S1.

Statistics

Statistical analysis was performed by unpaired Student's t test. Differences were considered statistically significant when $p < 0.05$.

SUPPLEMENTAL INFORMATION

Supplemental Information includes Supplemental Experimental Procedures, seven figures, and one table and can be found with this article online at http://dx.doi.org/10.1016/j.celrep.2016.07.062.

AUTHOR CONTRIBUTIONS

Y.Y., T.O., and T.A. conceived the project. Y.Y., Y.S.-S., S.S., Y.K., and K.F. performed experiments. Y.O., T.Y., and H.K. generated *Mex3b*$^{-/-}$ mice. O.S., M.I., K.Y., and M.D. worked on the experimental asthma model. S.N. and S.K. analyzed T cell development. Y.Y. and T.A. wrote the paper.

ACKNOWLEDGMENTS

We are grateful to R. Le Goffic for A549 and MLE-15 cells. We thank K. Watanabe, M. Kobayashi, and A. Miyazawa for genotyping, A. Kamiya and H. Matsuoka for discussion, help, and support, and A. Kawai and Y. Koreeda for technical assistance in generating knockout mouse lines. This work was supported by Grants-in-Aid for Scientific Research on Innovative Areas (Integrative Research on Cancer Microenvironment Network) and Research Program of the Project for Development of Innovative Research on Cancer Therapeutics (P-Direct), Research Program of Innovative Cell Biology by Innovative Technology (Integrated Systems Analysis of Cellular Oncogenic Signaling Networks), Ministry of Education, Culture, Sports, Science and Technology of Japan.

Received: October 20, 2015
Revised: June 20, 2016
Accepted: July 25, 2016
Published: August 18, 2016

REFERENCES

Allakhverdi, Z., Allam, M., Guimond, A., Ferrari, N., Zemzoumi, K., Séguin, R., Paquet, L., and Renzi, P.M. (2006). Multitargeted approach using antisense oligonucleotides for the treatment of asthma. Ann. N Y Acad. Sci. *1082*, 62–73.

Allakhverdi, Z., Comeau, M.R., Jessup, H.K., Yoon, B.R., Brewer, A., Chartier, S., Paquette, N., Ziegler, S.F., Sarfati, M., and Delespesse, G. (2007). Thymic stromal lymphopoietin is released by human epithelial cells in response to microbes, trauma, or inflammation and potently activates mast cells. J. Exp. Med. *204*, 253–258.

Ameres, S.L., Horwich, M.D., Hung, J.H., Xu, J., Ghildiyal, M., Weng, Z., and Zamore, P.D. (2010). Target RNA-directed trimming and tailing of small silencing RNAs. Science *328*, 1534–1539.

Bartel, D.P. (2009). MicroRNAs: target recognition and regulatory functions. Cell *136*, 215–233.

Bhattacharyya, S.N., Habermacher, R., Martine, U., Closs, E.I., and Filipowicz, W. (2006). Relief of microRNA-mediated translational repression in human cells subjected to stress. Cell *125*, 1111–1124.

Buchet-Poyau, K., Courchet, J., Le Hir, H., Séraphin, B., Scoazec, J.Y., Duret, L., Domon-Dell, C., Freund, J.N., and Billaud, M. (2007). Identification and characterization of human Mex-3 proteins, a novel family of evolutionarily conserved RNA-binding proteins differentially localized to processing bodies. Nucleic Acids Res. *35*, 1289–1300.

Byers, D.E., Alexander-Brett, J., Patel, A.C., Agapov, E., Dang-Vu, G., Jin, X., Wu, K., You, Y., Alevy, Y., Girard, J.P., et al. (2013). Long-term IL-33-producing epithelial progenitor cells in chronic obstructive lung disease. J. Clin. Invest. *123*, 3967–3982.

Cano, F., Bye, H., Duncan, L.M., Buchet-Poyau, K., Billaud, M., Wills, M.R., and Lehner, P.J. (2012). The RNA-binding E3 ubiquitin ligase MEX-3C links ubiquitination with MHC-I mRNA degradation. EMBO J. *31*, 3596–3606.

Casolaro, V., Fang, X., Tancowny, B., Fan, J., Wu, F., Srikantan, S., Asaki, S.Y., De Fanis, U., Huang, S.K., Gorospe, M., et al. (2008). Posttranscriptional regulation of IL-13 in T cells: role of the RNA-binding protein HuR. J. Allergy Clin. Immunol. *121*, 853–9.e4.

Cayrol, C., and Girard, J.P. (2014). IL-33: an alarmin cytokine with crucial roles in innate immunity, inflammation and allergy. Curr. Opin. Immunol. *31*, 31–37.

de la Mata, M., Gaidatzis, D., Vitanescu, M., Stadler, M.B., Wentzel, C., Scheiffele, P., Filipowicz, W., and Großhans, H. (2015). Potent degradation of neuronal miRNAs induced by highly complementary targets. EMBO Rep. *16*, 500–511.

Donnini, M., Lapucci, A., Papucci, L., Witort, E., Jacquier, A., Brewer, G., Nicolin, A., Capaccioli, S., and Schiavone, N. (2004). Identification of TINO: a new evolutionarily conserved BCL-2 AU-rich element RNA-binding protein. J. Biol. Chem. *279*, 20154–20166.

Evers, M.M., Toonen, L.J., and van Roon-Mom, W.M. (2015). Antisense oligonucleotides in therapy for neurodegenerative disorders. Adv. Drug Deliv. Rev. *87*, 90–103.

Fabian, M.R., Sonenberg, N., and Filipowicz, W. (2010). Regulation of mRNA translation and stability by microRNAs. Annu. Rev. Biochem. *79*, 351–379.

Filipowicz, W., Bhattacharyya, S.N., and Sonenberg, N. (2008). Mechanisms of post-transcriptional regulation by microRNAs: are the answers in sight? Nat. Rev. Genet. *9*, 102–114.

Gudbjartsson, D.F., Bjornsdottir, U.S., Halapi, E., Helgadottir, A., Sulem, P., Jonsdottir, G.M., Thorleifsson, G., Helgadottir, H., Steinthorsdottir, V., Stefansson, H., et al. (2009). Sequence variants affecting eosinophil numbers associate with asthma and myocardial infarction. Nat. Genet. *41*, 342–347.

Hammad, H., and Lambrecht, B.N. (2008). Dendritic cells and epithelial cells: linking innate and adaptive immunity in asthma. Nat. Rev. Immunol. *8*, 193–204.

Herrick, C.A., and Bottomly, K. (2003). To respond or not to respond: T cells in allergic asthma. Nat. Rev. Immunol. *3*, 405–412.

Iikura, M., Suto, H., Kajiwara, N., Oboki, K., Ohno, T., Okayama, Y., Saito, H., Galli, S.J., and Nakae, S. (2007). IL-33 can promote survival, adhesion and cytokine production in human mast cells. Lab. Invest. *87*, 971–978.

John, B., Enright, A.J., Aravin, A., Tuschl, T., Sander, C., and Marks, D.S. (2004). Human MicroRNA targets. PLoS Biol. *2*, e363.

Kafasla, P., Skliris, A., and Kontoyiannis, D.L. (2014). Post-transcriptional coordination of immunological responses by RNA-binding proteins. Nat. Immunol. *15*, 492–502.

Kedde, M., and Agami, R. (2008). Interplay between microRNAs and RNA-binding proteins determines developmental processes. Cell Cycle *7*, 899–903.

Kedde, M., Strasser, M.J., Boldajipour, B., Oude Vrielink, J.A., Slanchev, K., le Sage, C., Nagel, R., Voorhoeve, P.M., van Duijse, J., Ørom, U.A., et al. (2007). RNA-binding protein Dnd1 inhibits microRNA access to target mRNA. Cell *131*, 1273–1286.

Kedde, M., van Kouwenhove, M., Zwart, W., Oude Vrielink, J.A., Elkon, R., and Agami, R. (2010). A Pumilio-induced RNA structure switch in p27-3′ UTR controls miR-221 and miR-222 accessibility. Nat. Cell Biol. *12*, 1014–1020.

Khabar, K.S. (2010). Post-transcriptional control during chronic inflammation and cancer: a focus on AU-rich elements. Cell. Mol. Life Sci. *67*, 2937–2955.

Kim, B.S., and Artis, D. (2015). Group 2 innate lymphoid cells in health and disease. Cold Spring Harb. Perspect. Biol. *7*, 7.

Kim, H.Y., DeKruyff, R.H., and Umetsu, D.T. (2010). The many paths to asthma: phenotype shaped by innate and adaptive immunity. Nat. Immunol. *11*, 577–584.

Kondo, Y., Yoshimoto, T., Yasuda, K., Futatsugi-Yumikura, S., Morimoto, M., Hayashi, N., Hoshino, T., Fujimoto, J., and Nakanishi, K. (2008). Administration of IL-33 induces airway hyperresponsiveness and goblet cell hyperplasia in the lungs in the absence of adaptive immune system. Int. Immunol. *20*, 791–800.

La Rocca, G., Olejniczak, S.H., González, A.J., Briskin, D., Vidigal, J.A., Spraggon, L., DeMatteo, R.G., Radler, M.R., Lindsten, T., Ventura, A., et al. (2015). In vivo, Argonaute-bound microRNAs exist predominantly in a reservoir of low molecular weight complexes not associated with mRNA. Proc. Natl. Acad. Sci. USA *112*, 767–772.

Le Borgne, M., Chartier, N., Buchet-Poyau, K., Destaing, O., Faurobert, E., Thibert, C., Rouault, J.P., Courchet, J., Nègre, D., Bouvard, D., et al. (2014). The RNA-binding protein Mex3b regulates the spatial organization of the Rap1 pathway. Development *141*, 2096–2107.

Lieber, M., Smith, B., Szakal, A., Nelson-Rees, W., and Todaro, G. (1976). A continuous tumor-cell line from a human lung carcinoma with properties of type II alveolar epithelial cells. Int. J. Cancer *17*, 62–70.

Liew, F.Y., Pitman, N.I., and McInnes, I.B. (2010). Disease-associated functions of IL-33: the new kid in the IL-1 family. Nat. Rev. Immunol. *10*, 103–110.

Lindow, M., and Kauppinen, S. (2012). Discovering the first microRNA-targeted drug. J. Cell Biol. *199*, 407–412.

Lloyd, C.M., and Hessel, E.M. (2010). Functions of T cells in asthma: more than just T(H)2 cells. Nat. Rev. Immunol. *10*, 838–848.

Louten, J., Rankin, A.L., Li, Y., Murphy, E.E., Beaumont, M., Moon, C., Bourne, P., McClanahan, T.K., Pflanz, S., and de Waal Malefyt, R. (2011). Endogenous IL-33 enhances Th2 cytokine production and T-cell responses during allergic airway inflammation. Int. Immunol. *23*, 307–315.

Lundin, K.E., Gissberg, O., and Smith, C.I. (2015). Oligonucleotide Therapies: The Past and the Present. Hum. Gene Ther. *26*, 475–485.

Malmhäll, C., Alawieh, S., Lu, Y., Sjöstrand, M., Bossios, A., Eldh, M., and Rådinger, M. (2014). MicroRNA-155 is essential for T(H)2-mediated allergen-induced eosinophilic inflammation in the lung. J. Allergy Clin. Immunol. *133*, 1429–1438, 1438.e1–1438.e7.

Masamune, A., Watanabe, T., Kikuta, K., Satoh, K., Kanno, A., and Shimosegawa, T. (2010). Nuclear expression of interleukin-33 in pancreatic stellate cells. Am. J. Physiol. Gastrointest. Liver Physiol. *299*, G821–G832.

Matsuura, K., Jigami, T., Taniue, K., Morishita, Y., Adachi, S., Senda, T., Nonaka, A., Aburatani, H., Nakamura, T., and Akiyama, T. (2011). Identification of a link between Wnt/β-catenin signalling and the cell fusion pathway. Nat. Commun. *2*, 548.

Moffatt, M.F., Gut, I.G., Demenais, F., Strachan, D.P., Bouzigon, E., Heath, S., von Mutius, E., Farrall, M., Lathrop, M., and Cookson, W.O.; GABRIEL Consortium (2010). A large-scale, consortium-based genomewide association study of asthma. N. Engl. J. Med. *363*, 1211–1221.

Moro, K., Yamada, T., Tanabe, M., Takeuchi, T., Ikawa, T., Kawamoto, H., Furusawa, J., Ohtani, M., Fujii, H., and Koyasu, S. (2010). Innate production of T(H)2 cytokines by adipose tissue-associated c-Kit(+)Sca-1(+) lymphoid cells. Nature *463*, 540–544.

Nakagome, K., Okunishi, K., Imamura, M., Harada, H., Matsumoto, T., Tanaka, R., Miyazaki, J., Yamamoto, K., and Dohi, M. (2009). IFN-gamma attenuates antigen-induced overall immune response in the airway as a Th1-type immune regulatory cytokine. J. Immunol. *183*, 209–220.

Nunes, T., Bernardazzi, C., and de Souza, H.S. (2014). Interleukin-33 and inflammatory bowel diseases: lessons from human studies. Mediators Inflamm. *2014*, 423957.

Oboki, K., Ohno, T., Kajiwara, N., Arae, K., Morita, H., Ishii, A., Nambu, A., Abe, T., Kiyonari, H., Matsumoto, K., et al. (2010). IL-33 is a crucial amplifier of innate rather than acquired immunity. Proc. Natl. Acad. Sci. USA *107*, 18581–18586.

Ørom, U.A., Kauppinen, S., and Lund, A.H. (2006). LNA-modified oligonucleotides mediate specific inhibition of microRNA function. Gene *372*, 137–141.

Pereira, B., Sousa, S., Barros, R., Carreto, L., Oliveira, P., Oliveira, C., Chartier, N.T., Plateroti, M., Rouault, J.P., Freund, J.N., et al. (2013). CDX2 regulation by the RNA-binding protein MEX3A: impact on intestinal differentiation and stemness. Nucleic Acids Res. *41*, 3986–3999.

Pharmaxis. (2012). Pharmaxis Completes Phase II Clinical Study with ASM8 in Asthma Patients. http://www.evaluategroup.com/Universal/View.aspx?type=Story&id=288742.

Préfontaine, D., Nadigel, J., Chouiali, F., Audusseau, S., Semlali, A., Chakir, J., Martin, J.G., and Hamid, Q. (2010). Increased IL-33 expression by epithelial cells in bronchial asthma. J. Allergy Clin. Immunol. *125*, 752–754.

Ray, P.S., Jia, J., Yao, P., Majumder, M., Hatzoglou, M., and Fox, P.L. (2009). A stress-responsive RNA switch regulates VEGFA expression. Nature *457*, 915–919.

Saglani, S., Lui, S., Ullmann, N., Campbell, G.A., Sherburn, R.T., Mathie, S.A., Denney, L., Bossley, C.J., Oates, T., Walker, S.A., et al. (2013). IL-33 promotes airway remodeling in pediatric patients with severe steroid-resistant asthma. J. Allergy Clin. Immunol. *132*, 676–685.e13.

Schmitz, J., Owyang, A., Oldham, E., Song, Y., Murphy, E., McClanahan, T.K., Zurawski, G., Moshrefi, M., Qin, J., Li, X., et al. (2005). IL-33, an interleukin-1-like cytokine that signals via the IL-1 receptor-related protein ST2 and induces T helper type 2-associated cytokines. Immunity *23*, 479–490.

Simpson, L.J., Patel, S., Bhakta, N.R., Choy, D.F., Brightbill, H.D., Ren, X., Wang, Y., Pua, H.H., Baumjohann, D., Montoya, M.M., et al. (2014). A

microRNA upregulated in asthma airway T cells promotes TH2 cytokine production. Nat. Immunol. *15*, 1162–1170.

Sponheim, J., Pollheimer, J., Olsen, T., Balogh, J., Hammarström, C., Loos, T., Kasprzycka, M., Sørensen, D.R., Nilsen, H.R., Küchler, A.M., et al. (2010). Inflammatory bowel disease-associated interleukin-33 is preferentially expressed in ulceration-associated myofibroblasts. Am. J. Pathol. *177*, 2804–2815.

Suojalehto, H., Toskala, E., Kilpeläinen, M., Majuri, M.L., Mitts, C., Lindström, I., Puustinen, A., Plosila, T., Sipilä, J., Wolff, H., and Alenius, H. (2013). MicroRNA profiles in nasal mucosa of patients with allergic and nonallergic rhinitis and asthma. Int. Forum Allergy Rhinol. *3*, 612–620.

Wang, Y.H., Angkasekwinai, P., Lu, N., Voo, K.S., Arima, K., Hanabuchi, S., Hippe, A., Corrigan, C.J., Dong, C., Homey, B., et al. (2007). IL-25 augments type 2 immune responses by enhancing the expansion and functions of TSLP-DC-activated Th2 memory cells. J. Exp. Med. *204*, 1837–1847.

Wikenheiser, K.A., Vorbroker, D.K., Rice, W.R., Clark, J.C., Bachurski, C.J., Oie, H.K., and Whitsett, J.A. (1993). Production of immortalized distal respiratory epithelial cell lines from surfactant protein C/simian virus 40 large tumor antigen transgenic mice. Proc. Natl. Acad. Sci. USA *90*, 11029–11033.

Xiang, Y., Eyers, F., Herbert, C., Tay, H.L., Foster, P.S., and Yang, M. (2016). MicroRNA-487b is a negative regulator of macrophage activation by targeting IL-33 production. J. Immunol. *196*, 3421–3428.

Yang, Y., and Seed, B. (2003). Site-specific gene targeting in mouse embryonic stem cells with intact bacterial artificial chromosomes. Nat. Biotechnol. *21*, 447–451.

Yarovinsky, T.O., Butler, N.S., Monick, M.M., and Hunninghake, G.W. (2006). Early exposure to IL-4 stabilizes IL-4 mRNA in CD4+ T cells via RNA-binding protein HuR. J. Immunol. *177*, 4426–4435.

Ziegler, S.F., and Artis, D. (2010). Sensing the outside world: TSLP regulates barrier immunity. Nat. Immunol. *11*, 289–293.

Cell Reports, Volume *16*

Supplemental Information

The RNA Binding Protein Mex-3B Is Required for IL-33 Induction in the Development of Allergic Airway Inflammation

Yusuke Yamazumi, Oh Sasaki, Mitsuru Imamura, Takeaki Oda, Yoko Ohno, Yumi Shiozaki-Sato, Shigenori Nagai, Saki Suyama, Yuki Kamoshida, Kosuke Funato, Teruhito Yasui, Hitoshi Kikutani, Kazuhiko Yamamoto, Makoto Dohi, Shigeo Koyasu, and Tetsu Akiyama

Inventory of supplemental information

Seven figures with Figure legends. Figures S1 - S3 relate to Figure 1 in the main document; Figure S4 relate to Figure 2 in the main document; Figure S5 relates to Figure 3 in the main document; Figure S6 relate to Figure 4 in the main document; Figure S7 relate to Figure 6 in the main document.

Table S1: Primers Used in Quantitative RT-PCR Experiments

Yamazumi et al Figure S1, related to Figure 1

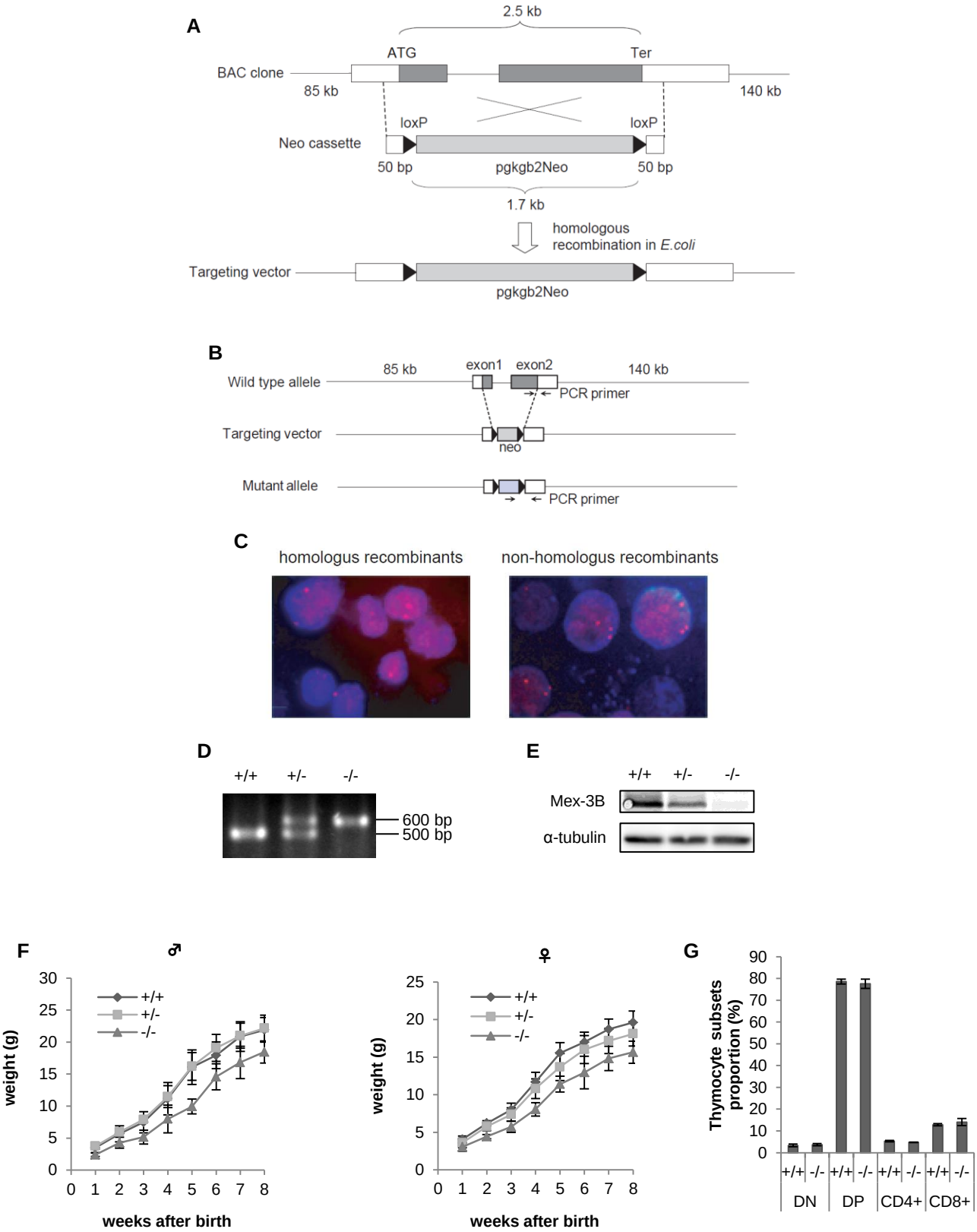

Yamazumi et al Figure S2, related to Figure 1

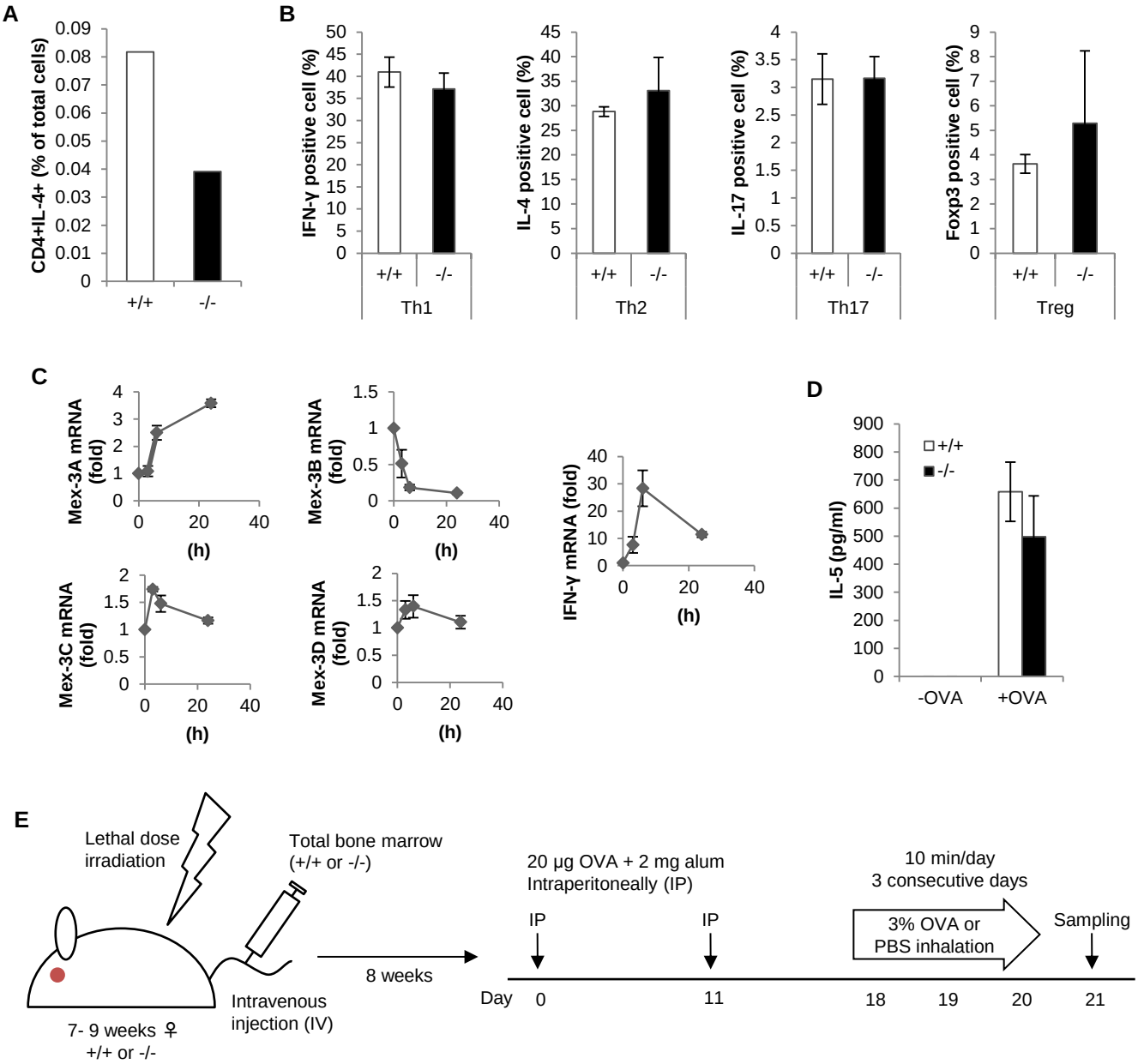

	Donor	Recipient
+/+ → +/+	+/+	+/+
-/- → +/+	-/-	+/+
+/+ → -/-	+/+	-/-

Yamazumi et al Figure S3, related to Figure 1

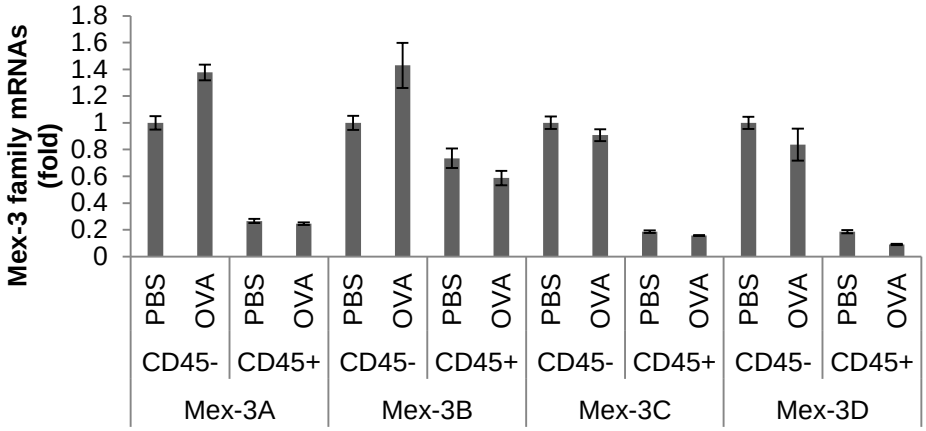

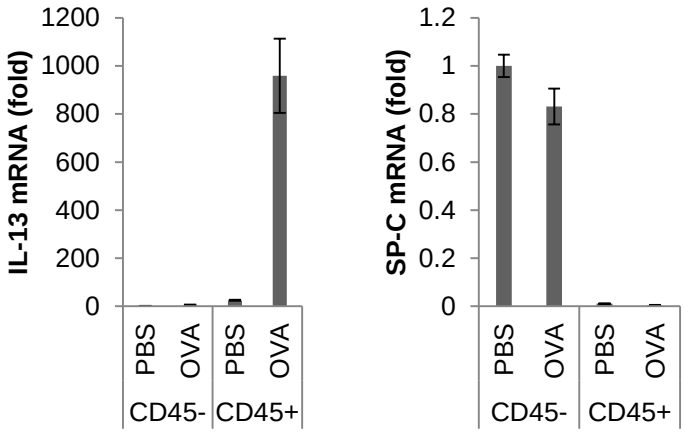

Yamazumi et al Figure S4, related to Figure 2

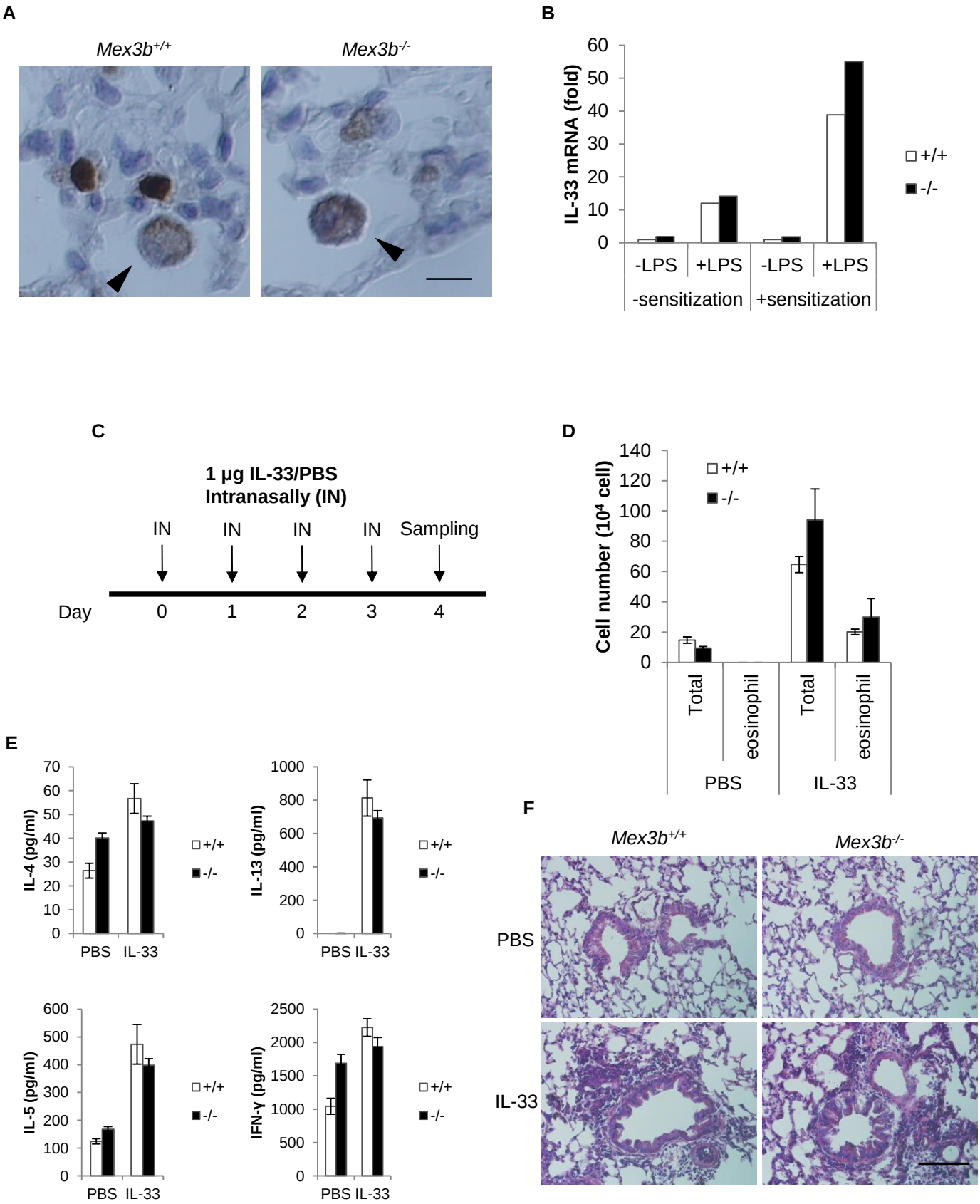

Yamazumi et al Figure S5, related to Figure 3

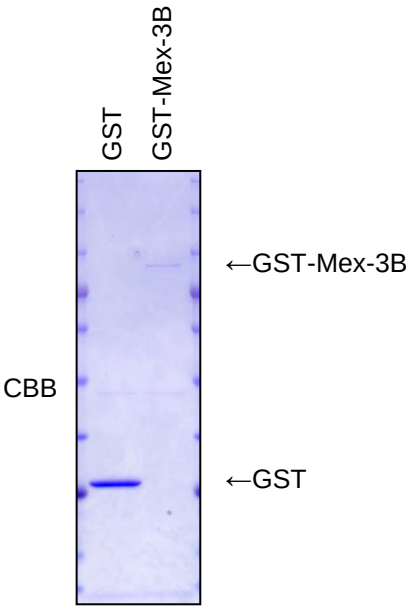

Yamazumi et al Figure S6, related to Figure 4

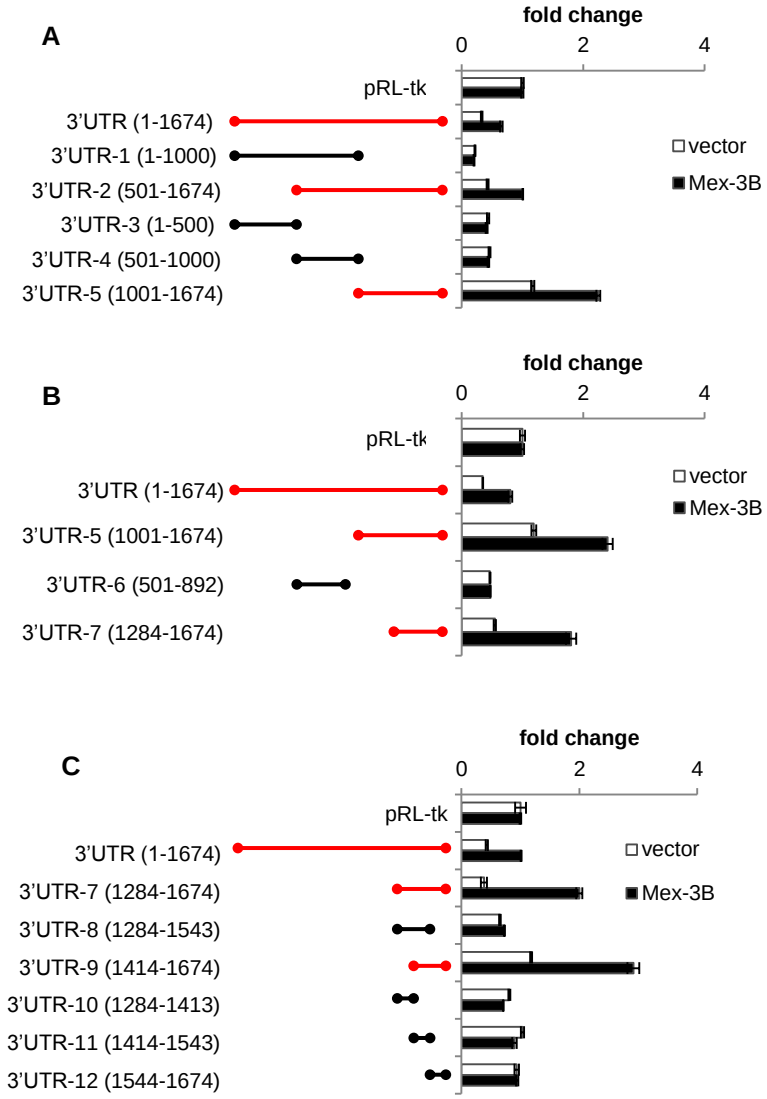

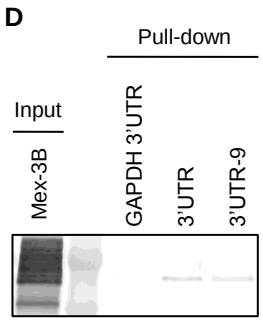

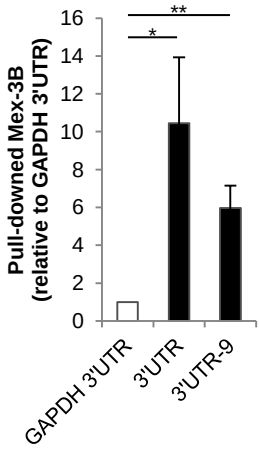

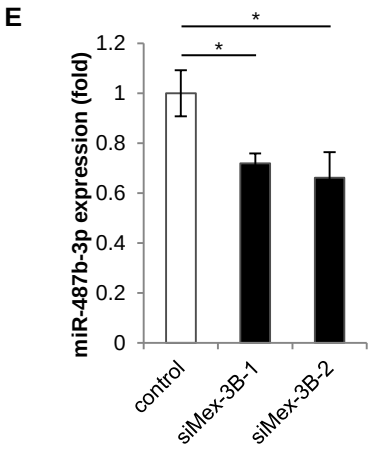

Yamazumi et al Figure S7, related to Figure 6

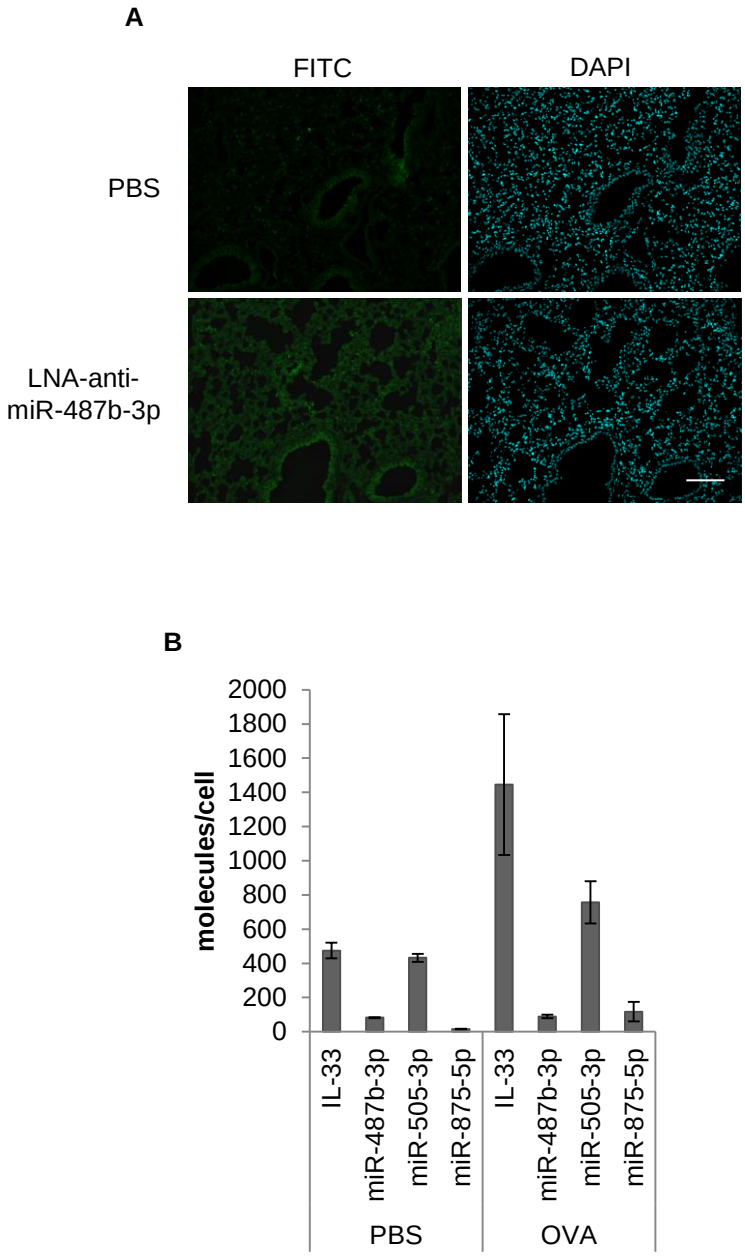

Supplemental Figure legends

Figure S1. Related to Figure 1

(A) The BAC clone, Neo cassette and targeting vector are shown.

(B) The wild-type *Mex3b* allele, targeting vector and mutant allele are shown. Arrows indicate primers used in PCR genotyping.

(C) FISH analysis of G418-resistant clones.

(D) Genotyping of mouse tail genomic DNA by PCR with primers amplifying the wild-type locus (500 bp) and the mutant locus (600 bp), respectively.

(E) Extracts from the thymus of *Mex3b*$^{+/+}$, *Mex3b*$^{+/-}$, and *Mex3b*$^{-/-}$ mice were subjected to immunoblotting analysis with anti-Mex-3B antibody. α-tubulin was used as a loading control.

(F) Weight gain in *Mex3b*$^{+/+}$, *Mex3b*$^{+/-}$ and *Mex3b*$^{-/-}$ mice (n = 4 - 14).

(G) Composition of thymocyte subsets (n = 3). Data are represented as mean ± SD.

Figure S2. Related to Figure 1

(A) Lung bronchial lymph node (LN) cells were isolated from the lungs of OVA-challenged *Mex3b*$^{+/+}$ and *Mex3b*$^{-/-}$ mice. LN cells from four mice were pooled in each group and stimulated *ex vivo* with Leukocyte Activation Cocktail. The number of Th2 cells was measured by intracellular IL-4 staining.

(B) Efector and regulatory T cells were generated from *Mex3b*$^{+/+}$ and *Mex3b*$^{-/-}$ CD4^{+}CD62L^{+} naïve T cells using standard cytokine cocktails. Th1, Th2, Th17 and Treg cells were detected by intracellular IL-4, IL-5, IL-17 and Foxp3 staining, respectively.

(C) CD4^{+} T cells were stimulated with anti-CD3/CD28 antibody for the indicated time and subjected to qRT-PCR. IFN-γ mRNA was used as a marker of T cell activation.

(D) Splenocytes containing dendritic cells from OVA-sensitized mice were cultured with OVA. The levels of IL-5 in the supernatant of splenocytes were measured by ELISA.

(E) Protocol for bone marrow transplantation.

(F) Bronchoalveolar lavage (BAL) fluid analyses were performed. Leukocytes were identified by morphological criteria. Data are represented as mean ± SD (B - D: n = 3) or ± SEM (F: n = 3 - 8)

Figure S3. Related to Figure 1

CD45-positive leukocytes and CD45-negative cells were separated from the lungs of control or OVA-challenged wild-type mice. RNAs were extracted from CD45-negative cells (CD45-) or CD45-positive cells (CD45+) and subjected to qRT-PCR. IL-13 or SP-C mRNA were used as markers of inflammation and airway epithelial cells, respectively. Data are represented as mean ± SEM (n = 4).

Figure S4. Related to Figure 2

(A) Alveolar macrophages (indicated by arrowheads) derived from OVA-inflamed lungs were stained with anti-IL-33 antibody.

(B) Alveolar macrophages from OVA-sensitized or unsensitized mice and were stimulated with LPS. The levels of IL-33 mRNA were measured by qRT-PCR.

(C) Scheme of IL-33-triggered airway inflammation.

(D - F) Effects of intra-nasal administration of IL-33 on lung inflammation in *Mex3b*$^{+/+}$ and *Mex3b*$^{-/-}$ mice. The number of cells in BAL fluids (D), cytokine concentrations (E) and lung sections stained with HE (F) at 24 h after the last IL-33 or PBS administration are shown. Scale bar, 20 μm (A) or 100 μm (F). Data are represented as mean ± SEM (n = 3 - 7).

Figure S5. Related to Figure 3

The purity of GST-Mex-3B was confirmed by CBB staining.

Figure S6. Related to Figure 4

(A - C) Luciferase activity of A549 cells transfected with the indicated reporter plasmid along with control vector or FLAG-tagged Mex-3B.

(D) Immunoblot analysis of exogenously expressed FLAG-tagged Mex-3B protein co-precipitated with the indicated IL-33 3'UTR fragments. GAPDH 3'UTR was used as a negative control.

(E) MLE-15 cells were transfected with the indicated siRNAs and subjected to qRT-PCR. miR-487b-3p expression was normalized to U6 snRNA. Data are represented as mean ± SD (n = 3). *: $p < 0.05$.

Figure S7. Related to Figure 6

(A) Immunofluorescence staining of LNA-anti-miRNA (green; left) in lung tissues treated for 24 h with PBS or Alexa 488-LNA-anti-miR-487b-3p. Nuclei were stained with DAPI (blue; right). (B) The absolute copy numbers of miRNAs and IL-33 mRNA per cells in the lungs of control or OVA-challenged wild-type mice were measured by qRT-PCR. Scale bar, 100 μm. Data are represented as mean ± SEM (n = 3 - 6).

Supplemental Tables

Supplemental table 1. Primers Used in Quantitative RT-PCR Experiments

Name	Sequence (5' → 3')
mouse β-actin-F	GGATGCAGAAGGAGATTACTGC
mouse β-actin-R	CCACCGATCCACACAGAGCA
mouse GAPDH-F	TGTGTCCGTCGTGGATCTGA
mouse GAPDH-R	TTGCTGTTGAAGTCGCAGGAG
mouse Mex-3A-F	TGGGAGAGAAGTCTGGAGAGTG
mouse Mex-3A-R	CCGTCTCAAACTGATTCTTTGG
mouse Mex-3B-F	AGATCGTAGGGAGGCAAGG
mouse Mex-3B-R	GCCCGTCACAACAAAGACA
mouse Mex-3C-F	CAGTGGGTCCCAGAGCCTA
mouse Mex-3C-R	GGCAGCACTGGAAGTGTCA
mouse Mex-3D-F	CGTGTCGCAAACAGCTTTAAC
mouse Mex-3D-R	TGTCACCGGCTCACTCAATAC
mouse IFN-γ-F	ATCTGGAGGAACTGGCAAAA
mouse IFN-γ-R	TTCAAGACTTCAAAGAGTCTGAGGTA
mouse IL-13-F	CCTCTGACCCTTAAGGAGCTTAT
mouse IL-13-R	CGTTGCACAGGGGAGTCT
mouse SP-C-F	GGTCCTGATGGAGAGTCCAC
mouse SP-C-R	GATGAGAAGGCGTTTGAGGT
mouse IL-33-F	GACACATTGAGCATCCAAGG
mouse IL-33-R	AACAGATTGGTCATTGTATGTACTCAG
mouse TSLP-F	CAGCTTGTCTCCTGAAAATCG
mouse TSLP-R	AAATGTTTTGTCGGGGAGTG
mouse GM-CSF-F	GCATGTAGAGGCCATCAAAGA
mouse GM-CSF-R	CGGGTCTGCACACATGTTA
human GAPDH-F	GCACCGTCAAGGCTGAGAAC
human GAPDH-R	TGGTGAAGACGCCAGTGGA
human IL-33-F	AGCAAAGTGGAAGAACACAGC
human IL-33-R	CTTCTTTGGCCTTCTGTTGG

miR-487b-3p	AAUCGUACAGGGUCAUCCACUU
miR-875-5p	TATACCTCAGTTTTATCAGGTG
miR-505-3p	CGTCAACACTTGCTGGTTTTCT

Supplemental Experimental Procedures

Genotype

Genomic DNA was prepared from tail biopsies and genotyped using the following primer sets: Mex-3B wild-type allele, GTCACTCAGGCCATCCGCATTTTTTCCTGA and GTGTTCTAGAACGAGCGCTGTAGGAACCCA; Mex-3B knockout allele, GTTGGTTTTTGTGTGCGGCGCGCCGTTTAA and GTGTTCTAGAACGAGCGCTGTAGGAACCCA.

Isolation of airway epithelial cells in the lung

Airway epithelial cells in the lungs were isolated from mice by the method described by Corti et al. (Corti et al. 1996) with minor modifications. Mice were exsanguinated under anesthesia, and the pulmonary vasculature was perfused with PBS via the right ventricle until the effluent was free of blood. The lungs were isolated and immersed in 7 ml dispase (BD Biosciences) in 30 ml syringe. By piston action, the lungs were deaerated and filled with dispase, then placed in 1.5 ml dispase for 45 min at 37°C. The lungs were minced in DMEM/F12 with 0.01% DNase I (Roche) and gently swirled for 7.5 min. This crude cell mixture was passed successively through 100-, 40 μm nylon mesh filters (BD Biosciences) and then centrifuged at 130 x g for 5 min at 4°C. Cells were incubated with CD45 MicroBeads (Miltenyi Biotec) and CD45-positive (leukocyte) or CD45-negative cell fractions were separated by autoMACS^{tm} Separator (Miltenyi Biotec) according to the manufacturer's instruction.

Bone marrow transplantation

For the preparation of recipient mice, 7 - 9 weeks old female *Mex3b*$^{+/+}$ or *Mex3b*$^{-/-}$ mice were total body irradiated with 9.5 Gy (lethal dose) in an acrylic chamber. Bone marrow donor cells were harvested from 7 - 9 weeks old female *Mex3b*$^{+/+}$ or *Mex3b*$^{-/-}$ mice by gently flushing their femurs with 2%FBS/PBS. Cells were centrifuged, resuspended in PBS. Total bone marrow cells (6 x 10^5) in 0.3 ml PBS were intravenously injected into recipient mice immediately after irradiation. Eight weeks after transplantation, mice were subjected to OVA-induced model of allergic airway inflammation.

Analysis of thymocyte subsets

Thymocytes were isolated and stained with FITC-conjugated anti-CD8a (53-6.7: BD biosciences) antibody (Ab) and PE-conjugated anti-CD4 (GK1.5: BD biosciences) Ab to analyze DN, DP, CD4 SP and CD8 SP subsets. Flow cytometry was performed on a FACSCalibur (BD Biosciences) and the data was analyzed using FlowJo Software (Tree Star).

T cell activation

After splenocytes were reacted with cocktail of biotin-conjugated monoclonal anti-mouse antibodies against CD8a, CD45R, CD11b, CD11c, MHC class II, CD25, CD49b and Ter-119, $CD25^-CD4^+$ T cells were isolated with Anti-Biotin Microbeads (Miltenyi Biotec) by negative selection. Isolated T cells were stimulated with immobilized anti-CD3ε antibody (plates coated with 5 μg/ml anti-CD3ε antibody in 100 μl PBS) and 1 μg/ml soluble anti-CD28 antibody

Measurement of cytokines

The concentrations of IL-4, IL-5, IL-13 and IFN-γ were measured using ELISA kits (IL-5 and IFN-γ, BD Pharmingen; IL-4 and IL-13, R&D Systems).

Preparation of spleen and lymph node cells

Spleen cells were prepared as reported previously (Nakagome et al., 2005). For the preparation of bronchial lymph node cells, the pool of bronchial lymph nodes of 3 - 4 mice were minced and then incubated at 37°C for 30 min with 150 U of collagenase (Sigma) in complete DMEM. Cell suspensions were obtained by pressing the tissues through a 70 μm nylon filter (BD Biosciences).

Ag-induced immune response in spleen cells

Spleen cells (2.5 x 10^5 cell/well) were cultured with OVA (10 μg/ml) in complete Dulbecco's Modified Eagle's Medium (DMEM: Nissui) for 120 h and the cytokine concentrations in the supernatants were measured by ELISA.

Isolation and differentiation of Th subsets

$CD4^+CD25^-CD62L^{high}$ T cells were purified from splenocytes using the $CD4^+CD62L^+$ T cell isolation kit II (Miltenyi Biotec). Isolated naïve $CD4^+$ T cells were stimulated for 3 days with immobilized anti-CD3ε antibody (plates coated with 5 μg/ml anti-CD3ε antibody in 100 μl PBS) and 1 μg/ml soluble anti-CD28 antibody supplemented with 10 ng/ml IL-12 for Th1 differentiation, 10 ng/ml IL-4 for Th2 differentiation, 3 ng/ml TGF-β for iTreg differentiation, or 30 ng/ml IL-6 and 3 ng/ml TGF-β for Th17 differentiation.

Preparation of alveolar macrophage

Mex3b$^{+/+}$ and *Mex3b*$^{-/-}$ mice were sensitized with OVA/alum on days 0 and 11. On day 18, BAL cells were obtained. Over 95% of BAL cells were identified as macrophage by cellular morphology. Cells were stimulated with LPS (100 ng/ml) for 3 h. Cells were lysed in Trisure for qRT-PCR analysis.

Intracellular staining of cytokines and Foxp3

Bronchial lymph node cells were restimulated with Golgi Plug (BD Pharmingen) for 4 h. Th1, Th2 and Th17

cells were restimulated with 50 ng/ml PMA and 1 μM ionomycin for 2 to 4 h, followed by incubation with Brefeldin A for 2 h. Intracellular cytokine staining was performed using Intra Prep (Beckman Coulter). Intracellular staining of Foxp3 for Treg was performed with the PE anti-mouse/rat Foxp3 staining kit (eBioscience). Flow cytometry was performed on a FACSCalibur and the data was analyzed using FlowJo Software.

Plasmid construction

FLAG-tagged human Mex-3B was subcloned into the pcDNA3.1 (+) vector (Invitrogen). FLAG-tagged Mex-3B mutKH was created by standard PCR techniques using Pyrobest DNA polymerase (TAKARA). Murine IL-33 3'UTR and its deletion mutants were cloned into the pRL-tk vector (Promega) at *Xba* I and *Not* I sites. For preparation of GST-Mex-3B, cDNA fragments were subcloned into pGEX-5X-1 (GE Healthcare).

Production of recombinant protein

GST-Mex-3B was synthesized in *Escherichia coli* and isolated by adsorption to glutathione-conjugated Sepharose (GSH-Sepharose; GE Healthcare). GST-Mex-3B was purified by DEAE Sepharose (GE Healthcare). The purity of GST-Mex-3B was confirmed by CBB staining.

Quantification of absolute copy numbers of RNAs

Quantification of absolute copy numbers of RNAs were performed by the method described by de la Mata et al. (de la Mata et al., 2015) with modifications. For quantification of miRNAs or U6, total RNA was reverse transcribed using miR-X miRNA First-Strand Synthesis Kit (Clontech), followed by qRT-PCR. Absolute estimation of miRNA copy numbers per cell was performed by generating standard curves using PAGE-purified 5'phosphorylated oligoribonucleotide (FASMAC) corresponding to the following reference sequence: miR-487b-3p, 5'-AAUCGUACAGGGUCAUCCACUU-3'; miR-505-3p, 5'-CGTCAACACTTGCTGGTTTTCT-3', miR-875-5p, 5'-TATACCTCAGTTTTATCAGGTG-3'. Absolute

estimation of IL-33 mRNA copy numbers per cell was performed by generating standard curves using *in vitro*-transcribed IL-33 mRNA [subcloned into pBlueScript II SK (+)]. The Ct values obtained from different reactions were converted to absolute copy numbers of miRNAs or IL-33 mRNA per 20 pg of total RNA (approximately one cell) by interpolating the Ct values of individual samples into the corresponding standard curves. miRNAs and IL-33 mRNA levels were normalized to U6 and β-actin, respectively.

Supplemental References

Corti, M., Brody, A.R., and Harrison, J.H. (1996). Isolation and primary culture of murine alveolar type II cells. American journal of respiratory cell and molecular biology 14, 309-315.

Nakagome, K., Dohi, M., Okunishi, K., Komagata, Y., Nagatani, K., Tanaka, R., Miyazaki, J., and Yamamoto, K. (2005). In vivo IL-10 gene delivery suppresses airway eosinophilia and hyperreactivity by down-regulating APC functions and migration without impairing the antigen-specific systemic immune response in a mouse model of allergic airway inflammation. J Immunol 174, 6955-6966.

Cell Reports

Article

The RNA Binding Protein Mex-3B Is Required for IL-33 Induction in the Development of Allergic Airway Inflammation

Graphical Abstract

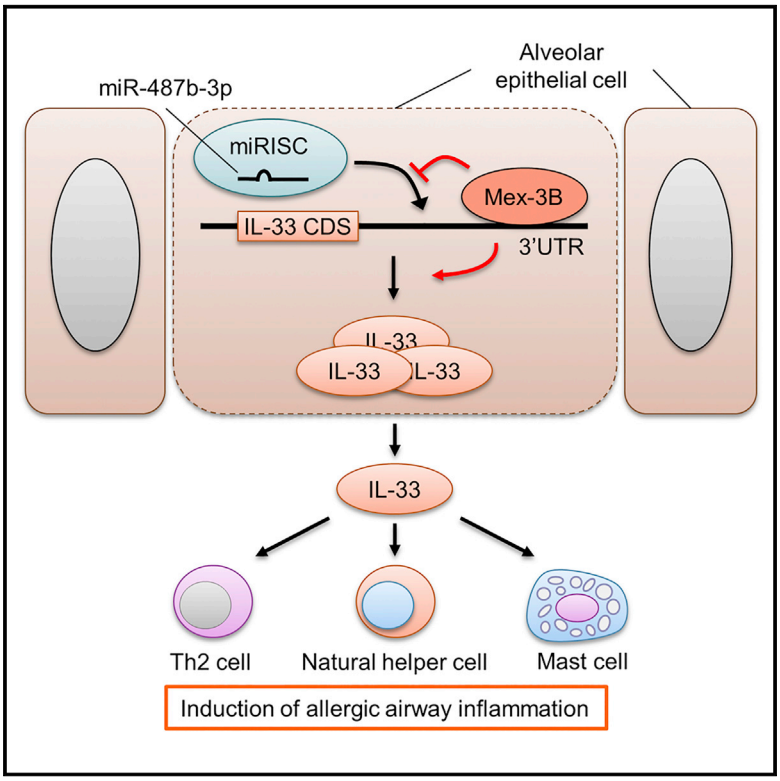

Highlights

- Mex-3B induces IL-33 in the development of allergic airway inflammation
- *Mex3b*$^{-/-}$ mice develop less airway inflammation due to reduced induction of IL-33
- Mex-3B upregulates IL-33 expression by inhibiting miR-487b-3p-mediated repression
- Inhalation of an antisense oligo targeting Mex-3B suppresses airway inflammation

Authors

Yusuke Yamazumi, Oh Sasaki, Mitsuru Imamura, ..., Makoto Dohi, Shigeo Koyasu, Tetsu Akiyama

Correspondence

akiyama@iam.u-tokyo.ac.jp

In Brief

Yamazumi et al. show that Mex-3B-mediated post-transcriptional upregulation of IL-33 is required for the development of allergic airway inflammation. Inhalation of an antisense oligonucleotide targeting Mex-3B suppresses allergic airway inflammation, suggesting that Mex-3B could be a promising molecular target for the treatment of allergic asthma.

Yamazumi et al., 2016, Cell Reports *16*, 2456–2471
August 30, 2016 © 2016 The Author(s).
http://dx.doi.org/10.1016/j.celrep.2016.07.062

OPEN ACCESS
CellPress

Cell Reports
Article

The RNA Binding Protein Mex-3B Is Required for IL-33 Induction in the Development of Allergic Airway Inflammation

Yusuke Yamazumi,[1] Oh Sasaki,[2] Mitsuru Imamura,[2] Takeaki Oda,[1] Yoko Ohno,[1] Yumi Shiozaki-Sato,[1] Shigenori Nagai,[3] Saki Suyama,[1] Yuki Kamoshida,[1] Kosuke Funato,[1] Teruhito Yasui,[4] Hitoshi Kikutani,[4] Kazuhiko Yamamoto,[2] Makoto Dohi,[2,5] Shigeo Koyasu,[6] and Tetsu Akiyama[1,7,*]

[1]Laboratory of Molecular and Genetic Information, Institute for Molecular and Cellular Biosciences, The University of Tokyo, 1-1-1 Yayoi, Bunkyo-ku, Tokyo 113-0032, Japan
[2]Department of Allergy and Rheumatology, Graduate School of Medicine, University of Tokyo, 7-3-1 Hongo, Bunkyo-ku, Tokyo 113-8655, Japan
[3]Department of Molecular Immunology, Graduate School of Medical and Dental Sciences, Tokyo Medical and Dental University, 1-5-45 Yushima, Bunkyo-ku, Tokyo 113-8549, Japan
[4]Department of Molecular Immunology, Research Institute for Microbial Diseases, Osaka University, 3-1 Yamada-oka, Suita, Osaka 565-0871, Japan
[5]Institute of Respiratory Immunology, Shibuya Clinic for Respiratory Diseases and Allergology, Tokyo 150-0002, Japan
[6]Laboratory for Immune Cell Systems, RIKEN Research Center for Integrative Medical Sciences (IMS), 1-7-22 Suehiro-cho, Tsurumi-ku, Yokohama 230-0045, Japan
[7]Lead Contact
*Correspondence: akiyama@iam.u-tokyo.ac.jp
http://dx.doi.org/10.1016/j.celrep.2016.07.062

SUMMARY

Allergic airway inflammation is one of the primary features of allergic asthma. Interleukin-33 (IL-33) is recognized as a key pro-inflammatory cytokine that mediates allergic airway inflammation, and its expression is elevated in this condition, but little is known about the regulatory mechanisms underlying IL-33 induction. Here, we show that the RNA binding protein Mex-3B plays a critical role in the induction of IL-33 in the development of allergic airway inflammation. We generated *Mex3b*$^{-/-}$ mice and found that they develop significantly less airway inflammation than wild-type mice due to reduced induction of IL-33. Furthermore, we show that Mex-3B directly upregulates IL-33 expression by inhibiting miR-487b-3p-mediated repression of IL-33. Moreover, we show that inhalation of an antisense oligonucleotide targeting Mex-3B suppresses allergic airway inflammation. Our data identify a signaling pathway that post-transcriptionally regulates IL-33 expression and suggest that Mex-3B could be a promising molecular target for the treatment of allergic asthma.

INTRODUCTION

Allergic asthma is a chronic inflammatory disease of the lungs that affects nearly 300 million people worldwide. Allergic airway inflammation is one of the primary features of allergic asthma and is generally considered to be mediated by a T helper type 2 (Th2) response (Kim et al., 2010). Leucocytes have long been focused as the key players in the development of allergic airway inflammation. However, there is increasing evidence that epithelial cells act as active immune regulators that produce inflammatory factors, such as TSLP and interleukin-33 (IL-33) (Liew et al., 2010; Ziegler and Artis, 2010). IL-33 is a member of the IL-1 family, which plays important roles in type 2 innate immunity and human asthma (Cayrol and Girard, 2014). It has been shown that mice deficient for IL-33 are resistant to allergen-induced airway inflammation (Oboki et al., 2010). Furthermore, *IL-33* has been identified as a susceptibility gene for human asthma (Gudbjartsson et al., 2009; Moffatt et al., 2010). In addition, its expression in epithelial cells is higher in patients with allergic asthma than in healthy individuals (Préfontaine et al., 2010), and upregulation of IL-33 expression is observed in an experimental asthma model (Louten et al., 2011). Although several studies have shown that IL-33 expression is induced upon pro-inflammatory cytokine stimulation in several cell types (Masamune et al., 2010; Sponheim et al., 2010), the importance of IL-33 induction in the development of allergic airway inflammation, and the mechanisms underlying this induction are not well understood.

MicroRNAs (miRNAs) are small non-coding RNAs that can regulate gene expression and have been shown to play a role in various pathologies, including inflammation and cancer. miRNAs interact with Argonaute (Ago) and other proteins to form RNA-induced silencing complexes (RISCs), and guide these RISCs to 3′ UTRs of target RNAs via sequence-specific binding (Bartel, 2009; Fabian et al., 2010). This results in the destabilization of the target RNA and inhibition of translation. RNA binding proteins can also interact with 3′ UTRs and regulate gene expression (Filipowicz et al., 2008; Kedde and Agami, 2008). Recently, several groups have obtained evidence that miRNAs and RNA binding proteins can co-operate at common

 © 2016 The Author(s).
This is an open access article under the CC BY-NC-ND license (http://creativecommons.org/licenses/by-nc-nd/4.0/).

target 3′ UTRs under certain conditions (Bhattacharyya et al., 2006; Ray et al., 2009).

Mex-3B, a member of the Mex-3 family, contains two K homology (KH)-type RNA-recognition domains and a RING finger domain (Buchet-Poyau et al., 2007). It has been shown that these family members associate with specific mRNAs and regulate expression of their proteins (Cano et al., 2012; Donnini et al., 2004; Pereira et al., 2013). Mex-3D (also known as TINO or RKHD1) has been shown to destabilize *BCL2* mRNA by binding to an AU-rich element in its 3′ UTR (Donnini et al., 2004). Mex-3C regulates HLA-A2 levels through its mRNA 3′ UTR (Cano et al., 2012). Mex-3A has been shown to repress CDX2 expression post-transcriptionally through binding to the CDX2 3′ UTR (Pereira et al., 2013). *Mex3b*-deficient mice exhibit defects in Sertoli cells and have low fertility (Le Borgne et al., 2014). However, the physiological role of post-transcriptional regulation of target genes by Mex-3B has not been elucidated.

In this study, we generated *Mex3b*$^{-/-}$ mice and used them in an experimental model of allergic airway inflammation. We show that *Mex3b*$^{-/-}$ mice develop significantly less airway inflammation, due to reduced induction of IL-33. We also demonstrate that Mex-3B binds to the IL-33 3′ UTR and upregulates IL-33 expression by inhibiting miR-487b-3p-mediated repression of IL-33. Furthermore, we show that inhalation of a locked nucleic acid (LNA)-modified antisense oligonucleotide targeting Mex-3B (LNA-anti-Mex-3B) suppresses the development of allergic airway inflammation.

RESULTS

Mice Deficient in *Mex3b* Have Normal Phenotype

To gain insight into Mex-3B function in vivo, we generated *Mex3b*$^{-/-}$ mice through homologous recombination in mouse embryonic stem cells (Figures S1A–S1E). Homozygous *Mex3b* mutant animals were born in a Mendelian ratio (~25% of progeny), showing no evidence of embryonic lethality. *Mex3b*$^{-/-}$ newborns were indistinguishable from wild-type littermates except that they were smaller and had reduced body weight (Figure S1F). Consistent with a previous report (Le Borgne et al., 2014), *Mex3b*$^{-/-}$ mice were fertile, but fertility is low. Macroscopic and histological examination did not reveal any morphological abnormalities in the major organs of young adult mice. In addition, *Mex3b*$^{-/-}$ mice showed no detectable abnormalities in the development of B cells in the spleen or T cells in the thymus (Figure S1G).

Mex-3B Is Required for the Ovalbumin-Induced Allergic Airway Inflammation

It has previously been reported that Mex-3B is relatively highly expressed in human lung and thymus (Buchet-Poyau et al., 2007). Consistent with these results, we found that Mex-3B is also highly expressed in mouse lung and thymus (Y.Y., unpublished data). We therefore speculated that Mex-3B could play a role in the immune system in the lung. We examined this possibility using an experimental model of allergic airway inflammation (Figure 1A). Mice were sensitized with ovalbumin (OVA)/alum and then challenged with nebulized OVA or PBS. Compared to wild-type mice, *Mex3b*$^{-/-}$ mice exhibited decreased lung leukocytic infiltration and mucus secretion (Figure 1B) and decreased numbers of bronchoalveolar lavage (BAL) eosinophils (Figure 1C) in response to OVA challenge. The Th2-type cytokines, IL-4, IL-5, and IL-13, were less efficiently induced in the lungs of *Mex3b*$^{-/-}$ mice (Figure 1D). By contrast, the Th1-type cytokine interferon-γ (IFN)-γ was induced normally. We also examined the number of Th2 cells in bronchial lymph nodes by measuring intracellular cytokine levels of lung bronchial lymph node cells stimulated ex vivo with leukocyte activation cocktail. We observed decreased percentages of IL-4-positive CD4^{+} cells in primary cultured bronchial lymph node cells from *Mex3b*$^{-/-}$ mice (Figure S2A). These results suggest that Mex-3B is required for the development of allergic airway inflammation.

Th2 cells are known to play critical roles in the pathogenesis of allergic airway inflammation by producing a variety of cytokines such as IL-4, IL-5, IL-9, and IL-13 (Herrick and Bottomly, 2003). In addition to Th2 cells, it has recently been shown that Th1, regulatory T (Treg), and Th17 cells play important roles in allergic airway inflammation (Lloyd and Hessel, 2010). To understand how Mex-3B regulates the induction of allergic airway inflammation, we first examined T cell differentiation in *Mex3b*$^{-/-}$ mice. Effector and regulatory T cells were generated from wild-type and *Mex3b*$^{-/-}$ CD4^{+}CD62L^{+} naive T cells by standard methods. We found that the percentage of each T cell subset generated was very similar regardless of their *Mex3b* status (Figure S2B). Furthermore, we stimulated CD4^{+} T cells with anti-CD3/CD28 antibody in vitro and examined the expression of Mex-3B and the other family members. IFN-γ was used as a marker of T cell activation. We found that stimulation with anti-CD3/CD28 antibody resulted in reduced expression of only Mex-3B (Figure S2C). We next examined antigen-induced immune responses in the spleens. When splenocytes from OVA-sensitized mice were cultured with OVA, similar levels of IL-5 were secreted into the culture media by wild-type and *Mex3b*$^{-/-}$ splenocytes (Figure S2D). These results suggest that immune cell function in the spleen is comparable between wild-type and *Mex3b*$^{-/-}$ mice.

To further clarify the role of Mex-3B in hematopoietic cells, we performed bone marrow transplantation experiments. BAL fluid analysis revealed that *Mex3b*$^{-/-}$ mice transplanted with bone marrow cells from wild-type mice had less inflammation than wild-type mice transplanted with bone marrow cells from *Mex3b*$^{-/-}$ mice (Figures S2E and S2F). These results exclude the possibility that Mex-3B in hematopoietic cells plays a critical role in the development of allergic airway inflammation.

IL-33 Induction Is Suppressed in *Mex3b*-Deficient Mice

Recent studies have shown that airway epithelial cells play critical roles in the regulation of airway inflammation: airway epithelial cells influence the function of immune-competent cells, such as dendritic cells (Hammad and Lambrecht, 2008), mast cells (Allakhverdi et al., 2007), and Th2 cells (Wang et al., 2007) by producing many inflammatory factors in response to allergen exposure. We therefore examined the expression of Mex-3B in lung tissues from control and OVA-challenged mice. We separated airway epithelial and non-epithelial cells using anti-CD45 antibody and performed qRT-PCR analysis. IL-13 and SP-C were used as markers of inflammation and airway epithelial cells,

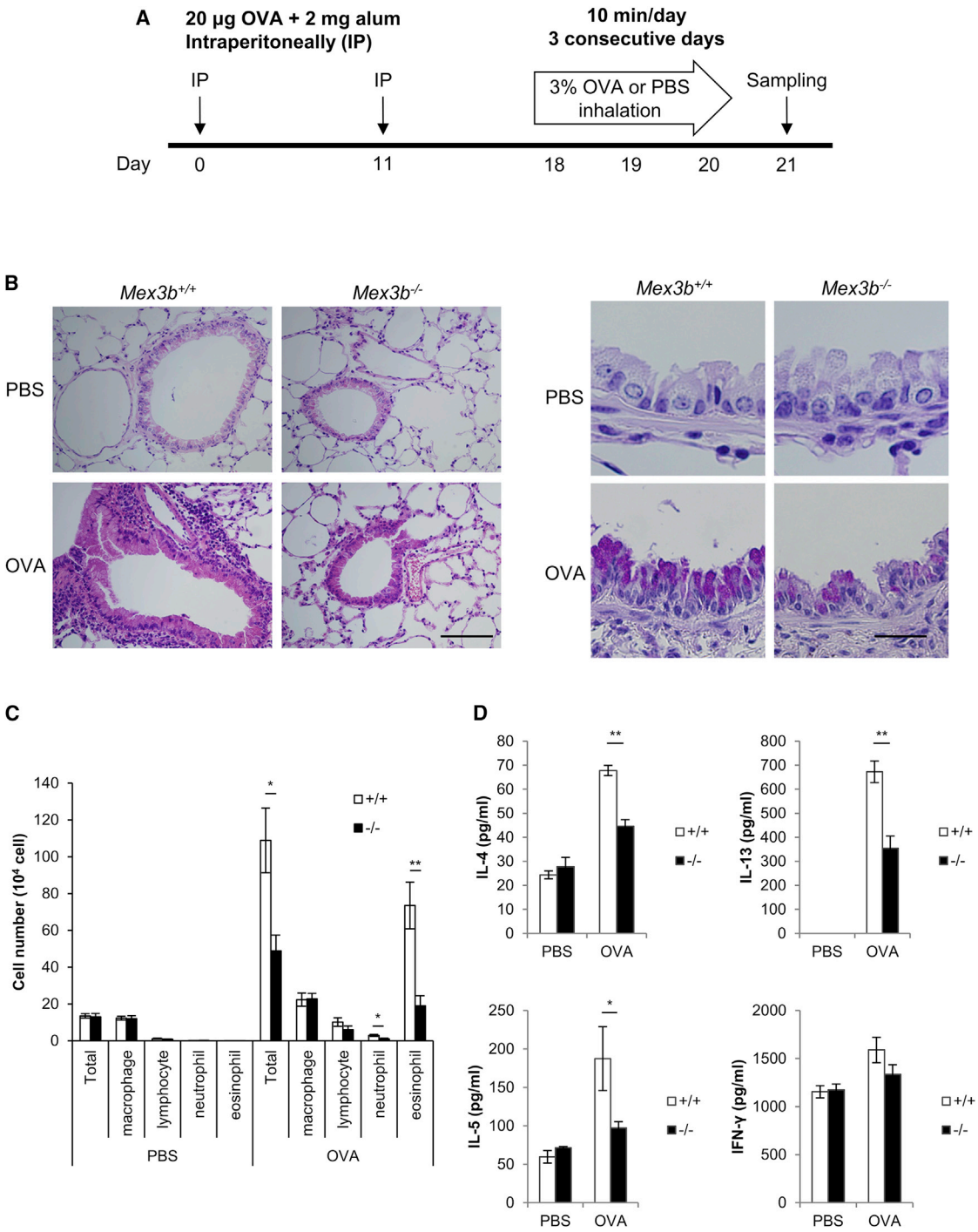

Figure 1. Mex-3B Is Critical for the Development of Airway Inflammation

(A) Scheme of the experimental asthma model. *Mex3b*$^{+/+}$ and *Mex3b*$^{-/-}$ mice were sensitized with OVA/alum on days 0 and 11. The mice were nebulized with OVA or PBS from day 18 to 20 and analyzed on day 21.

(B) OVA-induced infiltration of eosinophils into the peribronchial area and mucus hypersecretion by bronchial epithelial cells. (left) H&E staining. Scale bar, 100 μm. (right) Periodic acid-Schiff staining. Scale bar, 15 μm.

(C) Bronchoalveolar lavage (BAL) fluid analyses were performed. Leukocytes were identified by morphological criteria.

(D) Cytokine concentrations in the lungs of OVA-challenged or control mice. Lung homogenates were assayed for cytokine concentrations by ELISA. Data are represented as mean ± SEM (n = 3–7). *$p < 0.05$, **$p < 0.01$.

See also Figures S1–S3.

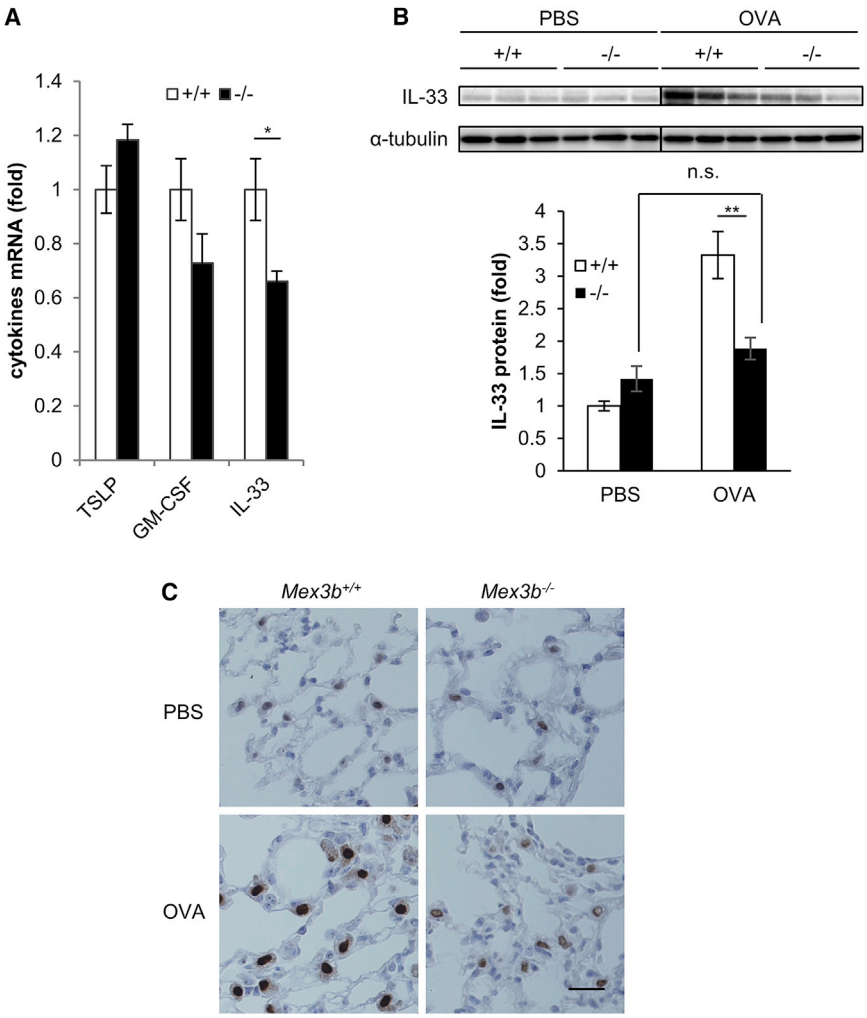

Figure 2. Mex-3B Is Required for the Induction of IL-33 Expression in the Development of Allergic Airway Inflammation

(A) The levels of inflammatory factor mRNAs in OVA-inflamed lungs of *Mex3b*$^{+/+}$ and *Mex3b*$^{-/-}$ mice.

(B) Immunoblot analysis of IL-33 protein in control or OVA-inflamed lungs.

(C) Lung sections were stained with anti-IL-33 antibody and counterstained with hematoxylin. Scale bar, 20 μm. Data are represented as mean ± SEM (n = 3–7). *p < 0.05, **p < 0.01.

See also Figure S4.

respectively. We found that Mex-3B was expressed in both airway epithelial and non-epithelial cells at similar levels and was upregulated by OVA challenge (Figure S3). We also found that the other Mex family genes, Mex-3A, -3C, and -3D, were highly expressed in airway epithelial cells compared with non-epithelial cells, and that only Mex-3A was upregulated by OVA challenge in airway epithelial cells. These results suggest that Mex-3B plays a role in airway epithelial cells in the development of allergic airway inflammation.

To investigate the role of Mex-3B in inflammatory factor production from airway epithelial cells, we examined the mRNA levels of epithelial cell-derived inflammatory factors in the lung tissues of OVA-challenged wild-type and *Mex3b*$^{-/-}$ mice. Among the inflammatory factors examined, IL-33 and GM-CSF mRNAs were found to be less efficiently induced in *Mex3b*$^{-/-}$ compared to wild-type lung (Figure 2A). Similarly, IL-33 protein was not significantly induced in the inflamed lungs of *Mex3b*$^{-/-}$ mice compared with wild-type mice (Figure 2B). In agreement with a previous report (Louten et al., 2011), immunostaining with anti-IL-33 antibody revealed that IL-33 was localized to the nuclei of alveolar epithelial cells of both wild-type and *Mex3b*$^{-/-}$ mice (Figure 2C). Following OVA challenge, we detected strong expression of IL-33 in the nuclei of alveolar epithelial cells from wild-type, but not *Mex3b*$^{-/-}$ mice (Figure 2C). By contrast, IL-33 was induced to similar levels in the cytoplasm of alveolar macrophages from either wild-type or *Mex3b*$^{-/-}$ mice (Figure S4A). Furthermore, the levels of IL-33 mRNA induced by LPS in OVA-sensitized or unsensitized alveolar macrophages were similar in wild-type and *Mex3b*$^{-/-}$ mice (Figure S4B). These results suggest that Mex-3B is required for the inflammation-induced upregulation of IL-33 in alveolar epithelial cells.

Mex-3B Deficiency Does Not Significantly Affect IL-33-Induced Airway Inflammation

IL-33 is a central player in the development of allergic inflammation. IL-33 stimulates Th2 cells (Schmitz et al., 2005), mast cells (Iikura et al., 2007), and natural helper cells (Moro et al., 2010). To clarify whether decreased IL-33 production in *Mex3b*$^{-/-}$ mice is responsible for the impaired development of airway inflammation, we examined the effects of intranasal administration of IL-33 on lung inflammation in wild-type and *Mex3b*$^{-/-}$ mice (Figure S4C). Administration of IL-33 for 4 consecutive days resulted in airway inflammation in both wild-type and *Mex3b*$^{-/-}$ mice, similar to that reported by Kondo et al. (2008), and was manifested by an increase in the numbers of eosinophils (Figure S4D), induction of Th2 cytokines (Figure S4E), and epithelial thickening and leukocytic infiltration (Figure S4F). Thus, in contrast to OVA-induced airway inflammation, IL-33-induced inflammation is not affected by *Mex3b* status. These results suggest that *Mex3b*$^{-/-}$ mice develop less airway inflammation than wild-type littermates due to reduced induction of IL-33.

Mex-3B Promotes IL-33 Expression Post-transcriptionally

We next investigated the mechanisms by which Mex-3B induces IL-33 expression using the transformed murine respiratory

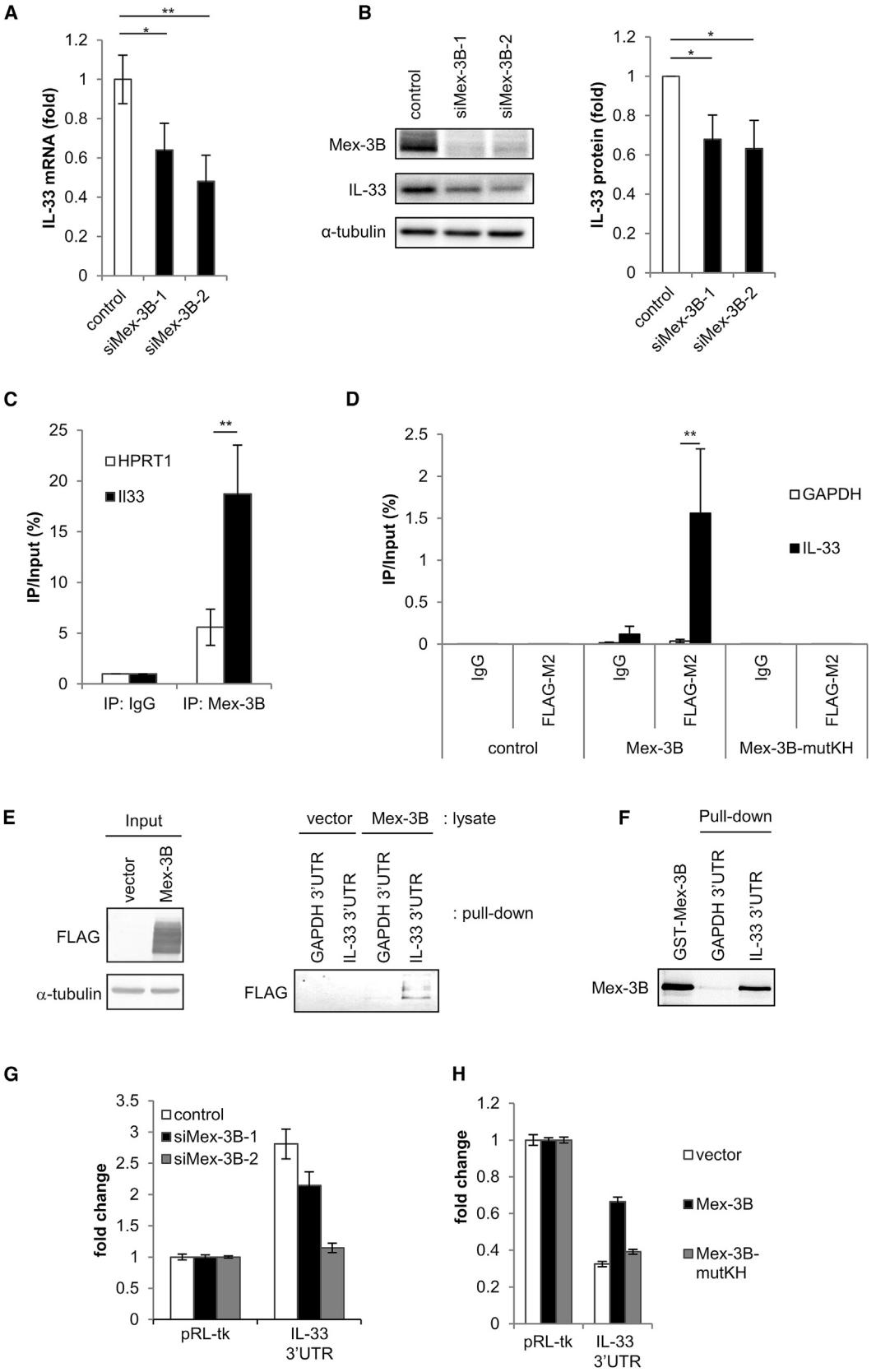

(legend on next page)

epithelial cell-derived cell line MLE-15 (Wikenheiser et al., 1993). We first examined whether IL-33 expression in MLE-15 cells is also regulated by Mex-3B. We found that knockdown of Mex-3B by small interfering RNA (siRNA) caused a decrease in both IL-33 mRNA and protein expression (Figures 3A and 3B). We therefore set out to examine whether Mex-3B directly regulates IL-33 expression using MLE-15 cells.

Since Mex-3B is a KH-type RNA binding protein, we investigated whether Mex-3B is associated with the IL-33 mRNA. We performed RNA immunoprecipitation assays: lysates prepared from MLE-15 cells were subjected to immunoprecipitation with anti-Mex-3B antibody and the IL-33 mRNA associated with the immunoprecipitates was detected by qRT-PCR analysis. We found that Mex-3B is associated with IL-33 mRNA, but not significantly with HPRT1 mRNA (Figure 3C). To examine the role of the KH domain in Mex-3B binding to IL-33 mRNA, we transfected FLAG-tagged wild-type or KH domain mutant Mex-3B into the alveolar epithelial cell-derived adenocarcinoma cell line A549 (Lieber et al., 1976) and performed RNA immunoprecipitation assays. We found that Mex-3B is associated with IL-33 mRNA, but not with GAPDH mRNA (Figure 3D). By contrast, we found that Mex-3B-mutKH did not co-precipitate with the IL-33 mRNA. Mex-3B-mutKH is mutated in key residues involved in RNA binding, i.e., Gly-83 and Gly-177 in the KH domains, which are replaced with Asp. Thus, Mex-3B may associate with the IL-33 mRNA through its KH domains.

An array of RNA binding proteins recognizes the 3′ UTR of target genes and exerts post-transcriptional control (Khabar, 2010). To examine whether Mex-3B binds to the IL-33 3′ UTR, we performed RNA binding protein pull-down assays. Lysates prepared from A549 cells transfected with FLAG-tagged Mex-3B were incubated with biotin-labeled IL-33 3′ UTR and subjected to precipitation with streptavidin-Dynabeads. Immunoblotting with anti-FLAG antibody revealed that Mex-3B co-precipitated with the IL-33 3′ UTR, but not with the GAPDH 3′ UTR (Figure 3E). Furthermore, we produced recombinant Mex-3B fused to glutathione *S*-transferase (GST-Mex-3B) (Figure S5) and examined its ability to interact directly with the IL-33 3′ UTR by RNA binding protein pull-down assays. Immunoblotting of the precipitates with anti-Mex-3B antibody revealed that GST-Mex-3B directly binds to the IL-33 3′ UTR (Figure 3F).

To clarify the significance of the association of Mex-3B with the IL-33 3′ UTR, we constructed a reporter vector containing the IL-33 3′ UTR region fused downstream of the luciferase gene. We found that knockdown of Mex-3B by siRNA caused a decrease in luciferase activity in MLE-15 cells (Figure 3G). Furthermore, we found that overexpression of Mex-3B, but not of Mex-3B-mutKH resulted in the enhancement of reporter activity in A549 cells (Figure 3H). These results suggest that Mex-3B post-transcriptionally activates IL-33 expression through binding to the IL-33 3′ UTR.

Identification of a Mex-3B-Responsive Region in the IL-33 3′ UTR

We next investigated which region of the IL-33 3′ UTR (region 1–12 in Figures S6A–S6D) is involved in Mex-3B-mediated upregulation of IL-33. We found that luciferase reporters containing region 9 [3′ UTR-9 (nucleotides 1414–1674)] were significantly upregulated by Mex-3B (Figure S6C). Furthermore, RNA binding protein pull-down assays revealed that Mex-3B binds 3′ UTR-9 (Figure S6D). These results suggest that Mex-3B regulates IL-33 expression through binding to 3′ UTR-9.

Mex-3B Promotes IL-33 Expression by Inhibiting miR-487b-3p-Mediated Repression

It has been shown that miRNAs suppress the expression of target genes by binding to their 3′ UTRs (Bartel, 2009). We therefore speculated that the Mex-3B-mediated regulation of IL-33 expression via the 3′ UTR might involve an miRNA species. We therefore searched for potential miRNA binding sites in 3′ UTR-9 using the microRNA.org database (John et al., 2004) and identified seven candidate sites (Figure 4A). Among these miRNAs, overexpression of miR-487b-3p most significantly suppressed IL-33 mRNA and protein expression in MLE-15 cells (Figures 4B and 4C). Overexpression of miR-487b-3p also resulted in a decrease in the activity of the luciferase reporters containing either the entire 3′ UTR or 3′ UTR-9 (Figure 4D). By contrast, overexpression of miR-487b-3p did not inhibit the activity of a luciferase reporter containing a mutated miR-487b-3p binding site (3′ UTR-9-mt487b in Figures 4E and 4F). In addition, this mutant reporter showed enhanced activity in the absence of Mex-3B. These results suggest that miR-487b-3p directly regulates IL-33 expression.

We next examined the significance of miR-487b-3p in Mex-3B-mediated upregulation of IL-33. We found that knockdown of miR-487b-3p by a locked nucleic-acid-modified antisense oligonucleotide (LNA-anti-miR487b-3p) (Ørom et al., 2006)

Figure 3. Mex-3B Post-transcriptionally Upregulates IL-33 Expression in the Alveolar Epithelial Cells

(A and B) Effects of Mex-3B knockdown on IL-33 mRNA (A) and protein (B) expression in MLE-15 cells.

(C) qRT-PCR analysis of IL-33 mRNA co-immunoprecipitated with rabbit immunoglobulin G (IgG) or anti-Mex-3B antibody in MLE-15 cells. HPRT1 mRNA was used as a negative control.

(D) qRT-PCR analysis of IL-33 mRNA co-immunoprecipitated with mouse IgG or anti-FLAG-M2 antibody in A549 cells, transfected with control vector, FLAG-tagged Mex-3B or FLAG-tagged Mex-3B-mutKH. GAPDH mRNA was used as a negative control.

(E) Immunoblot analysis of exogenously expressed FLAG-tagged Mex-3B protein co-precipitated with the indicated in vitro transcribed biotin-labeled RNAs. (left) Input. (right) Mex-3B pulled-down with biotin-labeled RNAs. GAPDH 3′ UTR was used as a negative control.

(F) Immunoblot analysis of GST-Mex-3B co-precipitated with the indicated in vitro transcribed biotin-labeled RNAs. GAPDH 3′ UTR was used as a negative control.

(G) Luciferase activity of Mex-3B-knockdowned MLE-15 cells transfected with a luciferase reporter fused to the IL-33 3′ UTR.

(H) Luciferase activity of A549 cells transfected with a luciferase reporter fused to the IL-33 3′ UTR along with control vector, FLAG-tagged Mex-3B or FLAG-tagged Mex-3B-mutKH. Data are represented as mean ± SD (n = 3). *$p < 0.05$, **$p < 0.01$.

See also Figure S5.

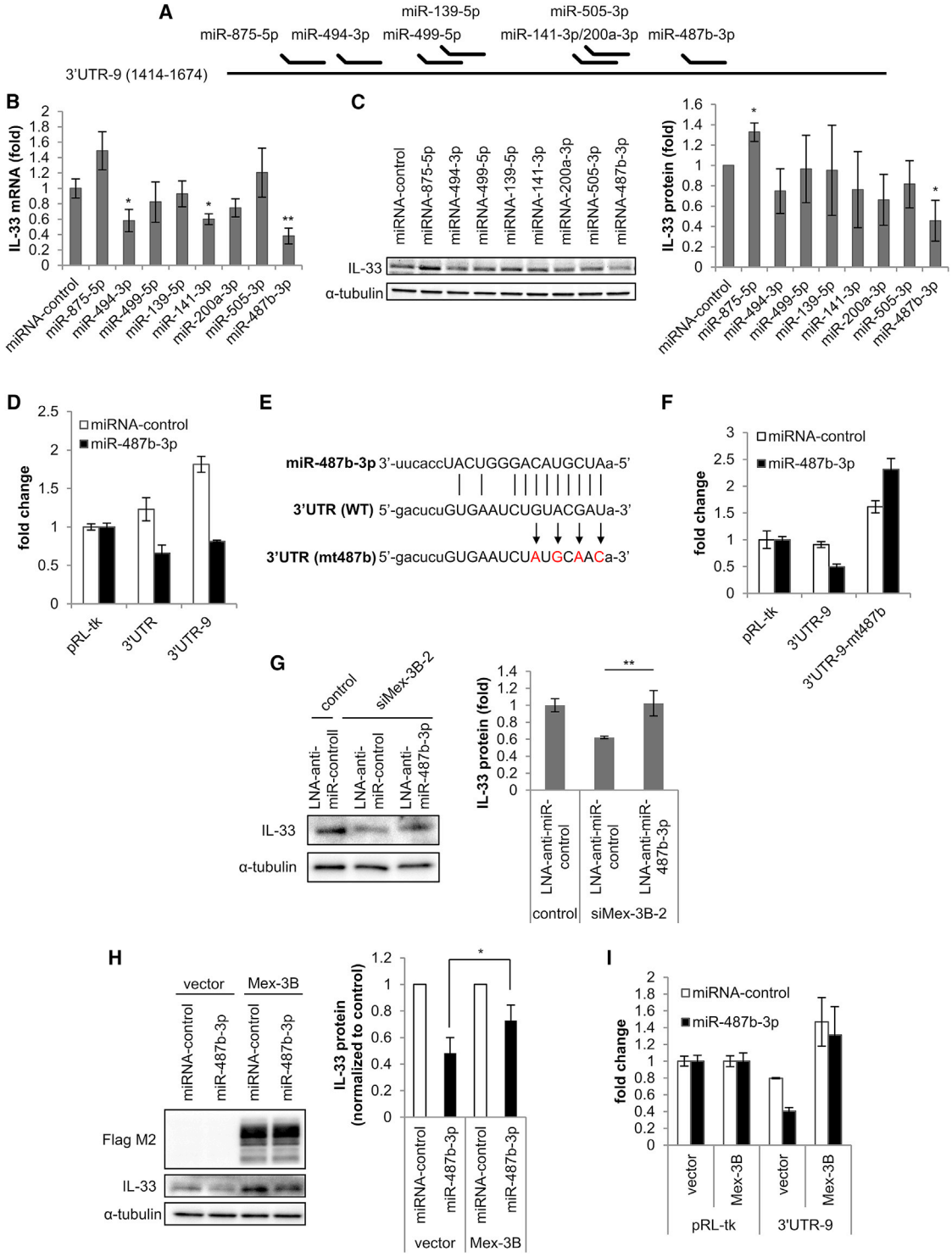

Figure 4. Mex-3B Inhibits the Effect of miR-487b-3p on the IL-33 3′ UTR

(A) Target sites of conserved miRNAs in IL-33 3′ UTR-9 predicted by mirSVR score (http://www.microRNA.org).

(B and C) Effect of miRNA overexpression on IL-33 mRNA (B) and protein (C) expression in MLE-15 cells.

(D) Luciferase activity of MLE-15 cells transfected with each reporter plasmid along with control miRNA or miR-487b-3p.

(E) Schematic representation of wild-type and mutated 3′ UTR-9 reporters.

(F) Luciferase activity of MLE-15 cells co-transfected with each reporter plasmid along with control miRNA or miR-487b-3p.

(G) Immunoblot analysis of IL-33 in MLE-15 cells transfected with the indicated anti-miRNAs along with the indicated siRNAs.

(legend continued on next page)

resulted in a restoration of IL-33 protein expression in MLE-15 cells in which Mex-3B was knocked down (Figure 4G). In addition, overexpression of Mex-3B restored IL-33 protein expression, as well as the activity of a luciferase reporter containing 3′ UTR-9 in cells in which miR-487b-3p was overexpressed (Figures 4H and 4I). We also found that knockdown of Mex-3B resulted in a decrease in miR-487b-3p expression (Figure S6E). These results suggest that Mex-3B promotes IL-33 expression by inhibiting miR-487b-3p-mediated suppression of IL-33.

Mex-3B Inhibits the Interaction of the miR-487b-3p-Ago2 Complex with the miR-487b-3p Target Site in the IL-33 3′ UTR

RNA binding proteins such as Dnd1 have been shown to inhibit miRNA access to their target mRNAs (Kedde et al., 2007). Thus, it is possible that Mex-3B competes with the miR-487b-3p-RISC complex for binding to the 3′ UTR of IL-33. To examine this possibility, we performed RNA binding protein pull-down assays. When miR-487b-3p was transfected into A549 cells, Ago2 was found to co-precipitate with 3′ UTR-9 (Figure 5A). However, co-transfection of Mex-3B with miR-487b-3p interfered with the co-precipitation of Ago2 and 3′ UTR-9 (Figure 5A). These results suggest that Mex-3B inhibits the interaction of the miR-487b-3p-Ago2 complex with the miR-487b-3p target site in the IL-33 3′ UTR.

We therefore examined whether the Mex-3B binding site overlaps with the miR-487b-3p binding site. However, we found that Mex-3B coprecipitated with a mutated 3′ UTR, 3′ UTR-9-Δseed, in which the miR-487b-3p seed match sequence in 3′ UTR-9 has deleted (Figures 5B and 5C). Thus, Mex-3B may not directly compete with the miR-487b-3p-RISC complex for binding to the 3′ UTR of IL-33 but indirectly inhibits their interaction presumably by changing the RNA secondary structure.

As shown in Figure S6C, we found that Mex-3B activated a luciferase reporter containing 3′ UTR-9, but not 3′ UTR-11 or 3′ UTR-12, which are the 5′ and 3′ halves of 3′ UTR-9, respectively. This may indicate that a region straddling 3′ UTR-11 and 3′ UTR-12 is important for Mex-3B binding. In addition, RNA secondary structure prediction indicated the presence of a stem-loop structure, within which this region is contained. We therefore constructed a mutated 3′ UTR-9, 3′ UTR-9-ΔSL, in which this predicted stem-loop structure (nucleotides 1514–1547) is deleted. Luciferase assays revealed that Mex-3B did not enhance the activity of a reporter containing 3′ UTR-9-ΔSL (Figure 5E). Moreover, RNA binding protein pull-down assays revealed that Mex-3B coprecipitated only weakly with 3′ UTR-9-ΔSL (Figure 5F). We also found that Ago2 coprecipitated only weakly with 3′ UTR-9-ΔSL and that miR-487b-3p did not affect this interaction (Figure 5G). Thus, the region containing nucleotides 1514–1547 is required for the interaction of both Mex-3B and the miR-487b-3p-Ago2 complex with the IL-33 3′ UTR.

miR-487b-3p Is Important for the Development of Allergic Airway Inflammation

To investigate whether miR-487b-3p plays a role in the negative regulation of allergic airway inflammation, LNA-anti-miR-487b-3p was administered into OVA-sensitized wild-type or *Mex3b*$^{-/-}$ mice according to the protocol shown in Figure 6A. Cytological analysis of BAL fluid revealed that nebulization of either LNA-anti-miR-487b-3p or a control LNA antisense oligonucleotide (LNA-anti-miR-control) had no effect on OVA-induced inflammation in wild-type mice (Figure 6B). By contrast, nebulization of LNA-anti-miRNA-487b-3p, but not an LNA-anti-miR-control, caused an increase in eosinophil infiltration in *Mex3b*$^{-/-}$ mice challenged with OVA (Figures 6A and 6B). We also found that nebulization of LNA-anti-miR-487b-3p restored IL-33 protein levels in *Mex3b*$^{-/-}$ mice (Figure 6C). In addition, we confirmed that Alexa-488-labeled LNA-anti-miR-487b-3p administered in a nebulized form accumulated in lung epithelial cells 24 hr after exposure (Figure S7A). These observations are consistent with the notion that miR-487b-3p plays an important role in the downregulation of IL-33 and thereby suppresses airway inflammation.

We performed qRT-PCR analysis to measure the approximate copy numbers of miR-487b-3p and IL-33 RNA per cell in the lung tissues of control and OVA-challenged *Mex3b*$^{+/+}$ and *Mex3b*$^{-/-}$ mice. We used miRNA-505-3p and miRNA-875-5p as controls, which are expressed in MLE-15 cells but do not suppress IL-33 expression. We found that the expression of miR-487b-3p and miR-875-5p was lower than that of IL-33 mRNA, while the expression of miR-505-3p was similar to that of IL-33 mRNA (Figure S7B). In addition, we observed that the expression of miR-487b-3p was similar between control and OVA-challenged mice. These results suggest that the suppression of IL-33 expression observed in OVA-challenged mice is not simply the result of altered expression of miR-487b-3p.

LNA Antisense Oligonucleotide-Mediated Knockdown of Mex-3B Suppresses Allergic Airway Inflammation

We finally investigated whether administration of an LNA antisense oligonucleotide targeting Mex-3B (LNA-anti-Mex-3B) could suppress the development of allergic airway inflammation. We confirmed that overexpression of LNA-anti-Mex-3B resulted in a decrease in the levels of Mex-3B and IL-33 in MLE-15 cells (Figure 7A). When LNA-anti-Mex-3B was administered into OVA-sensitized wild-type mice according to the protocol shown in Figure 7B, eosinophil infiltration was significantly inhibited (Figure 7C). Immunostaining with anti-IL-33 antibody revealed that LNA-anti-Mex-3B nebulization caused a decrease in the number of cells that were strongly positive for IL-33 (Figure 7D). These results suggest that suppression of Mex-3B expression using LNA antisense oligonucleotides suppresses allergic airway inflammation.

(H) Immunoblot analysis of IL-33 in MLE-15 cells transfected with the indicated miRNAs along with control vector or FLAG-tagged Mex-3B.
(I) Luciferase activity of MLE-15 cells co-transfected with each reporter plasmid and vector or FLAG-tagged Mex-3B along with control miRNA or miR-487b-3p. Data are represented as mean ± SD (n = 3). *$p < 0.05$, **$p < 0.01$.
See also Figure S6.

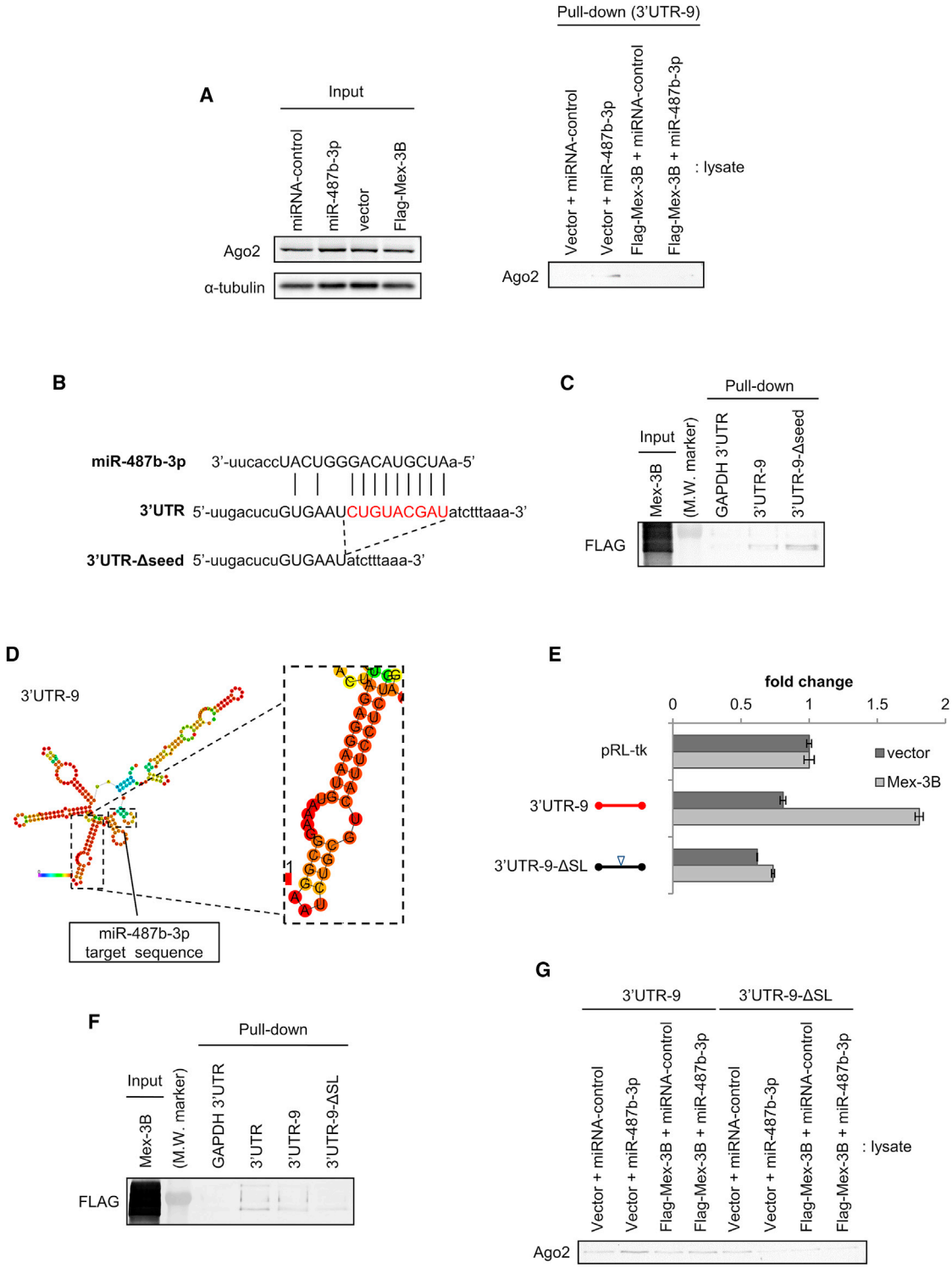

Figure 5. Mex-3B Inhibits the Interaction of the miR-487b-3p-Ago2 Complex with Its miR-487b-3p Target Site in the IL-33 3′ UTR

(A) Immunoblot analysis of Ago2 protein co-precipitated with the in vitro transcribed biotin-labeled 3′ UTR-9. Cell lysates mixed at 1:1 ratio as indicated were used in this assay. (left) Input. (right) Ago2 pulled down with biotin-labeled RNA.

(B) Schematic representation of wild-type and mutated 3′ UTR-9-Δseed reporters.

(C) Immunoblot analysis of exogenously expressed FLAG-tagged Mex-3B protein co-precipitated with the indicated in vitro transcribed biotin-labeled RNAs. GAPDH 3′ UTR was used as a negative control.

(legend continued on next page)

DISCUSSION

Post-transcriptional control of mRNAs encoding pro-inflammatory molecules by RNA binding proteins is considered to be a key determinant of many immunological responses (Kafasla et al., 2014). In the present study, we generated *Mex3b*$^{-/-}$ mice and found that the RNA binding protein Mex-3B plays an essential role in the development of allergic airway inflammation. *Mex3b*$^{-/-}$ mice had fewer inflammatory cell infiltrates and bronchovascular bundles as well as lower mucin production in pulmonary tissues compared to wild-type controls. Furthermore, Th2 cytokines such as IL-4, IL-5, and IL-13 were induced less efficiently in *Mex3b*$^{-/-}$ mice. Although the expression of Mex-3B in CD4^{+} T cells was suppressed by stimulation with anti-CD3/CD28 antibody in vitro, our bone marrow transplantation experiments suggest that the functions of Mex-3B in hematopoietic cells are not crucial for the development of allergic airway inflammation. Additionally, we observed that Mex-3B is upregulated in airway epithelial cells, but not in non-epithelial cells during the development of allergic airway inflammation. We therefore focused on inflammatory factors produced by airway epithelial cells and found that IL-33 induction is suppressed in *Mex3b*$^{-/-}$ mice. Furthermore, we showed that Mex-3B directly binds to the 3′ UTR of IL-33 and post-transcriptionally activates its expression. Thus, our results suggest that Mex-3B plays an important role in the development of airway inflammation by inducing IL-33, a cytokine required for the initiation of allergic airway inflammation.

Consistent with this notion, the degree of airway inflammation in *Mex3b*$^{-/-}$ mice provoked by intranasal administration of recombinant IL-33 was comparable to that in wild-type mice. In particular, we note that although several studies have shown that Th2 cytokines are post-transcriptionally regulated by RNA binding proteins such as HuR (Casolaro et al., 2008; Yarovinsky et al., 2006), the levels of Th2 cytokines induced by the administration of IL-33 in *Mex3b*$^{-/-}$ mice were comparable to those seen in wild-type mice. Thus, the effect of Mex-3B on Th2 cytokine expression appears to be indirect.

It has been shown that miRNAs play important roles in the development of allergic airway inflammation (Simpson et al., 2014). For example, it has been reported that miR-155 is overexpressed in the nasal mucosa of patients with allergic rhinitis and the skin of patients with atopic dermatitis (Suojalehto et al., 2013). It has also been shown that miR-155 deficiency abolishes allergic airway inflammation (Malmhäll et al., 2014). In this study, we found that miR-487b-3p directly suppresses IL-33 expression and that Mex-3B upregulates IL-33 by inhibiting the function of miR-487b-3p. Consistent with our results, it has recently been reported that miR-487b-3p negatively regulates macrophage activation by targeting IL-33 production (Xiang et al., 2016). Furthermore, we showed that inhalation of anti-miR-487b-3p restores IL-33 expression and causes airway inflammation in *Mex3b*$^{-/-}$ mice.

We found that the expression levels of miR-487b-3p are similar between control mice and OVA-challenged wild-type and *Mex3b*$^{-/-}$ mice. Thus, the suppression of IL-33 expression observed in OVA-challenged mice may be not be the simple result of altered expression of miR-487b-3p. Since the expression of Mex-3B is also not altered, activation of Mex-3B, presumably by modification and/or association with other proteins, may play an important role in the upregulation of IL-33 in OVA-challenged mice. Consistent with our results, it has recently been reported that miRNA-mediated mRNA repression in vivo does not necessarily require an alteration in specific miRNA expression (La Rocca et al., 2015) but may also be caused by alterations in the RISC assembly in response to intracellular signaling. Thus, it is possible that upregulation of IL-33 is induced by alterations in RISC assembly in OVA-challenged wild-type mice.

We showed that Mex-3B inhibits the interaction of the miR-487b-3p-Ago2 complex with the miR-487b-3p target site in the IL-33 3′ UTR. However, this inhibition may be indirect, since we found that the Mex-3B- and miR-487b-3p binding sites do not overlap. We therefore speculate that Mex-3B may induce a change in the IL-33 3′ UTR secondary structure that inhibits access of the miR-487b-3p-RISC complex. In line with this notion, it has been reported that the RNA binding protein Pumilio 1 (Pum 1) binds to the 3′ UTR of the p27 mRNA and induces a change in its secondary structure, which exposes miRNA target sites and promotes miRNA-mediated translational repression (Kedde et al., 2010). In addition, we found that Mex-3B binds only weakly to 3′ UTR-9-ΔSL, a mutant lacking a predicted stem-loop structure close to the miR-487b-3p binding site in the IL-33 3′ UTR. However, this result does not tell us whether the stem-loop structure itself is important for Mex-3B binding: it is also possible that this deletion simply removes a conventional binding sequence for Mex-3B. It is further possible that deletion of the stem-loop structure induces a change in mRNA secondary structure that is not favorable for Mex-3B binding. We also observed that the miR-487b-3p-RISC complex binds poorly to 3′ UTR-9-ΔSL, which could be similarly explained by a change in mRNA secondary structure. Further study is needed to determine the detailed regulatory mechanisms underlying Mex-3B-mediated upregulation of IL-33.

It has recently been reported that the expression levels of miRNAs can be regulated by their target mRNAs (Ameres et al., 2010; de la Mata et al., 2015). These reports show that target mRNAs accelerate the decay rate of miRNAs. Consistent with these reports, we found that knockdown of Mex-3B results in a decrease in miR-487b-3p expression. Our results suggest that, in the absence of Mex-3B, miR-487b-3p targets IL-33, and IL-33 may, in turn, accelerate the decay rate of miR-487b-3p.

(D) Predicted secondary structure of 3′ UTR-9. A characteristic stem-loop structure is enlarged in the right panel. The miR-487b-3p target site is also indicated.
(E) Luciferase activity of A549 cells transfected with the indicated reporter plasmid along with control vector or FLAG-tagged Mex-3B.
(F) Immunoblot analysis of exogenously expressed FLAG-tagged Mex-3B protein co-precipitated with the indicated in vitro transcribed biotin-labeled RNAs. GAPDH 3′ UTR was used as a negative control.
(G) Immunoblot analysis of Ago2 co-precipitated with the indicated in vitro transcribed biotin-labeled RNAs. Cell lysates mixed at 1:1 ratio as indicated were used in this assay. Data are represented as mean ± SD (n = 3).

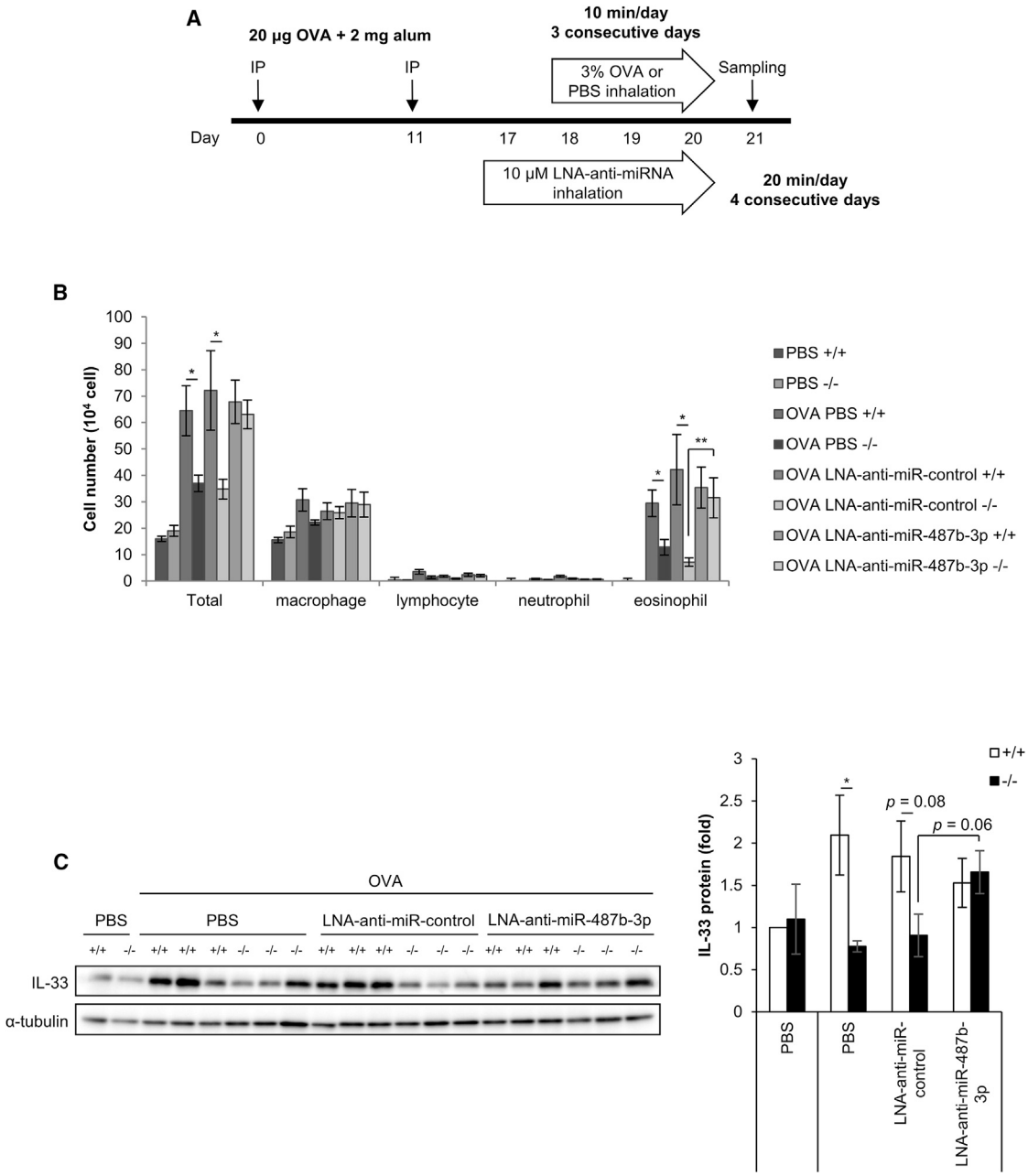

Figure 6. miR-487b-3p Is Important for the Development of Allergic Airway Inflammation

(A) Protocol for the administration of anti-miR-487b-3p into OVA-sensitized *Mex3b*$^{+/+}$ and *Mex3b*$^{-/-}$ mice.

(B) Bronchoalveolar lavage (BAL) fluid analyses. Leukocytes were identified by morphologic criteria.

(C) Immunoblot analysis of IL-33 protein in lungs. Data are represented as mean ± SEM (n = 3–7). *$p < 0.05$, **$p < 0.01$.

See also Figure S7.

Antisense oligonucleotides have been shown to be useful for the treatment of various diseases, including cancer and viral, inflammatory, and neurodegenerative diseases (Evers et al., 2015; Lindow and Kauppinen, 2012). For instance, simultaneous administration of two modified phosphorothioate antisense oligonucleotides targeting CCR3 and CCR4 (ASM8) has been shown to efficiently inhibit allergen-induced eosinophilia and airway dysfunction in sensitized rats and human asthmatics (Allakhverdi et al., 2006). These reagents are currently being evaluated in phase II clinical trials of asthma (Pharmaxis, 2012). We have also found that nebulized administration of an antisense oligonucleotide targeting Mex-3B (LNA-anti-Mex-3B) suppresses the development of allergic airway inflammation. In our experiments, we used LNA antisense

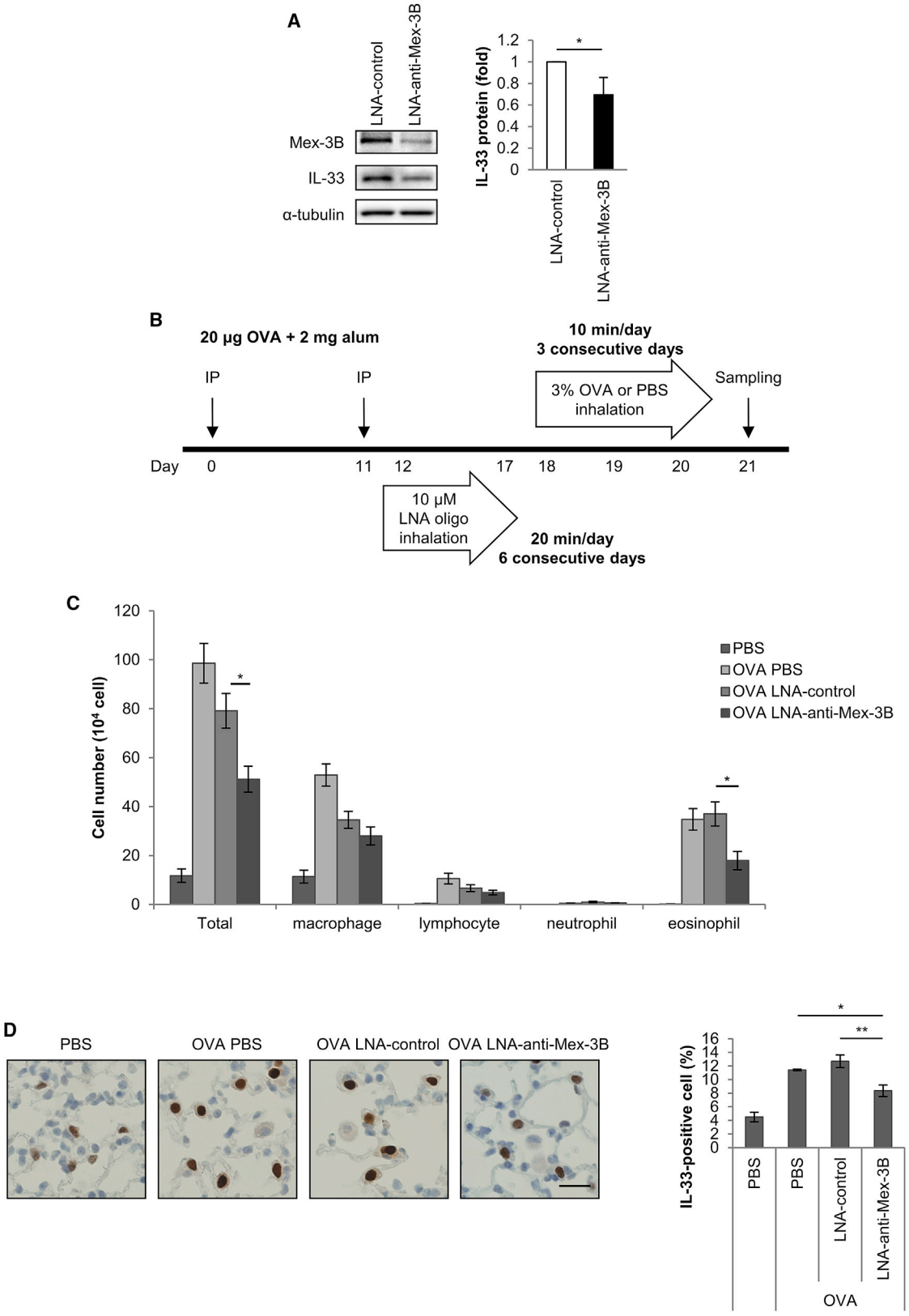

(legend on next page)

oligonucleotides, which contain an engineered O2′ to C4′ linkage within the ribose sugar and have markedly high target mRNA binding affinity and tissue stability (Lundin et al., 2015). We speculate that LNA-anti-Mex-3B could hold promise as a novel anti-asthma reagent. In particular, LNA-anti-Mex-3B could be effective against severe steroid-resistant asthma, a disease in which IL-33 plays an important role by promoting airway remodeling (Saglani et al., 2013).

Accumulating evidence indicates that IL-33 also plays critical roles in the development of various other inflammatory diseases, including chronic obstructive pulmonary disease (COPD) (Byers et al., 2013), inflammatory bowel diseases (Nunes et al., 2014), and atopic dermatitis (Kim and Artis, 2015). It would therefore be interesting to examine whether Mex-3B is involved in these inflammatory diseases and whether LNA-anti-Mex-3B is effective against them.

In conclusion, we showed that Mex-3B-mediated upregulation of IL-33 is critical for the development of allergic airway inflammation. We further showed that Mex-3B upregulates IL-33 by inhibiting miR-487b-3p-mediated repression of IL-33. Our results suggest that LNA-anti-Mex-3B could be useful for the treatment of inflammatory diseases in which the Mex-3B-IL-33 axis plays critical roles.

EXPERIMENTAL PROCEDURES

Mex3b$^{-/-}$ Mice

To construct the Mex-3B targeting vector, exon 1-2 of the *Mex3b* gene was replaced with a neomycin-resistant gene cassette using the bacterial artificial chromosome system (Yang and Seed, 2003). BALB/c embryonic stem cells were electroporated with the linearized Mex-3B targeting vector. G418-resistant clones were screened for homologous recombination by fluorescent in situ hybridization and PCR. *Mex3b*$^{+/-}$ mice were intercrossed to generate *Mex3b*$^{-/-}$ mice. All mice were housed under specific pathogen-free conditions at the Institute of Molecular and Cellular Biosciences, and animal care and experimental procedures were performed in accordance with the guidelines established by the Office for Life Science Research Ethics and Safety of the University of Tokyo.

In Vivo Treatment of Mice

For the OVA-induced model of allergic airway inflammation, mice were immunized as reported previously (Nakagome et al., 2009). For treatment with LNA-anti-miR-487b-3p, mice were exposed to LNA-control or LNA-anti-miR-487b-3p in PBS for 20 min on days 17–20. For treatment with LNA-anti-Mex-3B, mice were exposed to LNA-control or LNA-anti-Mex-3B in PBS for 20 min on days 12–17. Twenty-four hours after the final treatment, samples of BAL fluid and lungs were obtained for examination of the BAL cell profiles and lung histology. After centrifugation, BAL cells were resuspended in PBS and counted with a hemocytometer. A portion of each right lung was lysed in Trisure (Bioline) for qRT-PCR analysis or in RIPA-T buffer (50 mM Tris-HCl [pH 7.5], 150 mM NaCl, 1% Triton X-100, 0.5% NaDOC, 0.1% SDS) for immunoblotting, respectively. The left lungs were homogenized in 1.0 ml of PBS containing 0.5% Triton X-100 and complete protease inhibitor cocktail (Roche) and used for measurements of cytokine concentrations. Bronchial lymph nodes were also examined. Recombinant IL-33 (Invitrogen) treatment was performed as described previously (Kondo et al., 2008). Then, 24 hr after the final treatment, BAL fluid and lung tissues were harvested.

Histology

Tissues were fixed in 10% neutralized buffered formalin (Nacalai Tesque) and embedded in paraffin. Sections were subjected to H&E or periodic acid-Schiff staining. For immunohistochemical staining of lung tissues, rehydrated antigen-retrieved sections were incubated with anti-IL-33 antibody (AF3636: R&D Systems) and visualized by the avidin-biotin complex method using the chromogen diaminobenzidine (Vector Laboratories). For quantification of IL-33-positive cells, a total of 400 alveolar epithelial cells were counted and cells staining more intensely than the threshold value were counted as IL-33 positive. Results were expressed as the percentage of IL-33-positive cells over the total number of lung epithelial cells. Quantification was performed using automated computerized image analysis (CellSens dimension: Olympus). For immunofluorescence staining, nuclei were stained with DAPI (4′6-diamidino-2-phenylindole; Molecular Probes) and observed by fluorescence microscopy (BZ-X700; KEYENCE).

Cell Culture and Transfection

A549 cells were cultured in complete DMEM (Nissui) supplemented with 10% fetal bovine serum (FBS). MLE-15 cells were cultured in RPMI-1640 medium (Sigma-Aldrich) supplemented with 5% FBS, ITS (5 μg/ml insulin, 5 μg/ml transferrin, 5 μg/ml selenium: Sigma-Aldrich), 10 nM hydrocortisone (Sigma-Aldrich), 10 nM β-estradiol (Sigma-Aldrich), and 10 mM HEPES (GIBCO). Spleen cells were cultured in complete DMEM supplemented with 10% FBS. Alveolar macrophage, bronchial lymph node cells and CD4^{+} T cells were cultured in RPMI-1640 medium supplemented with 10% FBS. Plasmids were transfected into A549 or MLE-15 cells with Lipofectamine LTX (Invitrogen) or Lipofectamine 2000 (Invitrogen), respectively. Small oligonucleotides (siRNAs, miRNAs, and LNA oligonucleotides) were transfected into cells with Lipofectamine RNAiMAX (Invitrogen).

Immunoblotting

Cells were lysed in RIPA-T buffer. Samples were separated by SDS-PAGE and probed with specific antibodies. Antibodies were diluted as follows: anti-Mex-3B antibody (Ab) (Atlas), 1:1,000; anti-FLAG M2 Ab (Sigma-Aldrich), 1:2,000; anti-α-tubulin Ab (Calbiochem), 1:2,000; anti-IL-33 Ab (AF3626: R&D Systems), 1:1,000; anti-Ago2 Ab (Wako Pure Chemicals Industries), 1:500. α-tubulin was used as a loading control.

Oligonucleotide

Stealth siRNA targeting Mex-3B and Negative Control siRNA were purchased from Invitrogen. The sequences of siRNA targeting the mouse *Mex3b* cDNA were CACTCAGCTTTGCTCACAATGGGAA for siRNA-1 and TATGGTTTGTAA TCCGTCACAATCG for siRNA-2. Synthetic miRNAs and *mir*Vana mimic negative control were purchased from Ambion. The LNA oligonucleotides were synthesized as unconjugated and fully phosphorothiolated oligonucleotides (Gene Design). The perfectly matching LNA-anti-miR-487b-3p oligonucleotide: 5′-Atga^{m}C^{m}CcTgTa^{m}CGatT-3′ (uppercase, LNA; lowercase, DNA) was complementary to nucleotides 1–16 in the mature miR-487b-3p sequence. The mismatch control LNA oligonucleotide (LNA-anti-miR-control) was synthesized with the following sequence: 5′-aTga^{m}CTcTaTaTGacT-3′. For immunofluorescence analysis, Alexa 488 was conjugated to the 5′ UTR of LNA-anti-miR-487b-3p. LNA-anti-miR-control or LNA-anti-Mex-3B were synthesized by Exiqon.

Figure 7. Inhalation of Antisense Oligonucleotides Targeting Mex-3B Suppresses Allergic Airway Inflammation

(A) Effect of LNA-anti-Mex-3B on Mex-3B and IL-33 protein in MLE-15 cells.

(B) Protocol for the administration of LNA-anti-Mex-3B into OVA-sensitized wild-type mice.

(C) Bronchoalveolar lavage (BAL) fluid analyses. Leukocytes were identified by morphological criteria.

(D) Lung sections were stained with anti-IL-33 antibody and counterstained with hematoxylin. The numbers of IL-33-positive cells were counted. Scale bar, 20 μm. Data are represented as mean ± SEM (n = 3–7). *$p < 0.05$, **$p < 0.01$.

RNA Immunoprecipitation Assay

MLE-15 cells were lysed in NP-40 buffer (20 mM Tris-HCl [pH 7.5], 150 mM NaCl, 1 mM EDTA, 0.5 mM DTT, 0.5% Nonidet P-40, 120 U/ml RNase inhibitor, protease inhibitor cocktail). A549 cells were transfected with the Mex-3B expression constructs. Twenty-four hours after transfection, cytoplasmic cell extracts were prepared in buffer B (10 mM PIPES [pH 6.8], 300 mM sucrose, 100 mM NaCl, 3 mM $MgCl_2$, 1 mM EGTA, 0.5% Triton X-100, 120 U/ml RNase inhibitor, protease inhibitor cocktail). Immunoprecipitation was performed using Dynabeads protein G (Invitrogen). The beads were washed and bound RNA was eluted from the beads by directly adding Trisure (Bioline), followed by RNA extraction and qRT-PCR.

In Vitro Transcription

Murine IL-33 3′ UTRs were cloned into pBluescript II SK (+) at the KpnI and XhoI sites. These constructs were linearized by digestion with EcoRI and in vitro transcription was performed with the T7 MAXIscript Kit (Ambion). Biotin-labeled RNAs were synthesized in the presence of biotin-labeled dCTP during in vitro transcription. GAPDH 3′ UTR was used as a control.

mRNA Binding Protein Pull-down Assay

A549 cells were transfected with the Mex-3B expression construct. Twenty-four hours after transfection, cells were lysed in IP buffer (10 mM Tris-HCl [pH 7.5], 100 mM NaCl, 2.5 mM $MgCl_2$, 0.5% Triton X-100, 120 U/ml RNase inhibitor, protease inhibitor cocktail). Protein extracts were incubated with 350 ng of biotin-labeled UTRs with 15 μg tRNA in IP buffer for 1 hr at 4°C with constant mixing. The biotin-labeled RNA and associated mRNA binding proteins were incubated with 20 μl of paramagnetic streptavidin Dynabeads (Invitrogen) for 1 hr at 4°C with constant mixing. The beads were washed and associated proteins were solubilized in SDS sample buffer and subjected to immunoblotting to detect Mex-3B. For in vitro mRNA binding protein pull-down assays, GST-Mex-3B was incubated with 1 μg of biotin-labeled UTRs.

Luciferase Reporter Assay

A549 cells were transfected with the luciferase reporter construct along with the Mex-3B expression construct. Twenty-four hours after transfection, cells were lysed and luciferase activities were measured. For siRNA or miRNA experiments, MLE-15 cells were transfected with siRNA or miRNA 24 hr before reporter transfection. Twenty-four hours after reporter transfection, cells were lysed and luciferase activities were measured. Luciferase assays were performed with the Dual-Luciferase Reporter Assay System (Promega).

qRT-PCR

RNA extraction and reverse transcription were performed as described previously (Matsuura et al., 2011). Mouse β-actin, mouse GAPDH, and human GAPDH were used as control genes for normalization. Primers used are listed in Table S1.

Statistics

Statistical analysis was performed by unpaired Student's t test. Differences were considered statistically significant when $p < 0.05$.

SUPPLEMENTAL INFORMATION

Supplemental Information includes Supplemental Experimental Procedures, seven figures, and one table and can be found with this article online at http://dx.doi.org/10.1016/j.celrep.2016.07.062.

AUTHOR CONTRIBUTIONS

Y.Y., T.O., and T.A. conceived the project. Y.Y., Y.S.-S., S.S., Y.K., and K.F. performed experiments. Y.O., T.Y., and H.K. generated *Mex3b*$^{-/-}$ mice. O.S., M.I., K.Y., and M.D. worked on the experimental asthma model. S.N. and S.K. analyzed T cell development. Y.Y. and T.A. wrote the paper.

ACKNOWLEDGMENTS

We are grateful to R. Le Goffic for A549 and MLE-15 cells. We thank K. Watanabe, M. Kobayashi, and A. Miyazawa for genotyping, A. Kamiya and H. Matsuoka for discussion, help, and support, and A. Kawai and Y. Koreeda for technical assistance in generating knockout mouse lines. This work was supported by Grants-in-Aid for Scientific Research on Innovative Areas (Integrative Research on Cancer Microenvironment Network) and Research Program of the Project for Development of Innovative Research on Cancer Therapeutics (P-Direct), Research Program of Innovative Cell Biology by Innovative Technology (Integrated Systems Analysis of Cellular Oncogenic Signaling Networks), Ministry of Education, Culture, Sports, Science and Technology of Japan.

Received: October 20, 2015
Revised: June 20, 2016
Accepted: July 25, 2016
Published: August 18, 2016

REFERENCES

Allakhverdi, Z., Allam, M., Guimond, A., Ferrari, N., Zemzoumi, K., Séguin, R., Paquet, L., and Renzi, P.M. (2006). Multitargeted approach using antisense oligonucleotides for the treatment of asthma. Ann. N Y Acad. Sci. *1082*, 62–73.

Allakhverdi, Z., Comeau, M.R., Jessup, H.K., Yoon, B.R., Brewer, A., Chartier, S., Paquette, N., Ziegler, S.F., Sarfati, M., and Delespesse, G. (2007). Thymic stromal lymphopoietin is released by human epithelial cells in response to microbes, trauma, or inflammation and potently activates mast cells. J. Exp. Med. *204*, 253–258.

Ameres, S.L., Horwich, M.D., Hung, J.H., Xu, J., Ghildiyal, M., Weng, Z., and Zamore, P.D. (2010). Target RNA-directed trimming and tailing of small silencing RNAs. Science *328*, 1534–1539.

Bartel, D.P. (2009). MicroRNAs: target recognition and regulatory functions. Cell *136*, 215–233.

Bhattacharyya, S.N., Habermacher, R., Martine, U., Closs, E.I., and Filipowicz, W. (2006). Relief of microRNA-mediated translational repression in human cells subjected to stress. Cell *125*, 1111–1124.

Buchet-Poyau, K., Courchet, J., Le Hir, H., Séraphin, B., Scoazec, J.Y., Duret, L., Domon-Dell, C., Freund, J.N., and Billaud, M. (2007). Identification and characterization of human Mex-3 proteins, a novel family of evolutionarily conserved RNA-binding proteins differentially localized to processing bodies. Nucleic Acids Res. *35*, 1289–1300.

Byers, D.E., Alexander-Brett, J., Patel, A.C., Agapov, E., Dang-Vu, G., Jin, X., Wu, K., You, Y., Alevy, Y., Girard, J.P., et al. (2013). Long-term IL-33-producing epithelial progenitor cells in chronic obstructive lung disease. J. Clin. Invest. *123*, 3967–3982.

Cano, F., Bye, H., Duncan, L.M., Buchet-Poyau, K., Billaud, M., Wills, M.R., and Lehner, P.J. (2012). The RNA-binding E3 ubiquitin ligase MEX-3C links ubiquitination with MHC-I mRNA degradation. EMBO J. *31*, 3596–3606.

Casolaro, V., Fang, X., Tancowny, B., Fan, J., Wu, F., Srikantan, S., Asaki, S.Y., De Fanis, U., Huang, S.K., Gorospe, M., et al. (2008). Posttranscriptional regulation of IL-13 in T cells: role of the RNA-binding protein HuR. J. Allergy Clin. Immunol. *121*, 853–9.e4.

Cayrol, C., and Girard, J.P. (2014). IL-33: an alarmin cytokine with crucial roles in innate immunity, inflammation and allergy. Curr. Opin. Immunol. *31*, 31–37.

de la Mata, M., Gaidatzis, D., Vitanescu, M., Stadler, M.B., Wentzel, C., Scheiffele, P., Filipowicz, W., and Großhans, H. (2015). Potent degradation of neuronal miRNAs induced by highly complementary targets. EMBO Rep. *16*, 500–511.

Donnini, M., Lapucci, A., Papucci, L., Witort, E., Jacquier, A., Brewer, G., Nicolin, A., Capaccioli, S., and Schiavone, N. (2004). Identification of TINO: a new evolutionarily conserved BCL-2 AU-rich element RNA-binding protein. J. Biol. Chem. *279*, 20154–20166.

Evers, M.M., Toonen, L.J., and van Roon-Mom, W.M. (2015). Antisense oligonucleotides in therapy for neurodegenerative disorders. Adv. Drug Deliv. Rev. *87*, 90–103.

Fabian, M.R., Sonenberg, N., and Filipowicz, W. (2010). Regulation of mRNA translation and stability by microRNAs. Annu. Rev. Biochem. *79*, 351–379.

Filipowicz, W., Bhattacharyya, S.N., and Sonenberg, N. (2008). Mechanisms of post-transcriptional regulation by microRNAs: are the answers in sight? Nat. Rev. Genet. *9*, 102–114.

Gudbjartsson, D.F., Bjornsdottir, U.S., Halapi, E., Helgadottir, A., Sulem, P., Jonsdottir, G.M., Thorleifsson, G., Helgadottir, H., Steinthorsdottir, V., Stefansson, H., et al. (2009). Sequence variants affecting eosinophil numbers associate with asthma and myocardial infarction. Nat. Genet. *41*, 342–347.

Hammad, H., and Lambrecht, B.N. (2008). Dendritic cells and epithelial cells: linking innate and adaptive immunity in asthma. Nat. Rev. Immunol. *8*, 193–204.

Herrick, C.A., and Bottomly, K. (2003). To respond or not to respond: T cells in allergic asthma. Nat. Rev. Immunol. *3*, 405–412.

Iikura, M., Suto, H., Kajiwara, N., Oboki, K., Ohno, T., Okayama, Y., Saito, H., Galli, S.J., and Nakae, S. (2007). IL-33 can promote survival, adhesion and cytokine production in human mast cells. Lab. Invest. *87*, 971–978.

John, B., Enright, A.J., Aravin, A., Tuschl, T., Sander, C., and Marks, D.S. (2004). Human MicroRNA targets. PLoS Biol. *2*, e363.

Kafasla, P., Skliris, A., and Kontoyiannis, D.L. (2014). Post-transcriptional coordination of immunological responses by RNA-binding proteins. Nat. Immunol. *15*, 492–502.

Kedde, M., and Agami, R. (2008). Interplay between microRNAs and RNA-binding proteins determines developmental processes. Cell Cycle *7*, 899–903.

Kedde, M., Strasser, M.J., Boldajipour, B., Oude Vrielink, J.A., Slanchev, K., le Sage, C., Nagel, R., Voorhoeve, P.M., van Duijse, J., Ørom, U.A., et al. (2007). RNA-binding protein Dnd1 inhibits microRNA access to target mRNA. Cell *131*, 1273–1286.

Kedde, M., van Kouwenhove, M., Zwart, W., Oude Vrielink, J.A., Elkon, R., and Agami, R. (2010). A Pumilio-induced RNA structure switch in p27-3′ UTR controls miR-221 and miR-222 accessibility. Nat. Cell Biol. *12*, 1014–1020.

Khabar, K.S. (2010). Post-transcriptional control during chronic inflammation and cancer: a focus on AU-rich elements. Cell. Mol. Life Sci. *67*, 2937–2955.

Kim, B.S., and Artis, D. (2015). Group 2 innate lymphoid cells in health and disease. Cold Spring Harb. Perspect. Biol. *7*, 7.

Kim, H.Y., DeKruyff, R.H., and Umetsu, D.T. (2010). The many paths to asthma: phenotype shaped by innate and adaptive immunity. Nat. Immunol. *11*, 577–584.

Kondo, Y., Yoshimoto, T., Yasuda, K., Futatsugi-Yumikura, S., Morimoto, M., Hayashi, N., Hoshino, T., Fujimoto, J., and Nakanishi, K. (2008). Administration of IL-33 induces airway hyperresponsiveness and goblet cell hyperplasia in the lungs in the absence of adaptive immune system. Int. Immunol. *20*, 791–800.

La Rocca, G., Olejniczak, S.H., González, A.J., Briskin, D., Vidigal, J.A., Spraggon, L., DeMatteo, R.G., Radler, M.R., Lindsten, T., Ventura, A., et al. (2015). In vivo, Argonaute-bound microRNAs exist predominantly in a reservoir of low molecular weight complexes not associated with mRNA. Proc. Natl. Acad. Sci. USA *112*, 767–772.

Le Borgne, M., Chartier, N., Buchet-Poyau, K., Destaing, O., Faurobert, E., Thibert, C., Rouault, J.P., Courchet, J., Nègre, D., Bouvard, D., et al. (2014). The RNA-binding protein Mex3b regulates the spatial organization of the Rap1 pathway. Development *141*, 2096–2107.

Lieber, M., Smith, B., Szakal, A., Nelson-Rees, W., and Todaro, G. (1976). A continuous tumor-cell line from a human lung carcinoma with properties of type II alveolar epithelial cells. Int. J. Cancer *17*, 62–70.

Liew, F.Y., Pitman, N.I., and McInnes, I.B. (2010). Disease-associated functions of IL-33: the new kid in the IL-1 family. Nat. Rev. Immunol. *10*, 103–110.

Lindow, M., and Kauppinen, S. (2012). Discovering the first microRNA-targeted drug. J. Cell Biol. *199*, 407–412.

Lloyd, C.M., and Hessel, E.M. (2010). Functions of T cells in asthma: more than just T(H)2 cells. Nat. Rev. Immunol. *10*, 838–848.

Louten, J., Rankin, A.L., Li, Y., Murphy, E.E., Beaumont, M., Moon, C., Bourne, P., McClanahan, T.K., Pflanz, S., and de Waal Malefyt, R. (2011). Endogenous IL-33 enhances Th2 cytokine production and T-cell responses during allergic airway inflammation. Int. Immunol. *23*, 307–315.

Lundin, K.E., Gissberg, O., and Smith, C.I. (2015). Oligonucleotide Therapies: The Past and the Present. Hum. Gene Ther. *26*, 475–485.

Malmhäll, C., Alawieh, S., Lu, Y., Sjöstrand, M., Bossios, A., Eldh, M., and Rådinger, M. (2014). MicroRNA-155 is essential for T(H)2-mediated allergen-induced eosinophilic inflammation in the lung. J. Allergy Clin. Immunol. *133*, 1429–1438, 1438.e1–1438.e7.

Masamune, A., Watanabe, T., Kikuta, K., Satoh, K., Kanno, A., and Shimosegawa, T. (2010). Nuclear expression of interleukin-33 in pancreatic stellate cells. Am. J. Physiol. Gastrointest. Liver Physiol. *299*, G821–G832.

Matsuura, K., Jigami, T., Taniue, K., Morishita, Y., Adachi, S., Senda, T., Nonaka, A., Aburatani, H., Nakamura, T., and Akiyama, T. (2011). Identification of a link between Wnt/β-catenin signalling and the cell fusion pathway. Nat. Commun. *2*, 548.

Moffatt, M.F., Gut, I.G., Demenais, F., Strachan, D.P., Bouzigon, E., Heath, S., von Mutius, E., Farrall, M., Lathrop, M., and Cookson, W.O.; GABRIEL Consortium (2010). A large-scale, consortium-based genomewide association study of asthma. N. Engl. J. Med. *363*, 1211–1221.

Moro, K., Yamada, T., Tanabe, M., Takeuchi, T., Ikawa, T., Kawamoto, H., Furusawa, J., Ohtani, M., Fujii, H., and Koyasu, S. (2010). Innate production of T(H)2 cytokines by adipose tissue-associated c-Kit(+)Sca-1(+) lymphoid cells. Nature *463*, 540–544.

Nakagome, K., Okunishi, K., Imamura, M., Harada, H., Matsumoto, T., Tanaka, R., Miyazaki, J., Yamamoto, K., and Dohi, M. (2009). IFN-gamma attenuates antigen-induced overall immune response in the airway as a Th1-type immune regulatory cytokine. J. Immunol. *183*, 209–220.

Nunes, T., Bernardazzi, C., and de Souza, H.S. (2014). Interleukin-33 and inflammatory bowel diseases: lessons from human studies. Mediators Inflamm. *2014*, 423957.

Oboki, K., Ohno, T., Kajiwara, N., Arae, K., Morita, H., Ishii, A., Nambu, A., Abe, T., Kiyonari, H., Matsumoto, K., et al. (2010). IL-33 is a crucial amplifier of innate rather than acquired immunity. Proc. Natl. Acad. Sci. USA *107*, 18581–18586.

Ørom, U.A., Kauppinen, S., and Lund, A.H. (2006). LNA-modified oligonucleotides mediate specific inhibition of microRNA function. Gene *372*, 137–141.

Pereira, B., Sousa, S., Barros, R., Carreto, L., Oliveira, P., Oliveira, C., Chartier, N.T., Plateroti, M., Rouault, J.P., Freund, J.N., et al. (2013). CDX2 regulation by the RNA-binding protein MEX3A: impact on intestinal differentiation and stemness. Nucleic Acids Res. *41*, 3986–3999.

Pharmaxis. (2012). Pharmaxis Completes Phase II Clinical Study with ASM8 in Asthma Patients. http://www.evaluategroup.com/Universal/View.aspx?type=Story&id=288742.

Préfontaine, D., Nadigel, J., Chouiali, F., Audusseau, S., Semlali, A., Chakir, J., Martin, J.G., and Hamid, Q. (2010). Increased IL-33 expression by epithelial cells in bronchial asthma. J. Allergy Clin. Immunol. *125*, 752–754.

Ray, P.S., Jia, J., Yao, P., Majumder, M., Hatzoglou, M., and Fox, P.L. (2009). A stress-responsive RNA switch regulates VEGFA expression. Nature *457*, 915–919.

Saglani, S., Lui, S., Ullmann, N., Campbell, G.A., Sherburn, R.T., Mathie, S.A., Denney, L., Bossley, C.J., Oates, T., Walker, S.A., et al. (2013). IL-33 promotes airway remodeling in pediatric patients with severe steroid-resistant asthma. J. Allergy Clin. Immunol. *132*, 676–685.e13.

Schmitz, J., Owyang, A., Oldham, E., Song, Y., Murphy, E., McClanahan, T.K., Zurawski, G., Moshrefi, M., Qin, J., Li, X., et al. (2005). IL-33, an interleukin-1-like cytokine that signals via the IL-1 receptor-related protein ST2 and induces T helper type 2-associated cytokines. Immunity *23*, 479–490.

Simpson, L.J., Patel, S., Bhakta, N.R., Choy, D.F., Brightbill, H.D., Ren, X., Wang, Y., Pua, H.H., Baumjohann, D., Montoya, M.M., et al. (2014). A

microRNA upregulated in asthma airway T cells promotes TH2 cytokine production. Nat. Immunol. *15*, 1162–1170.

Sponheim, J., Pollheimer, J., Olsen, T., Balogh, J., Hammarström, C., Loos, T., Kasprzycka, M., Sørensen, D.R., Nilsen, H.R., Küchler, A.M., et al. (2010). Inflammatory bowel disease-associated interleukin-33 is preferentially expressed in ulceration-associated myofibroblasts. Am. J. Pathol. *177*, 2804–2815.

Suojalehto, H., Toskala, E., Kilpeläinen, M., Majuri, M.L., Mitts, C., Lindström, I., Puustinen, A., Plosila, T., Sipilä, J., Wolff, H., and Alenius, H. (2013). MicroRNA profiles in nasal mucosa of patients with allergic and nonallergic rhinitis and asthma. Int. Forum Allergy Rhinol. *3*, 612–620.

Wang, Y.H., Angkasekwinai, P., Lu, N., Voo, K.S., Arima, K., Hanabuchi, S., Hippe, A., Corrigan, C.J., Dong, C., Homey, B., et al. (2007). IL-25 augments type 2 immune responses by enhancing the expansion and functions of TSLP-DC-activated Th2 memory cells. J. Exp. Med. *204*, 1837–1847.

Wikenheiser, K.A., Vorbroker, D.K., Rice, W.R., Clark, J.C., Bachurski, C.J., Oie, H.K., and Whitsett, J.A. (1993). Production of immortalized distal respiratory epithelial cell lines from surfactant protein C/simian virus 40 large tumor antigen transgenic mice. Proc. Natl. Acad. Sci. USA *90*, 11029–11033.

Xiang, Y., Eyers, F., Herbert, C., Tay, H.L., Foster, P.S., and Yang, M. (2016). MicroRNA-487b is a negative regulator of macrophage activation by targeting IL-33 production. J. Immunol. *196*, 3421–3428.

Yang, Y., and Seed, B. (2003). Site-specific gene targeting in mouse embryonic stem cells with intact bacterial artificial chromosomes. Nat. Biotechnol. *21*, 447–451.

Yarovinsky, T.O., Butler, N.S., Monick, M.M., and Hunninghake, G.W. (2006). Early exposure to IL-4 stabilizes IL-4 mRNA in CD4+ T cells via RNA-binding protein HuR. J. Immunol. *177*, 4426–4435.

Ziegler, S.F., and Artis, D. (2010). Sensing the outside world: TSLP regulates barrier immunity. Nat. Immunol. *11*, 289–293.

Cell Reports, Volume *16*

Supplemental Information

The RNA Binding Protein Mex-3B Is Required for IL-33 Induction in the Development of Allergic Airway Inflammation

Yusuke Yamazumi, Oh Sasaki, Mitsuru Imamura, Takeaki Oda, Yoko Ohno, Yumi Shiozaki-Sato, Shigenori Nagai, Saki Suyama, Yuki Kamoshida, Kosuke Funato, Teruhito Yasui, Hitoshi Kikutani, Kazuhiko Yamamoto, Makoto Dohi, Shigeo Koyasu, and Tetsu Akiyama

Inventory of supplemental information

Seven figures with Figure legends. Figures S1 - S3 relate to Figure 1 in the main document; Figure S4 relate to Figure 2 in the main document; Figure S5 relates to Figure 3 in the main document; Figure S6 relate to Figure 4 in the main document; Figure S7 relate to Figure 6 in the main document.

Table S1: Primers Used in Quantitative RT-PCR Experiments

Yamazumi et al Figure S1, related to Figure 1

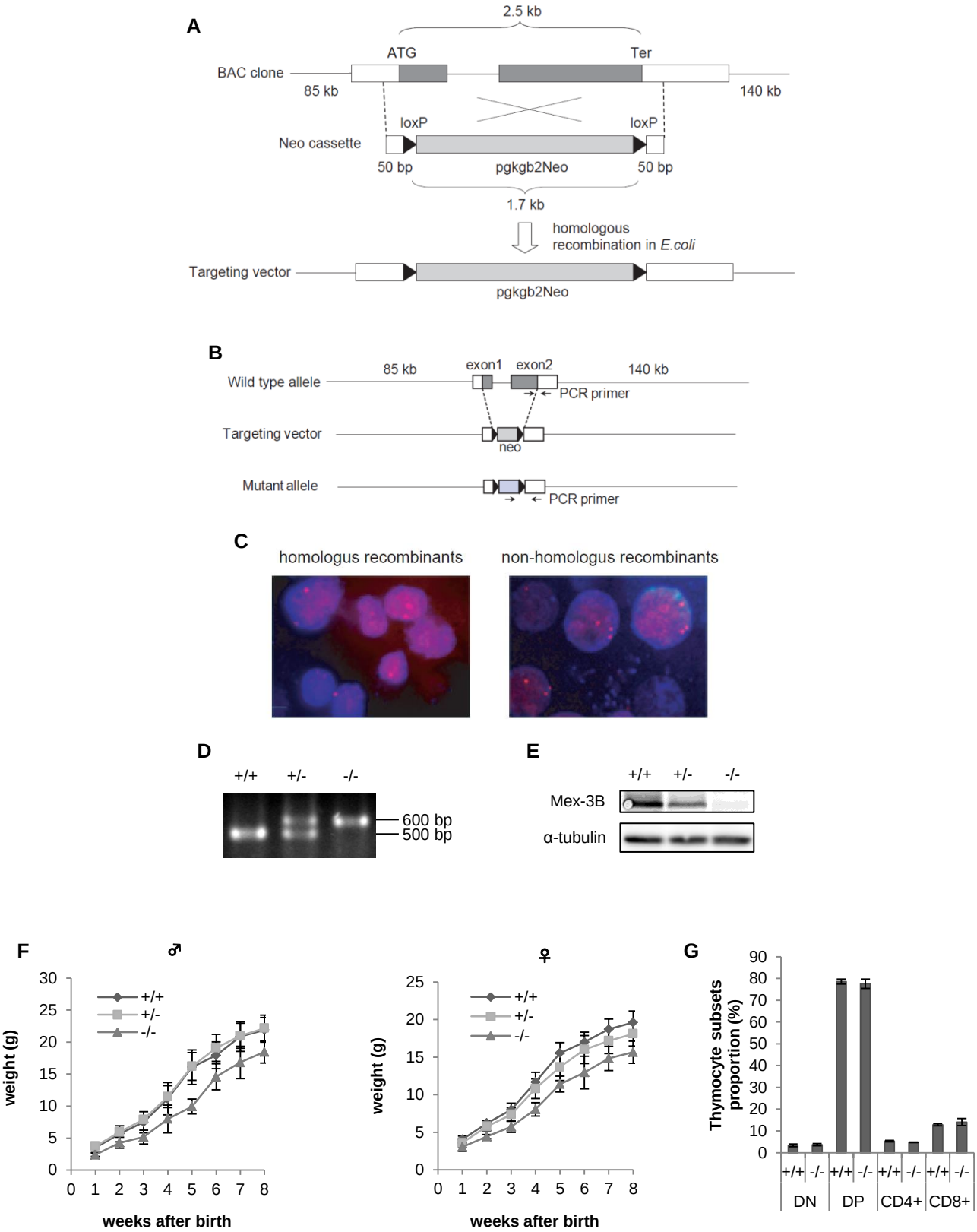

Yamazumi et al Figure S2, related to Figure 1

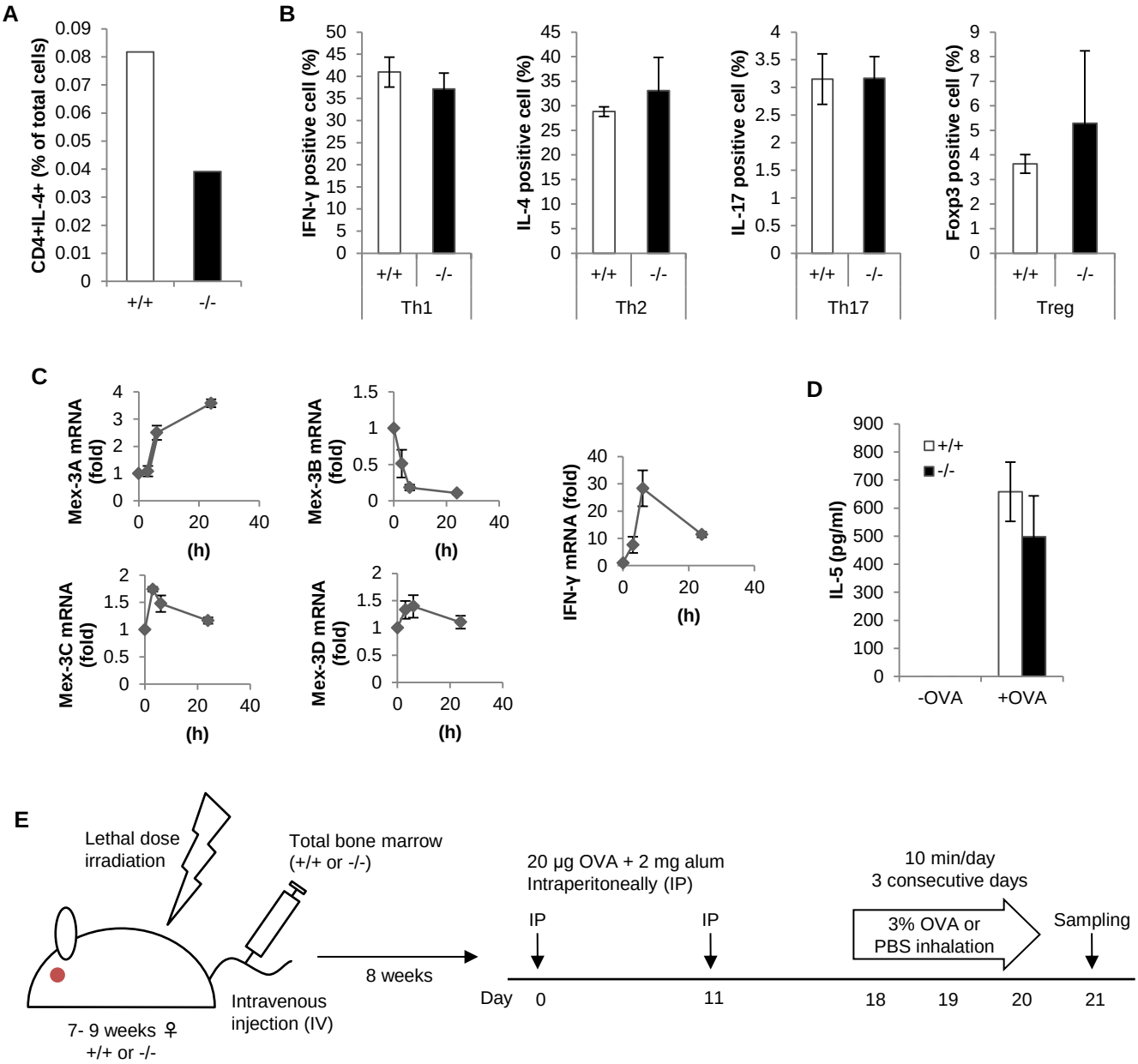

	Donor	Recipient
+/+ → +/+	+/+	+/+
-/- → +/+	-/-	+/+
+/+ → -/-	+/+	-/-

Yamazumi et al Figure S3, related to Figure 1

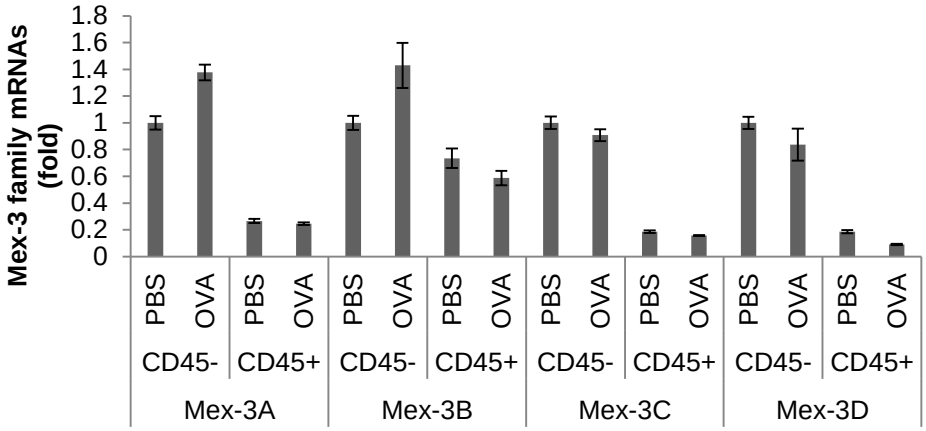

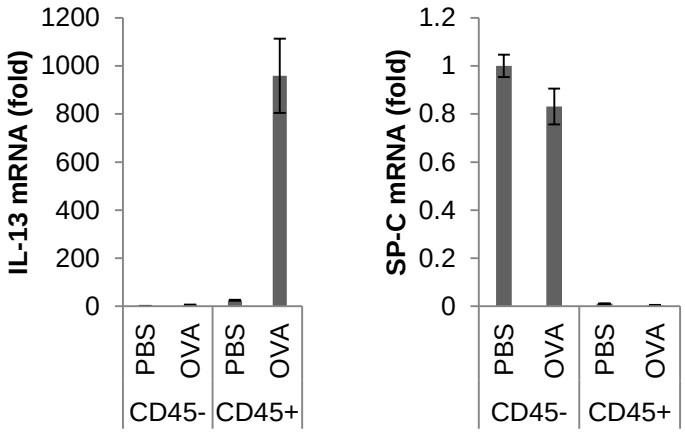

Yamazumi et al Figure S4, related to Figure 2

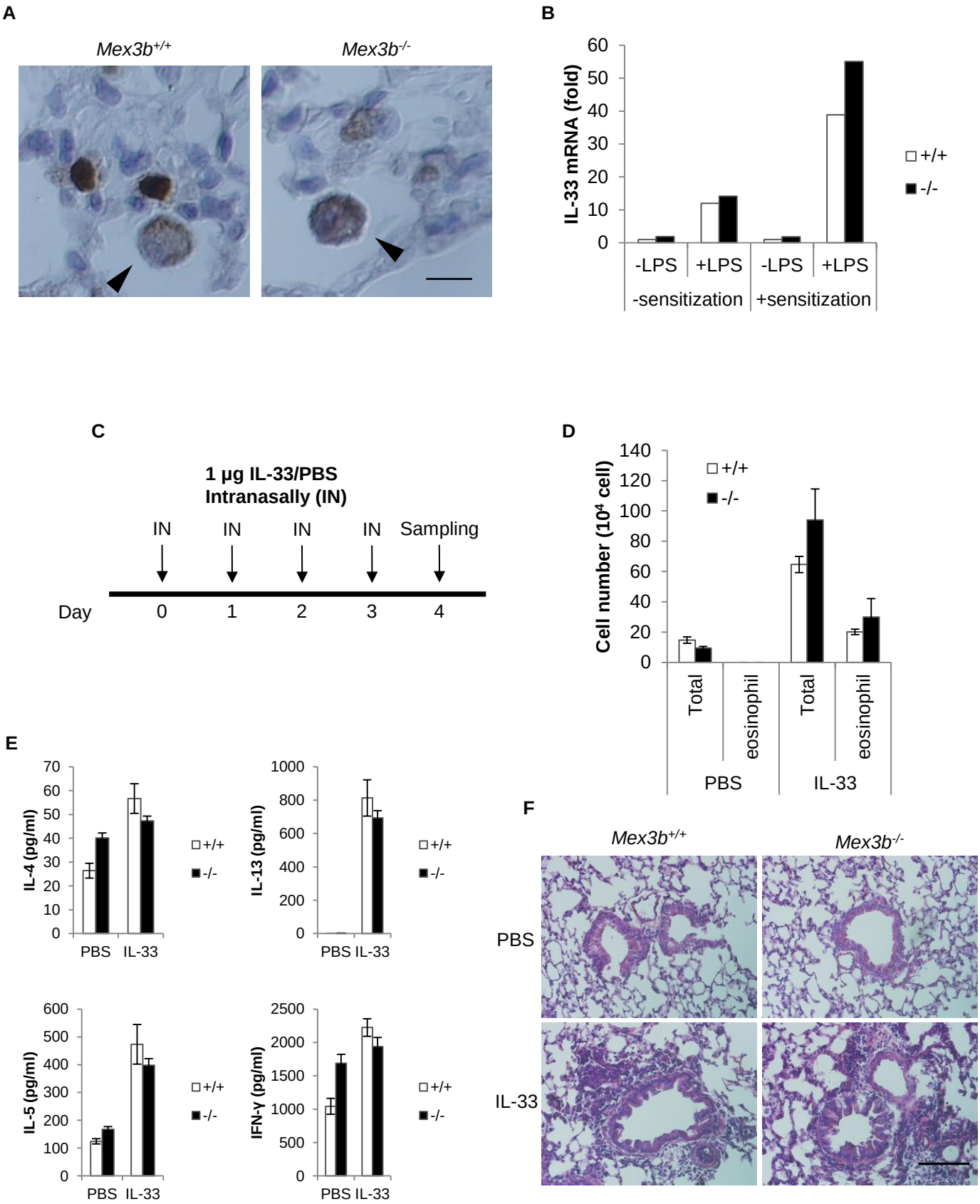

Yamazumi et al Figure S5, related to Figure 3

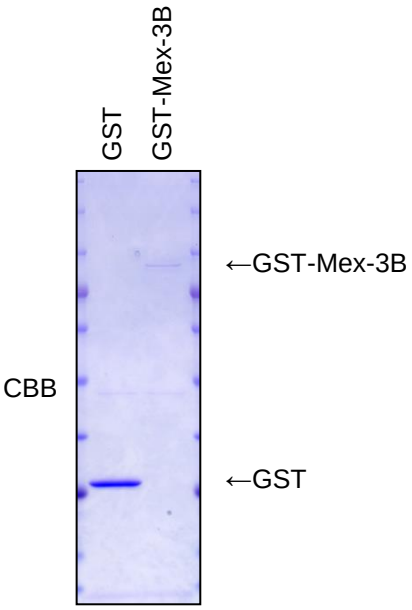

Yamazumi et al Figure S6, related to Figure 4

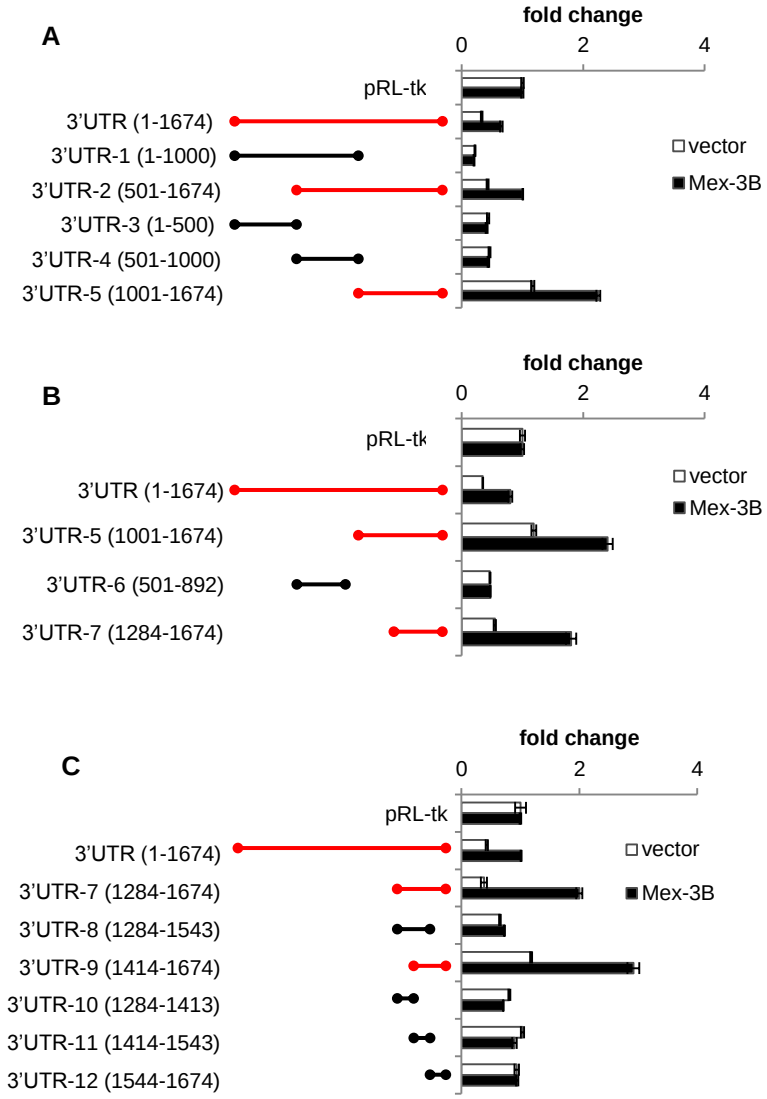

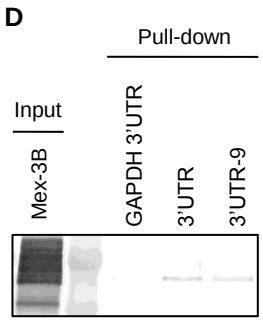

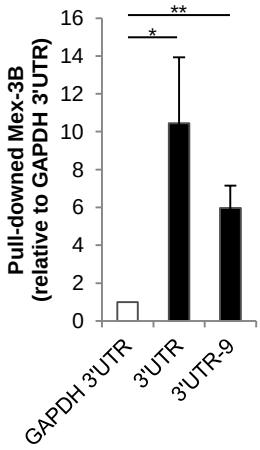

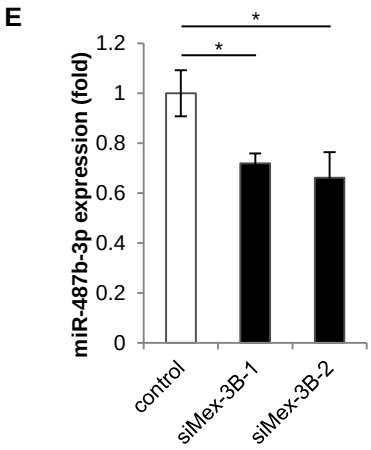

Yamazumi et al Figure S7, related to Figure 6

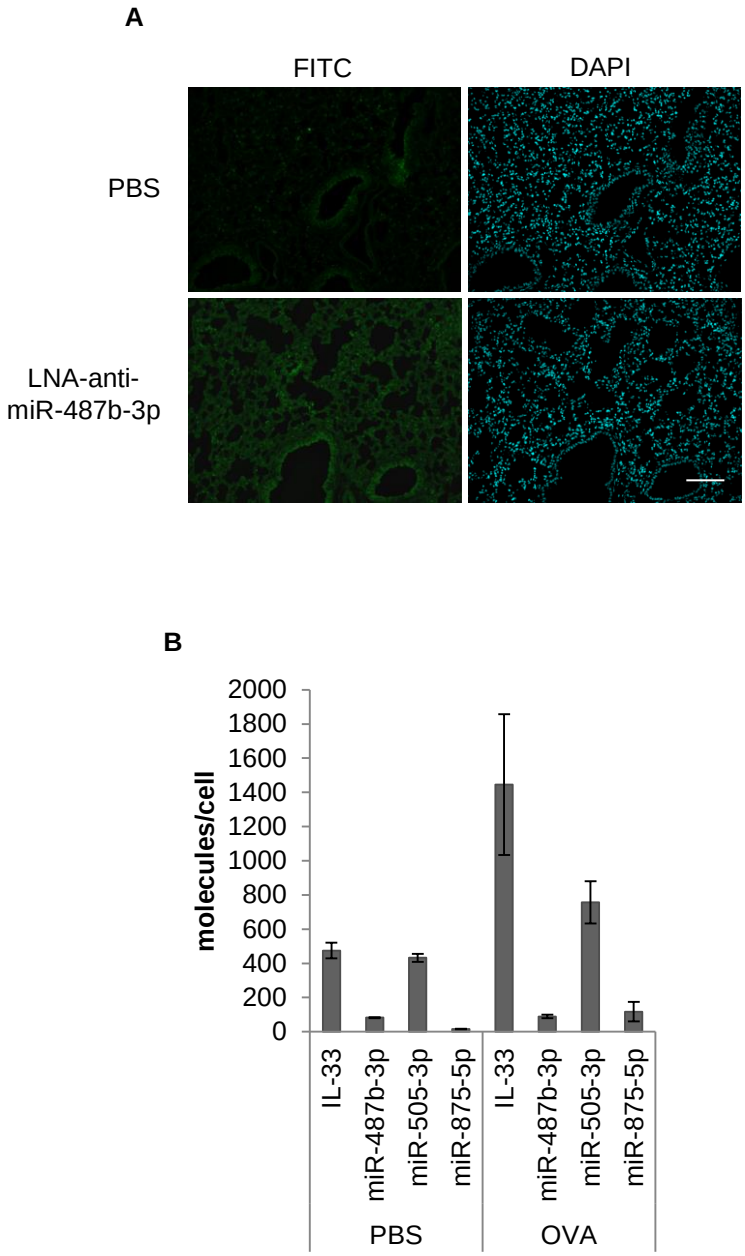

Supplemental Figure legends

Figure S1. Related to Figure 1

(A) The BAC clone, Neo cassette and targeting vector are shown.

(B) The wild-type *Mex3b* allele, targeting vector and mutant allele are shown. Arrows indicate primers used in PCR genotyping.

(C) FISH analysis of G418-resistant clones.

(D) Genotyping of mouse tail genomic DNA by PCR with primers amplifying the wild-type locus (500 bp) and the mutant locus (600 bp), respectively.

(E) Extracts from the thymus of *Mex3b*$^{+/+}$, *Mex3b*$^{+/-}$, and *Mex3b*$^{-/-}$ mice were subjected to immunoblotting analysis with anti-Mex-3B antibody. α-tubulin was used as a loading control.

(F) Weight gain in *Mex3b*$^{+/+}$, *Mex3b*$^{+/-}$ and *Mex3b*$^{-/-}$ mice (n = 4 - 14).

(G) Composition of thymocyte subsets (n = 3). Data are represented as mean ± SD.

Figure S2. Related to Figure 1

(A) Lung bronchial lymph node (LN) cells were isolated from the lungs of OVA-challenged *Mex3b*$^{+/+}$ and *Mex3b*$^{-/-}$ mice. LN cells from four mice were pooled in each group and stimulated *ex vivo* with Leukocyte Activation Cocktail. The number of Th2 cells was measured by intracellular IL-4 staining.

(B) Efector and regulatory T cells were generated from *Mex3b*$^{+/+}$ and *Mex3b*$^{-/-}$ CD4^{+}CD62L^{+} naïve T cells using standard cytokine cocktails. Th1, Th2, Th17 and Treg cells were detected by intracellular IL-4, IL-5, IL-17 and Foxp3 staining, respectively.

(C) CD4^{+} T cells were stimulated with anti-CD3/CD28 antibody for the indicated time and subjected to qRT-PCR. IFN-γ mRNA was used as a marker of T cell activation.

(D) Splenocytes containing dendritic cells from OVA-sensitized mice were cultured with OVA. The levels of IL-5 in the supernatant of splenocytes were measured by ELISA.

(E) Protocol for bone marrow transplantation.

(F) Bronchoalveolar lavage (BAL) fluid analyses were performed. Leukocytes were identified by morphological criteria. Data are represented as mean ± SD (B - D: n = 3) or ± SEM (F: n = 3 - 8)

Figure S3. Related to Figure 1

CD45-positive leukocytes and CD45-negative cells were separated from the lungs of control or OVA-challenged wild-type mice. RNAs were extracted from CD45-negative cells (CD45-) or CD45-positive cells (CD45+) and subjected to qRT-PCR. IL-13 or SP-C mRNA were used as markers of inflammation and airway epithelial cells, respectively. Data are represented as mean ± SEM (n = 4).

Figure S4. Related to Figure 2

(A) Alveolar macrophages (indicated by arrowheads) derived from OVA-inflamed lungs were stained with anti-IL-33 antibody.

(B) Alveolar macrophages from OVA-sensitized or unsensitized mice and were stimulated with LPS. The levels of IL-33 mRNA were measured by qRT-PCR.

(C) Scheme of IL-33-triggered airway inflammation.

(D - F) Effects of intra-nasal administration of IL-33 on lung inflammation in *Mex3b*$^{+/+}$ and *Mex3b*$^{-/-}$ mice. The number of cells in BAL fluids (D), cytokine concentrations (E) and lung sections stained with HE (F) at 24 h after the last IL-33 or PBS administration are shown. Scale bar, 20 μm (A) or 100 μm (F). Data are represented as mean ± SEM (n = 3 - 7).

Figure S5. Related to Figure 3

The purity of GST-Mex-3B was confirmed by CBB staining.

Figure S6. Related to Figure 4

(A - C) Luciferase activity of A549 cells transfected with the indicated reporter plasmid along with control vector or FLAG-tagged Mex-3B.

(D) Immunoblot analysis of exogenously expressed FLAG-tagged Mex-3B protein co-precipitated with the indicated IL-33 3'UTR fragments. GAPDH 3'UTR was used as a negative control.

(E) MLE-15 cells were transfected with the indicated siRNAs and subjected to qRT-PCR. miR-487b-3p expression was normalized to U6 snRNA. Data are represented as mean ± SD (n = 3). *: $p < 0.05$.

Figure S7. Related to Figure 6

(A) Immunofluorescence staining of LNA-anti-miRNA (green; left) in lung tissues treated for 24 h with PBS or Alexa 488-LNA-anti-miR-487b-3p. Nuclei were stained with DAPI (blue; right). (B) The absolute copy numbers of miRNAs and IL-33 mRNA per cells in the lungs of control or OVA-challenged wild-type mice were measured by qRT-PCR. Scale bar, 100 μm. Data are represented as mean ± SEM (n = 3 - 6).

Supplemental Tables

Supplemental table 1. Primers Used in Quantitative RT-PCR Experiments

Name	Sequence (5' → 3')
mouse β-actin-F	GGATGCAGAAGGAGATTACTGC
mouse β-actin-R	CCACCGATCCACACAGAGCA
mouse GAPDH-F	TGTGTCCGTCGTGGATCTGA
mouse GAPDH-R	TTGCTGTTGAAGTCGCAGGAG
mouse Mex-3A-F	TGGGAGAGAAGTCTGGAGAGTG
mouse Mex-3A-R	CCGTCTCAAACTGATTCTTTGG
mouse Mex-3B-F	AGATCGTAGGGAGGCAAGG
mouse Mex-3B-R	GCCCGTCACAACAAAGACA
mouse Mex-3C-F	CAGTGGGTCCCAGAGCCTA
mouse Mex-3C-R	GGCAGCACTGGAAGTGTCA
mouse Mex-3D-F	CGTGTCGCAAACAGCTTTAAC
mouse Mex-3D-R	TGTCACCGGCTCACTCAATAC
mouse IFN-γ-F	ATCTGGAGGAACTGGCAAAA
mouse IFN-γ-R	TTCAAGACTTCAAAGAGTCTGAGGTA
mouse IL-13-F	CCTCTGACCCTTAAGGAGCTTAT
mouse IL-13-R	CGTTGCACAGGGGAGTCT
mouse SP-C-F	GGTCCTGATGGAGAGTCCAC
mouse SP-C-R	GATGAGAAGGCGTTTGAGGT
mouse IL-33-F	GACACATTGAGCATCCAAGG
mouse IL-33-R	AACAGATTGGTCATTGTATGTACTCAG
mouse TSLP-F	CAGCTTGTCTCCTGAAAATCG
mouse TSLP-R	AAATGTTTTGTCGGGGAGTG
mouse GM-CSF-F	GCATGTAGAGGCCATCAAAGA
mouse GM-CSF-R	CGGGTCTGCACACATGTTA
human GAPDH-F	GCACCGTCAAGGCTGAGAAC
human GAPDH-R	TGGTGAAGACGCCAGTGGA
human IL-33-F	AGCAAAGTGGAAGAACACAGC
human IL-33-R	CTTCTTTGGCCTTCTGTTGG

miR-487b-3p	AAUCGUACAGGGUCAUCCACUU
miR-875-5p	TATACCTCAGTTTTATCAGGTG
miR-505-3p	CGTCAACACTTGCTGGTTTTCT

Supplemental Experimental Procedures

Genotype

Genomic DNA was prepared from tail biopsies and genotyped using the following primer sets: Mex-3B wild-type allele, GTCACTCAGGCCATCCGCATTTTTTCCTGA and GTGTTCTAGAACGAGCGCTGTAGGAACCCA; Mex-3B knockout allele, GTTGGTTTTTGTGTGCGGCGCGCCGTTTAA and GTGTTCTAGAACGAGCGCTGTAGGAACCCA.

Isolation of airway epithelial cells in the lung

Airway epithelial cells in the lungs were isolated from mice by the method described by Corti et al. (Corti et al. 1996) with minor modifications. Mice were exsanguinated under anesthesia, and the pulmonary vasculature was perfused with PBS via the right ventricle until the effluent was free of blood. The lungs were isolated and immersed in 7 ml dispase (BD Biosciences) in 30 ml syringe. By piston action, the lungs were deaerated and filled with dispase, then placed in 1.5 ml dispase for 45 min at 37°C. The lungs were minced in DMEM/F12 with 0.01% DNase I (Roche) and gently swirled for 7.5 min. This crude cell mixture was passed successively through 100-, 40 μm nylon mesh filters (BD Biosciences) and then centrifuged at 130 x g for 5 min at 4°C. Cells were incubated with CD45 MicroBeads (Miltenyi Biotec) and CD45-positive (leukocyte) or CD45-negative cell fractions were separated by autoMACS^{tm} Separator (Miltenyi Biotec) according to the manufacturer's instruction.

Bone marrow transplantation

For the preparation of recipient mice, 7 - 9 weeks old female *Mex3b*$^{+/+}$ or *Mex3b*$^{-/-}$ mice were total body irradiated with 9.5 Gy (lethal dose) in an acrylic chamber. Bone marrow donor cells were harvested from 7 - 9 weeks old female *Mex3b*$^{+/+}$ or *Mex3b*$^{-/-}$ mice by gently flushing their femurs with 2%FBS/PBS. Cells were centrifuged, resuspended in PBS. Total bone marrow cells (6 x 10^5) in 0.3 ml PBS were intravenously injected into recipient mice immediately after irradiation. Eight weeks after transplantation, mice were subjected to OVA-induced model of allergic airway inflammation.

Analysis of thymocyte subsets

Thymocytes were isolated and stained with FITC-conjugated anti-CD8a (53-6.7: BD biosciences) antibody (Ab) and PE-conjugated anti-CD4 (GK1.5: BD biosciences) Ab to analyze DN, DP, CD4 SP and CD8 SP subsets. Flow cytometry was performed on a FACSCalibur (BD Biosciences) and the data was analyzed using FlowJo Software (Tree Star).

T cell activation

After splenocytes were reacted with cocktail of biotin-conjugated monoclonal anti-mouse antibodies against CD8a, CD45R, CD11b, CD11c, MHC class II, CD25, CD49b and Ter-119, $CD25^-CD4^+$ T cells were isolated with Anti-Biotin Microbeads (Miltenyi Biotec) by negative selection. Isolated T cells were stimulated with immobilized anti-CD3ε antibody (plates coated with 5 μg/ml anti-CD3ε antibody in 100 μl PBS) and 1 μg/ml soluble anti-CD28 antibody

Measurement of cytokines

The concentrations of IL-4, IL-5, IL-13 and IFN-γ were measured using ELISA kits (IL-5 and IFN-γ, BD Pharmingen; IL-4 and IL-13, R&D Systems).

Preparation of spleen and lymph node cells

Spleen cells were prepared as reported previously (Nakagome et al., 2005). For the preparation of bronchial lymph node cells, the pool of bronchial lymph nodes of 3 - 4 mice were minced and then incubated at 37°C for 30 min with 150 U of collagenase (Sigma) in complete DMEM. Cell suspensions were obtained by pressing the tissues through a 70 μm nylon filter (BD Biosciences).

Ag-induced immune response in spleen cells

Spleen cells (2.5 x 10^5 cell/well) were cultured with OVA (10 μg/ml) in complete Dulbecco's Modified Eagle's Medium (DMEM: Nissui) for 120 h and the cytokine concentrations in the supernatants were measured by ELISA.

Isolation and differentiation of Th subsets

$CD4^+CD25^-CD62L^{high}$ T cells were purified from splenocytes using the $CD4^+CD62L^+$ T cell isolation kit II (Miltenyi Biotec). Isolated naïve $CD4^+$ T cells were stimulated for 3 days with immobilized anti-CD3ε antibody (plates coated with 5 μg/ml anti-CD3ε antibody in 100 μl PBS) and 1 μg/ml soluble anti-CD28 antibody supplemented with 10 ng/ml IL-12 for Th1 differentiation, 10 ng/ml IL-4 for Th2 differentiation, 3 ng/ml TGF-β for iTreg differentiation, or 30 ng/ml IL-6 and 3 ng/ml TGF-β for Th17 differentiation.

Preparation of alveolar macrophage

Mex3b$^{+/+}$ and *Mex3b*$^{-/-}$ mice were sensitized with OVA/alum on days 0 and 11. On day 18, BAL cells were obtained. Over 95% of BAL cells were identified as macrophage by cellular morphology. Cells were stimulated with LPS (100 ng/ml) for 3 h. Cells were lysed in Trisure for qRT-PCR analysis.

Intracellular staining of cytokines and Foxp3

Bronchial lymph node cells were restimulated with Golgi Plug (BD Pharmingen) for 4 h. Th1, Th2 and Th17

cells were restimulated with 50 ng/ml PMA and 1 μM ionomycin for 2 to 4 h, followed by incubation with Brefeldin A for 2 h. Intracellular cytokine staining was performed using Intra Prep (Beckman Coulter). Intracellular staining of Foxp3 for Treg was performed with the PE anti-mouse/rat Foxp3 staining kit (eBioscience). Flow cytometry was performed on a FACSCalibur and the data was analyzed using FlowJo Software.

Plasmid construction

FLAG-tagged human Mex-3B was subcloned into the pcDNA3.1 (+) vector (Invitrogen). FLAG-tagged Mex-3B mutKH was created by standard PCR techniques using Pyrobest DNA polymerase (TAKARA). Murine IL-33 3'UTR and its deletion mutants were cloned into the pRL-tk vector (Promega) at *Xba* I and *Not* I sites. For preparation of GST-Mex-3B, cDNA fragments were subcloned into pGEX-5X-1 (GE Healthcare).

Production of recombinant protein

GST-Mex-3B was synthesized in *Escherichia coli* and isolated by adsorption to glutathione-conjugated Sepharose (GSH-Sepharose; GE Healthcare). GST-Mex-3B was purified by DEAE Sepharose (GE Healthcare). The purity of GST-Mex-3B was confirmed by CBB staining.

Quantification of absolute copy numbers of RNAs

Quantification of absolute copy numbers of RNAs were performed by the method described by de la Mata et al. (de la Mata et al., 2015) with modifications. For quantification of miRNAs or U6, total RNA was reverse transcribed using miR-X miRNA First-Strand Synthesis Kit (Clontech), followed by qRT-PCR. Absolute estimation of miRNA copy numbers per cell was performed by generating standard curves using PAGE-purified 5'phosphorylated oligoribonucleotide (FASMAC) corresponding to the following reference sequence: miR-487b-3p, 5'-AAUCGUACAGGGUCAUCCACUU-3'; miR-505-3p, 5'-CGTCAACACTTGCTGGTTTTCT-3', miR-875-5p, 5'-TATACCTCAGTTTTATCAGGTG-3'. Absolute

estimation of IL-33 mRNA copy numbers per cell was performed by generating standard curves using *in vitro*-transcribed IL-33 mRNA [subcloned into pBlueScript II SK (+)]. The Ct values obtained from different reactions were converted to absolute copy numbers of miRNAs or IL-33 mRNA per 20 pg of total RNA (approximately one cell) by interpolating the Ct values of individual samples into the corresponding standard curves. miRNAs and IL-33 mRNA levels were normalized to U6 and β-actin, respectively.

Supplemental References

Corti, M., Brody, A.R., and Harrison, J.H. (1996). Isolation and primary culture of murine alveolar type II cells. American journal of respiratory cell and molecular biology 14, 309-315.

Nakagome, K., Dohi, M., Okunishi, K., Komagata, Y., Nagatani, K., Tanaka, R., Miyazaki, J., and Yamamoto, K. (2005). In vivo IL-10 gene delivery suppresses airway eosinophilia and hyperreactivity by down-regulating APC functions and migration without impairing the antigen-specific systemic immune response in a mouse model of allergic airway inflammation. J Immunol 174, 6955-6966.